ECM Degradation, Matricryptic Peptides, and Stem Cell Recruitment

by

Vineet Agrawal

B.S.E., Biomedical Engineering, Electrical Engineering, Duke University, 2006

Submitted to the Graduate Faculty of

Cellular and Molecular Pathology in partial fulfillment

of the requirements for the degree of

Doctor of Philosophy

University of Pittsburgh

2011

UNIVERSITY OF PITTSBURGH

SCHOOL OF MEDICINE

This thesis dissertation was presented

by

Vineet Agrawal

It was defended on

July 27, 2011

and approved by

Alan Wells, MD, DMS, Professor, Department of Pathology

Timothy D. Oury, MD, PhD, Professor, Department of Pathology

Ira J. Fox, MD, Professor, Department of Surgery

Kacey G. Marra, PhD, Associate Professor, Department of Surgery

Alejandro Almarza, PhD, Assistant Professor, Department of Bioengineering

Dissertation Advisor: Stephen F. Badylak, DVM, PhD, MD, Professor, Department of

Surgery

ECM Degradation, Matricryptic Peptides, and Stem Cell Recruitment

Vineet Agrawal

University of Pittsburgh, 2011

Biologic scaffolds composed of extracellular matrix (ECM) have been used to promote site-specific, functional remodeling of tissue in both preclinical animal models and human clinical applications. Although the mechanisms of action of ECM scaffolds are not completely understood, proteolytic degradation of the ECM scaffold and subsequent progenitor cell recruitment are thought to be important mediators of the constructive remodeling process.

Proteolytic degradation of the ECM scaffolds results in the generation and release of cryptic peptides with novel bioactive properties not associated with their parent molecules such as angiogenic, antimicrobial, mitogenic, and chemotactic properties. While previous studies have suggested that degradation products of ECM scaffolds are chemotactic for progenitor cells *in vitro*, the present thesis expands upon these findings *in vivo*.

In a non-regenerating model of mid-second phalanx digit amputation, treatment with ECM degradation rpodcuts resulted in the accumulation of a heterogeneous population of cells with *in vitro* differentiation potential along osteogenic, adipogenic, and neuroectodermal lineages. Focusing specifically on the Sox2+ population of cells found at the site of injury, work in the present thesis showed that Sox2+ cells co-express bone marrow and periosteal stem cell markers CD90 and Sca1, but not dermal stem cell marker CD133 or circulating stem cell marker c-kit (CD117). Additionally, bone marrow chimeric studies utilizing wild type C57/BL6 and Sox2 eGFP/+ mice showed that the Sox2+ cells are not derived from the bone marrow, but more likely from a local tissue source such as the periosteum.

Fractionation of the ECM degradation products resulted in the identification of a highly conserved cryptic peptide derived from the C-terminal telopeptide of the collagen type IIIα molecule with chemotactic activity for multiple progenitor cells *in vitro*, IAGVGGEKSGGF. Administration of the cryptic peptide in a model of digit amputation resulted in the accumulation of Sox2+, Sca1+, Lin- cells at the site of amputation. Peptide treatment also resulted in the formation of a bone nodule at the site that coincided with the spatial location of Sox2+ cells. *In vitro*, the peptide accelerated osteogenesis of mesenchymal stem cells and increased the expression of osteogenic and chondrogenic genes.

The result of this body of work shows that degradation products of ECM scaffolds contain cryptic peptides with the ability to influence chemotaxis and differentiation of progenitor cells *in vitro* and *in vivo*. The ability to influence stem cell phenotype and fate may be useful in designing new therapies for regenerative medicine approaches to complex, composite tissue reconstruction. Additionally, the findings of the present thesis may serve as the basis for future studies investigating the importance of ECM degradation in the downstream constructive remodeling events at a site of ECM implantation in soft tissue models of injury.

TABLE OF CONTENTS

LIST OF TABLES

LIST OF FIGURES

Figure 7. P erivascular stem cells express mesenchymal stem cell markers over multiple passages. In order to confirm that the perivascular stem cells did not alter phenotype after in vitro culture, cell surface expression of various markers was investigated by flow cytometry. Perivascular stem cells expressed mesenchymal stem cell marker CD146, sm-actin, and NG2,

PREFACE

The work presented in this thesis is the culmination of my experience of as a graduate student. I owe my growth to a multitude of people that have been there with me throughout the process. I am eternally grateful for my experience as a student in the Badylak laboratory, and I cannot express enough gratitude towards everyone who has helped me throughout the process. First and foremost, I owe a debt of gratitude to Dr. Stephen Badylak. He was the only professor at the University of Pittsburgh who took a chance on me as an incoming MD/PhD student in 2006, and I am glad that it turned out to be such a fruitful learning experience for me. He always pushed me to be better than I can be, and I can confidently say that my growth as a researcher is due to his mentorship and guidance.

I would also like to thank Ann Stewart-Akers, Janet Reing, John Freund, and Li Zhang too for their tireless work to keep up the laboratory, as well for their valuable input at different stages of my work. I would like to thank Allison Beattie, Alex Huber, and Jeremy Kelly for their critical eyes with respect to my work. I would also like to thank Donald Freytes, John Wainwright, Ellen Brennan, Jolene Valentin, Tiffany Sellaro, Jillian Tengood, Chris Medberry, Matthew Wolf, Ricardo Londono, and Brian Sicari for being such valuable resources and great friends during my tenure as a student in the Badylak laboratory. I would like to thank Dr. Tom Gilbert for his valuable input as well as for giving me to opportunity to participate in other interesting projects within his laboratory. I also would like to thank Renee Atkinson, Dawn

Robertson, Jocelyn Runyon, Eve Simpson, Loren Gorgel, Neill Turner, and Maria Allie for their valuable assistance as well. I would like to thank the talented undergraduates that I had the honor to work with. I thank Alex Short for his creative ideas, Thu Nguyen for her careful thoughts and organization, Kathryn Hurley for her loyalty and hard work and overall presence, Sandy Liu for her work ethic and organization, and Bernard Siu for his intelligence and enthusiasm and incredible talent for research.

I owe a special debt of gratitude to Stephen Tottey, Kerry Daly, and Scott Johnson. Scott Johnson is perhaps the only other person who never gave up on the work that has culminated in this thesis dissertation. He was my greatest ally, and at times my greatest friend in the laboratory. He taught me much of what I know about my project today, and I can confidently say that the project would be nowhere without his help. Stephen Tottey is one of the most intelligent person I met in the Badylak laboratory, and he was not only a great mentor but also a great confidant. I learned so much about scientific inquiry from him, as well as the importance of balance in an academic career. Likewise, Kerry was a great ally of mine, a great confidant, and most importantly, a great mentor. I always felt that I could be completely open with both Kerry and Stephen, and I still respect their vast knowledge and aptitude for research. I can only wish them the best of luck in their future endeavors – I will cheer them on as they become successful professors in academia some day.

I would also like to personally thank my committee for their valuable input and critical eye for my work throughout my training. I can say without hesitation that our bi-annual meetings were some of the most nerve wracking moments that I have experienced in my graduate training. More importantly, though, they were the moments in which I learned the most about myself as a researcher as well as my project. My improvement as a scientist throughout my graduate training

student in his laboratory. While I may not have been very productive that first summer, I learned more about the basic tenants of research during that summer than in any other year I have spent as a graduate student. In that regard, Dr. Fox has always served as a self-less mentor for me. I only hope to find more mentors like him as I continue my training. I would also like to thank my two undergraduate mentors, Dr. Kathryn Nightingale and Gregg Trahey, for nurturing my love for science and research. Along with Jeremy Dahl and Mark Palmeri, they taught me that it is possible to immerse oneself in their work while maintaining a friendly research environment. To this day, I look back at my time as an undergraduate Pratt fellow in their laboratories with fond memories. I only hope to be able to create a similar friendly, nurturing environment for research some day as I progress through my career.

I would also like to thank the multitude of collaborators without whom my thesis project would not have been what it is today. I would like to thank Susan Braunhut from University of Massachusetts Lowell and David Kaplan from Tufts University. I would like to thank Gang Wang and Lorraine J. Gudas from Cornell University. I would like to thank Hsu Chao, Eric Raborn, Mary Moore, and Karen K. Hirschi from Baylor College of Medicine.

Last, but definitely not least, I must thank my family and friends. My MD/PhD class entering with me in 2006 has become a small family away from home in Pittsburgh: Samuel Shin, David Svilar, Liang-I Kang, Benjamin Mantell, David Wheeler, Amin Afrazi, Mark Doyal, Pavle Milutinovic, Vivek Patel, Jeffrey Koenitzer, and Michael Sung,. To my new friends that I have made, both near and far, I owe my sanity to you. Whether multiple texts and phone calls back and forth, or whether a weekend away, these last few months would not have been the same without you. I only hope to look forward to more days with you in my life.

My immediate family has been a n ever-ending source of support and love for me throughout this process. To my sister, Anshu, my brother-in-law, Himanshu Jijaji, my younger brother, Ankit, and both of my parents, you are the one constant in my life that has never changed. Your love has always been unconditional, and I hope that I can only begin to return the same love and support that you all have given to me over the years. To my parents, you taught us children the meaning of hard work. Coming from India with nothing and rebuilding your life all over again, I cannot even imagine the kind of hardships that you endured so that we may live a better life. You gave us everything we wanted or needed, regardless of how many difficulties you had to endure in order to give it to us. Everything I am is because of you, and everything I will accomplish (God willing) in the future will be a result of your upbringing.

1.0 INTRODUCTION

1.1 BIOLOGIC SCAFFOLDS COMPOSED OF EXTRACELLULAR MATRIX

The extracellular matrix (ECM) is composed of the secreted products of the resident cells in any given tissue, organ, or microenvironment. In addition to serving as a structural scaffold for the tissue, ECM is in a constant state of "dynamic equilibrium" with the resident cells of the given tissues or organ (Nelson and Bissell 2006). Through a unique composition and structure optimized for each tissue, ECM can regulate the phenotype of local cells through modulation of various factors including, but not limited to, mechanical forces, biochemical milieu, oxygen requirements/concentration, pH, and inherent gene expression. For these reasons, ECM plays a central role in mammalian development, normal physiology, and the response to injury (Nelson and Bissell 2006).

This dynamic reciprocity that exists between the cells and ECM of any given tissue also makes the ECM from any tissue or organ an ideal substrate for tissue engineering applications. Biologic scaffolds composed of allogeneic and xenogeneic ECM have been used in preclinical animal studies to facilitate constructive remodeling of a variety of muscular tissues including esophagus (Badylak, Hoppo et al. ; Badylak, Meurling et al. 2000; Badylak, Vorp et al. 2005; Lopes, Cabrita et al. 2006), myocardium (Kochupura, Azeloglu et al. 2005; Robinson, Li et al. 2005; Badylak, Kochupura et al. 2006; Ota, Gilbert et al. 2007), blood vessels (Badylak, Lantz et

al. 1989; Lantz, Badylak et al. 1990; Lantz, Badylak et al. 1992), urinary bladder (Kropp, Eppley et al. 1995; Kropp, Rippy et al. 1996; Pope, Davis et al. 1997; Record, Hillegonds et al. 2001), and skeletal muscle (Mase, Hsu et al. ; Prevel, Eppley et al. 1995; Clarke, Lantz et al. 1996; Badylak, Kokini et al. 2001; Badylak, Kokini et al. 2002). Additionally, commercially produced ECM scaffolds (Appendix A) have shown remarkable efficacy in certain human clinical applications (Mase, Hsu et al. 2010; Badylak, Hoppo et al. 2011) and have been implanted successfully in over one million patients (Badylak 2007).

When properly produced, the general host response to ECM scaffolds consists of rapid degradation of the scaffold with concomitant replacement by organized, site-appropriate, functional host tissue (Allman, McPherson et al. 2001; Record, Hillegonds et al. 2001; Allman, McPherson et al. 2002; Gilbert, Stewart-Akers et al. 2007). Within the context of the present thesis, this process of site-specific deposition of organized, site-appropriate, functional tissue will be referred to as "constructive remodeling." The otherwise default response to injury at similar sites of injury consists of an incomplete regenerative response concomitant with deposition of dense, disorganized connective tissue (Turner and Badylak). The mechanisms by which ECM scaffolds promote constructive remodeling are still only partially understood, but recent studies have begun to identify properties of the ECM scaffold as well components of the host response to the scaffold that may be important for constructive remodeling *in vivo*.

Some of the first studies to identify potential mechanisms by which ECM scaffolds remodel have done so through a time course analysis of remodeling at a site of injury following ECM implantation (Valentin, Badylak et al. 2006; Badylak, Valentin et al. 2008). So long as the scaffold is properly produced such that immunogenic remnants such as DNA and cellular debris are minimized, the remodeling of the ECM scaffold at the site of injury follows a very similar

pattern, regardless of the specific site at which the scaffold is implanted. This time course has led

to the identification of a number of contributing factors that correlate with a r egenerative

outcome in response to ECM scaffold implantation, as opposed to the default wound healing

response of scar tissue deposition. In order to understand why these observed factors are thought

to be important, it is important to understand how and why they represent a deviation from the

default wound healing response at a site of injury. Thus, the normal phases of the wound healing

response in adult mammals are briefly discussed to serve as a baseline for understanding the

importance of the differences observed at a site of injury following implantation of ECM derived

scaffolds.

1.2   THE NORMAL PHASES OF WOUND HEALING IN ADULT MAMMALS

Wound healing in an adult mammal is a well orchestrated integration of multiple systems within

a host that results in quick closure of the wound so as to maintain the integrity of the barrier

between the host and outside world (Falanga 2005). The phases of wound healing can be broadly

be broken into four phases (Figure 1). The coagulation phase is the initial response to injury.

Immediately after injury, hemostasis occurs via local platelet aggregation, fibrin deposition, and

activation of the coagulation cascade. The main purpose of this phase is to achieve hemostasis

and protect against pathogen colonization of the site of injury. This phase culminates in the

eventual release of inflammatory cytokines and mediators that then recruit innate immune cells

such as neutrophils and monocytes/macrophages to commence the inflammatory phase of wound

healing. N eutrophils and monocytes/macrophages are recruited to the site of injury during the

inflammatory phase, and they phagocytose cellular debris at a site of injury as well as release paracrine factors that then recruit other cell types (Lolmede, Campana et al. 2009).

This eventually gives rise to the proliferative phase of wound healing in which re-epithelialization and angiogenesis occurs via migration of epithelial and endothelial cells into the site of injury. Over the course of weeks, wound contraction occurs in the remodeling phase and the extracellular matrix at the site of injury is eventually replaced by ECM deposited by infiltrating fibroblasts and myofibroblasts at the site of injury. In some pathologic cases, inflammatory cells such as T cells may be present at later time points after injury. This is generally a sign of an ongoing chronic inflammatory response that deviates from the normal wound healing response.

Time	Phases	Main Cell Types	Specific Events
	Coagulation Phase	Platelets	Platelet aggregation, fibrin deposition, inflammatory mediators
Hours			
	Inflammatory Phase	Neutrophils / Monocytes, Macrophages	Cell diapedesis, chemotaxis, and wound debridement
Days			
	Proliferative Phase	Epithelial cells, endothelial cells	Epithelial closure, fibroplasia, angiogenesis, ECM deposition and contraction
Weeks			
	Remodeling Phase	+/- T cells / Fibroblasts	MMPs, integrin-crosstalk, cytokine mediated cell migration, ECM production, fibroblast maturation

Figure 1. A schematic depiction of the phases of normal wound healing in adult mammalian soft tissues (modified and adapted from (21)).

1.3   MECHANISMS OF REMODELING OF ECM SCAFFOLDS

While the coagulative phases and inflammatory phases still occur following implantation of an ECM scaffold at a site of injury (Wokalek and Ruh 1991; Allman, McPherson et al. 2001), the overall time course of remodeling deviates significantly from the default wound healing response in the later proliferative and remodeling phases. The specific events that deviate from the normal injury response have most extensively been characterized in a rodent model of skeletal muscle injury in the abdominal wall (Valentin, Turner et al. ; Valentin, Badylak et al. 2006; Badylak, Valentin et al. 2008; Valentin, Stewart-Akers et al. 2009) (Figure 2). Immediately following injury and ECM implantation, the initial coagulative phase of wound healing occurs and results in the eventual recruitment of neutrophils (Allman, McPherson et al. 2001). As early as 48 hours post-ECM implantation, a dense mononuclear infiltrate of cells is observed at the site of injury that persists for weeks. At 4 weeks post-injury, the site of ECM scaffold implantation has been replaced with dense, connective tissue deposited by host cells. The ECM scaffold is no longer present in its intact form. At 16 weeks post-implantation, the site of ECM scaffold implantation is populated with multiple vascular structures, small islands of immature muscular tissue, and growing nerve fibers that histologically colocalize with the small islands of muscle, i.e. the start of constructive remodeling (Valentin, Turner et al. ; Valentin, Badylak et al. 2006; Agrawal, Brown et al. 2009; Brown, Valentin et al. 2009). By 26 weeks post-implantation, the site of ECM scaffold implantation has been replaced with site appropriate, functional muscular tissue that is grossly indistinguishable from the surrounding native muscle (Valentin, Turner et al. ; Valentin, Badylak et al. 2006; Badylak, Valentin et al. 2008; Valentin, Stewart-Akers et al. 2009). In this time course, the formation of new mature vascular structures and immature, but innervated,

muscular tissue (i.e. the events defined as "constructive remodeling") is consistently observed only after the scaffold is no longer histologically present and presumably degraded.
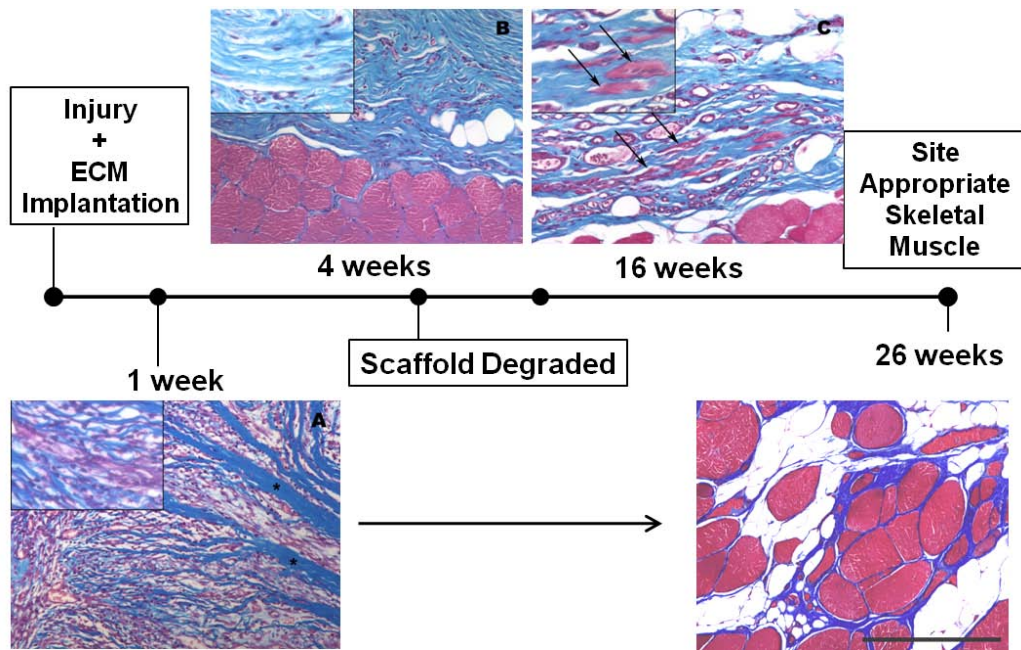
Figure 2. The time course of remodeling at a site of ECM scaffold implantation (adapted from data in (29, 31)).

From this time course analysis and other studies, the immune response, mechanotransduction at the site of injury, site directed recruitment of differentiated and progenitor cells, and rapid degradation of the ECM scaffold have all been identified as important factors that correlate with constructive remodeling *in vivo*. Although each contributing mechanism is discussed below in further detail, the present thesis will focus specifically on two of the four mechanisms. Specifically, the work in this thesis will aim to establish a link between the release of bioactive peptides from rapid degradation of the ECM scaffold and the site directed recruitment of progenitor cells to a site of ECM implantation.

1.3.1 The Immune Response to ECM Scaffold Implantation

Neutrophils, monocytes, macrophages, and T cells are all known to be found at a site of ECM implantation *in vivo* (Wokalek and Ruh 1991; Allman, McPherson et al. 2001; Valentin, Badylak et al. 2006; Crisan, Yap et al. 2008; Valentin, Stewart-Akers et al. 2009). However, the persistence of mononuclear cells at the site of injury for weeks after ECM implantation markedly differs from the time course of normal wound healing at a site of injury. While such a sustained mononuclear response may be considered a chronic inflammatory response as seen in pathologic conditions, the sustained mononuclear infiltration in response to ECM scaffold implantation eventually results in constructive remodeling (Valentin, Badylak et al. 2006), suggesting that mononuclear cells may play a role in mediating this process.

Previous studies have shown that one of the reasons why sustained persistence of mononuclear cells at a site of injury may actually be beneficial is the polarization of the immune cells towards a more anti-inflammatory healing phenotype (Badylak, Valentin et al. 2008), as opposed to the classic pro-inflammatory phenotype. Immune cells such as T cells and monocytes/macrophages exhibit various phenotypes, or polarizations, that dictate their overall function at a site of injury. For example, T cells can broadly be classified into pro-inflammatory (Th1), anti-inflammatory (Th2), or regulatory (Treg) T cells (Gatenby, Callard et al. 1984). Likewise, macrophages can broadly be classified into pro-inflammatory M1 macrophages or anti-inflammatory, pro-wound healing M2 macrophages (Mantovani, Sica et al. 2004). Recently a third subgroup of regulatory macrophages has also been reported in the literature (Zorro Manrique, Duque Correa et al. ; Mosser and Zhang 2008).

Properly decellularized and unmodified ECM scaffolds that promote constructive remodeling and functional restoration at a site of injury have been showed to elicit a Th2

restricted T cell response *in vivo* (Allman, McPherson et al. 2001). Additionally, ECM scaffolds induce an early and sustained anti-inflammatory, M2 phenotype in the recruited monocytes and macrophages at the site of injury (Valentin, Badylak et al. 2006; Badylak, Valentin et al. 2008). Furthermore, removal of the macrophages via depletion of circulating monocytes inhibits the constructive remodeling response to ECM scaffolds and results in fibrous encapsulation *in vivo* (Valentin, Stewart-Akers et al. 2009). In each case with a poor remodeling outcome, the predominant phenotype of mononuclear phagocytes at the site of ECM implantation is the pro-inflammatory M1 phenotype (Crisan, Yap et al. 2008; Brown, Valentin et al. 2009).

Although the role of the immune system in ECM scaffold remodeling is not directly addressed in the present thesis, the importance of and the contribution of the immune system towards is revisited in the final discussion of the work presented in chapter 5.

1.3.2 Mechanical Stimulation and Mechanotransduction at the Site of ECM Implantation

Previous studies have also shown that the microenvironment in which the ECM scaffold is placed can influence the overall remodeling outcome. For example, an ECM scaffold derived from the porcine urinary bladder can remodel into abdominal wall (Brown, Valentin et al. 2009), bladder (Boruch, Nieponice et al. 2010), trachea (Gilbert, Gilbert et al. 2008), or myocardium (Kochupura, Azeloglu et al. 2005) depending on the conditions in which it is placed *in vivo*. One component of the microenvironment that is thought to mediate this remodeling response to scaffolds is the spatiotemporal pattern of mechanical forces sensed by the ECM scaffold and cells at the site of injury. Previous studies shown that mechanical forces can be transduced through the scaffold to influence the phenotype and response of local cells in contact with the scaffold *in vitro* (Androjna, Spragg et al. 2007; Gilbert, Stewart-Akers et al. 2007). Other studies

have then confirmed that physiologic mechanical load is essential for site appropriate constructive remodeling of ECM scaffolds *in vivo* (Boruch, Nieponice et al. 2010). While local mechanical forces within the microenvironment are not further investigated in the present thesis, the role of the microenvironment in ECM scaffold remodeling is revisited in the final discussions of this thesis in chapter 5.

1.3.3 Rapid Degradation of the ECM Scaffold and Release of Bioactive Peptides

One of the hallmarks of unmodified ECM scaffolds is their rapid degradation *in vivo* within 60-90 days post-implantation (Record, Hillegonds et al. 2001; Gilbert, Stewart-Akers et al. 2007). As discussed in the time course of remodeling, the constructive remodeling response only occurs _after_ the scaffold is predominantly degraded. Inhibition of the degradation of the scaffold through any of a number of means including chemical cross-linking (Valentin, Badylak et al. 2006; Valentin, Stewart-Akers et al. 2009), or host depletion of phagocytic cells partially responsible for degrading the scaffold (Valentin, Stewart-Akers et al. 2009), results in a poor remodeling outcome *in vivo*. Based on these observations in the time course of remodeling, rapid degradation of ECM scaffolds is an important prerequisite for constructive remodeling at the site of injury. In fact, it may be the initiating event for all subsequent events at the site of injury that deviate from the normal wound healing response.

One potential mechanism by which rapid degradation of ECM scaffolds results in constructive remodeling may be the release of bioactive peptides from degradation of the ECM scaffold. In addition to the release of sequestered growth factors and cytokines in the ECM, local proteolysis of the ECM scaffolds results in enzymatic digestion of the structural proteins (i.e. collagen, fibronectin, laminin) that comprise a majority of the ECM scaffold (Badylak 2002).

The resulting degradation products of ECM have been shown to possess novel bioactive properties that are not present in the parent ECM structural proteins. These peptides are called "matricryptic peptides" (Davis, Bayless et al. 2000; Autelitano, Rajic et al. 2006; Ng and Ilag 2006; Pimenta and Lebrun 2007; Mukai, Hokari et al. 2008; Mukai, Seki et al. 2009; Davis 2010). Antimicrobial activity has been attributed to such peptides in the form of defensins (Ganz 2003), cecropins (Moore, Devine et al. 1994; Moore, Beazley et al. 1996), and magainins (Berkowitz, Bevins et al. 1990). Other matricryptic peptides have been shown to be able to regulate angiogenesis, with separate peptides possessing angiogenic and anti-angiogenic activity (Davis, Bayless et al. 2000; Li, Li et al. 2004). Other cryptic peptides have also been identified that modulate the local and systemic immune response by modulating phagocytic activity, gene expression, and chemotaxis of various immune cells (Adair-Kirk and Senior 2008). Within the context of tissue engineering, cryptic peptides have been identified with mitogenic and chemotactic activity for other cell types such as endothelial, Schwann, and smooth muscle cells (Davis, Bayless et al. 2000; Li, Li et al. 2004; Agrawal, Brown et al. 2009). The sustained generation and release of these matricryptic peptides may be a potential explanation for how ECM scaffolds promote constructive remodeling after their degradation. The work presented in the present thesis focuses on addressing the contribution of matryptic peptides, subsequently referred to as "ECM degradation products," upon *in vivo* constructive remodeling.

1.3.4 Site Directed Recruitment of Progenitor Cells

Although previous studies have focused on the immune contribution to the cell infiltrate at the site of injury (Valentin, Badylak et al. 2006; Badylak, Valentin et al. 2008), circulating bone-marrow derived cells are known to partially comprise the dense mononuclear infiltrate that

populates the site of ECM implantation (Valentin, Badylak et al. 2006; Badylak, Valentin et al. 2008). Previous studies have further shown that bone marrow derived progenitor cells persist at the site of injury and eventually contribute to functionally remodeled tissue (Badylak, Park et al. 2001; Zantop, Gilbert et al. 2006). Although the mechanisms underlyling the site directed accumulation of progenitor-like cells at the site of injury by ECM scaffolds are not well understood, it has been previously been hypothesized that ECM scaffold degradation products may play a potential role in progenitor cell recruitment. In addition to possessing chemotactic properties for site-specific differentiated cells (Li, Li et al. 2004; Agrawal, Brown et al. 2009), recent evidence suggests that peptides generated from *ex vivo* degradation of ECM scaffolds may have a net chemotactic effect upon multiple progenitor cell types *in vitro*. These cells include mouse ear blastemal cells (Reing, Zhang et al. 2009) (derived from the regenerating ear of an MRL/MpJ mouse (Clark, Clark et al. 1998)), fetal keratinocyte progenitor cells (Brennan, Tang et al. 2008), adult keratinocyte progenitor cells (Brennan, Tang et al. 2008), and human mesenchymal perivascular stem cells (Crisan, Yap et al. 2008; Tottey, Corselli et al. 2011). However, the *in vivo* chemotactic properties of these same degradation products have not been investigated.

Thus, as presented in future chapters of the present thesis, a primary goal of the present work will be to establish an *in vivo* link between two major mechanisms by ECM scaffolds remodel, namely the generation of bioactive ECM degradation products and the site directed recruitment of progenitor cells. If indeed degradation products of ECM scaffolds can promote site directed recruitment of progenitor cells *in vitro*, this approach may be a viable therapy for altering the default wound healing response towards regeneration in more complex models of injury that currently cannot be engineered using conventional approaches. Because other species

capable of spontaneous regeneration of complex tissues do so via the site directed recruitment of multipotent stem cells to a site of injury (Kumar, Godwin et al. 2007; Kragl, Knapp et al. 2009; Monaghan, Epp et al. 2009), a similar type of "endogenous stem cell therapy" in adult mammals might be a valuable and new tissue engineering approach for more complex tissue engineering in adult mammals (Lee, Cook et al. ; Kim, Xin et al. 2010).

1.4   CLINICAL SIGNIFICANCE OF LIMB/DIGIT REGROWTH

Limb and digit amputation is a life altering procedure that is completed secondary to intractable malignancy (Steinau, Daigeler et al. 2010), unremitting complications of chronic disease (Dec 2006), or acute tramautic injury such as motor vehicle accidents (Barmparas, Inaba et al. 2010) or battle related injuries. Amputations can occur to patients of all ages. In addition to potentially multiple and irreversible functional deficiencies, amputation can also leave a patient with multiple psychological and psychosomatic aberrations such as phantom limb syndrome. Such aberrations and deficiencies constitute a decrease in overall quality of life.

Specifically with respect to acute traumatic injuries, although although medical therapies have improved survival rates following, an unfortunate side effect of these advances has been a concomitant increase in patients and soldiers living with life-altering limb amputations (Baer, Dubick et al. 2009; Ritenour, Blackbourne et al. 2010). Within the US Army from 2002-2010, a cumulative total of 791 soldiers have undergone distal extremities amputation following traumatic injuries, corresponding to 3.38% of U.S. military patients admitted to a Role III facility (e.g. combat support hospital). Stratified by anatomic location of amputation, there have been 522 finger amputees, 85 toe amputees, and 184 patients who have undergone multiple

amputations of fingers and/or toes (unpublished data from David G. Baer, U.S. Military). Additionally, over 950 soldiers have undergone more proximal limb amputations following combat-related wounds (Stinner, Burns et al. 2010).

There are currently no effective treatments for restoring function to composite tissues such as limbs and digits following extensive injury. Digit replantation has been attempted in the past with mixed reported success rates ranging from 59% to 91% success rates following replantation. In a meta analysis of published success rates of digit replantation, factors that correlated with a poor outcome included type of injury (crushing or avulsion injury as opposed to clean cut), location of injury (proximal as opposed to more distal), involved digits (thumbs correlate with a worse outcome than pinky finger), involvement of ischemia-prone tissues such as muscle, and comorbidities such as smoking (Dec 2006). Notably, a zero percent success rate was reported in cases where the patients were diabetic. Even with success of replantation, though, motor function of the replanted digit remains suboptimal, possibly secondary to post-amputation remodeling of central and peripheral neural circuitry (Schieber, Lang et al. 2009).

1.5 EPIMORPHIC REGENERATION AS A SOLUTION TO POOR COMPOSITE TISSUE REGENERATION IN ADULT MAMMALS

The canonical approach to engineering of new tissue following injury or tissue loss consists of utilizing a combination of cells, bioactive factors, and scaffold within a bioreactor system that mimics the nutritional and biomechanical environment of the native tissue (Langer and Vacanti 1993; Nichol and Khademhosseini 2009). Following sufficient maturation, this tissue engineered construct is then implanted *in vivo* at a site of injury to replace the missing tissue.

However, the use of bioactive factors, stem cell therapy, or scaffold therapy alone has been insufficient for certain applications, specifically tissue engineering of more complex tissues such as digits. For example, stem cell therapy and/or addition of exogenous bioactive factors have shown some clinical promise in limiting the extent of injury or progression of disease in human clinical trials (Brown, Hong et al. 1995; Harada, Friedman et al. 1996; Horwitz, Gordon et al. 2002; Okamoto, Yajima et al. 2002; Chen, Fang et al. 2004; Bang, Lee et al. 2005; Jeong, Sandhu et al. 2005; Janssens, Dubois et al. 2006; Janssens, Theunissen et al. 2006; Moist, Muirhead et al. 2006; Tyndall and Furst 2007; Zadrazil, Horak et al. 2009), the use of such therapies for complex tissue regeneration has been limited both by efficacy and regulatory concerns (Bongso, Fong et al. 2008). Scaffolds alone have been used very successfully in tissue engineering applications for restoration of tissue. However, most of the successful applications utilizing only scaffolds are limited to soft tissues with a repeatable microstructure, innate ability to respond favorably to tissue injury, and limited three dimensionality (Kropp, Eppley et al. 1995; Badylak, Meurling et al. 2000; Robinson, Li et al. 2005; Lopes, Cabrita et al. 2006). Thus, these methods alone have not been viable approaches for tissue engineering of more complex tissues.

The problem of complex and composite tissue regeneration in adult mammals is further complicated by the limited regenerative capacity of adult mammals. Besides select tissues including the bone marrow (Chan and Yoder 2004), intestinal lining (Oates and West 2006), superficial layers of the skin (Epstein and Maibach 1965), nailbeds (Lee, Lau et al. 1995), liver (Michalopoulos 2007), and deer antler (Li, Yang et al. 2009), the default response to injury in most other tissues involves processes of coagulation, inflammation, migration, and scar tissue deposition (Falanga 2005). However, scarless regeneration in the form of epimorphic

14

regeneration occurs following tissue injury in early human fetal development (Metcalfe and Ferguson 2005) and in urodeles (e.g. the newt and salamander) of all ages and has been divided into two relatively broad categories. The first category of epimorphic regeneration involves the formation of a blastema. A blastema is a pre-programmed accumulation of multipotential cells that spontaneously proliferate, migrate, differentiate, and spatially organize in three dimensions to form a perfect phenocopy of the missing or injured body part (Morgan 1901). The second category of epimorphic regeneration does not involve a blastema and instead utilizes mechanisms that include: (a) transdifferentiation of cells to replace the missing tissue; (b) limited dedifferentiation and proliferation of cells; and/or (c) proliferation and differentiation of stem and progenitor cells in the injured tissue (Sanchez Alvarado 2000). The specific origins of the cells, the genetic profile, and the upstream molecular signals that participate in the two categories of epimorphic regeneration are only partially known, but the microenviromental cues and cell populations required to initiate and sustain the process are gradually and systemically being identified (Brockes and Kumar 2005; Kumar, Godwin et al. 2007; Monaghan, Epp et al. 2009).

The equivalent of a blastema does not occur in adult mammals, but non-blastemal regeneration does occur in certain organs of adult mammals such as the liver (Ito, Hayashi et al. 1991). In the context of regenerative medicine strategies for adult mammals, including humans, non-blastemal approaches may be more plausible for the functional restoration of complex tissues and organs. Thus, recruitment of endogenous progenitor cells to a site of injury may alter the overall wound healing response from scar tissue deposition towards regeneration. While likely insufficient on its own, directed recruitment of endogenous progenitor cells would conceptually represent an essential component of a non-blastemal based approach to epimorphic regeneration of tissues and organs.

1.6   CENTRAL HYPOTHESIS

The work presented in the following chapters broadly aims to investigate whether degradation products of ECM scaffolds can promote site-directed recruitment of progenitor cells to a site of injury *in vivo*. A secondary goal of the present work is to utilize this property of ECM degradation products as a potential therapeutic approach towards tissue engineering of more complex, composite tissues such as digits.

Thus, the central hypothesis of the present body of work is that degradation products of bioscaffolds composed of extracellular matrix recruit progenitor cells to a site of injury in an adult murine model of digit amputation.

1.7   SPECIFIC AIMS

Specific Aim 1: To determine the effect of treatment with degradation products of ECM scaffolds upon recruitment of progenitor cells to a site of amputation in a non-regenerating adult mammalian model of digit amputation.

Corollary Hypothesis for Aim 1: Degradation products of ECM scaffolds promote the local accumulation of progenitor cells in a non-regenerating murine adult mammalian model of digit amputation.

Specific Aim 2: To determine the chemotactic potential of isolated fractions of degradation products of ECM scaffolds *in vivo* in an adult mammalian model of digit amputation.

Corollary Hypothesis for Aim 2: A single, purified chemotactic peptide promotes progenitor cell chemotaxis *in vitro* and the local accumulation of progenitor cells at a site of amputation in a murine model of digit amputation.

Specific Aim 3: To determine the effect of treatment with ECM degradation products upon tissue reconstruction in an adult mammalian model of digit amputation.

Corollary Hypothesis for Aim 3: A purified chemotactic peptide accelerates osteogenesis of adult mesenchymal stem cells *in vitro* and promotes bone formation *in vivo* in a murine model of digit amputation.

2.0   RECRUITMENT OF PROGENITOR CELLS BY ECM DEGRADATION PRODUCTS IN VIVO

2.1   INTRODUCTION

Sections of this chapter have been modified and adapted from (Agrawal, Johnson et al. 2010).

Biologic scaffolds composed of extracellular matrix (ECM) have been used to promote site-specific, functional remodeling of tissue in both preclinical animal models (Badylak, Lantz et al. 1989; Lantz, Badylak et al. 1990; Cobb, Badylak et al. 1996; Hodde, Badylak et al. 1997; Badylak, Meurling et al. 2000; Caione, Capozza et al. 2006; Zalavras, Gardocki et al. 2006; Ott, Matthiesen et al. 2008; Ott, Clippinger et al. 2010; Uygun, Soto-Gutierrez et al. 2010) and human clinical applications (Metcalf, Savoie et al. 2002; Witteman, Foxwell et al. 2009; Derwin, Badylak et al. 2010; Mase, Hsu et al. 2010). Although the mechanisms of remodeling are not completely known, proteolytic degradation of the ECM scaffold and concomitant accumulation of progenitor cells at a site of injury are two important mechanisms by which ECM scaffolds promote constructive tissue remodeling of the injury site (Badylak, Park et al. 2001; Zantop, Gilbert et al. 2006; Valentin, Stewart-Akers et al. 2009). Circulating bone-marrow derived cells are known to partially comprise the dense mononuclear infiltrate that populates the site of ECM implantation (Valentin, Badylak et al. 2006; Badylak, Valentin et al. 2008), and bone marrow derived progenitor cells persist at the site of injury and eventually contribute to functionally

18

remodeled tissue (Badylak, Park et al. 2001; Zantop, Gilbert et al. 2006). The degradation of the ECM scaffolds results in the release of small cryptic peptides with novel bioactivity not present in the parent ECM proteins (Davis, Bayless et al. 2000; Davis 2010). These cryptic fragments have been shown to possess antimicrobial, immunomodulatory, angiogenic and anti-angiogenic, mitogenic, and chemotactic properties, among others (Berkowitz, Bevins et al. 1990; Moore, Devine et al. 1994; Moore, Beazley et al. 1996; Davis, Bayless et al. 2000; Ganz 2003; Li, Li et al. 2004; Adair-Kirk and Senior 2008; Agrawal, Brown et al. 2009). Although full characterization of these bioactive peptides has not been completed to date, *ex vivo* enzymatic, chemical, and physical methods (Li, Li et al. 2004; Brennan, Reing et al. 2006; Reing, Zhang et al. 2009) have generated a heterogeneous population of ECM peptides (Brennan, Tang et al. 2008; Freytes, Martin et al. 2008) with both chemotactic and mitogenic properties for a variety of stem and progenitor cells (Zantop, Gilbert et al. 2006; Brennan, Tang et al. 2008; Crisan, Yap et al. 2008; Marra, Defail et al. 2008).

Thus, the work described in the present chapter aims to expand upon previous *in vitro* work and characterize the *in vivo* chemotactic potential of ECM degradation products in a non-regenerating model of mid-second-phalanx amputation in adult mice. In the absence of any intervention, wound healing is completed by 14 days post-amputation in this model (Schotte and Smith 1959; Schotte and Smith 1961). The work in the present chapter shows that treatment with ECM degradation products results in a deviation from the default wound healing response from scar tissue deposition and instead promotes site directed accumulation of progenitor cells at the site of amputation.

2.2   METHODS

2.2.1   Preparation of ECM degradation products:

Porcine urinary bladders were harvested from euthanized market weight (240-260 lb) pigs. The basement membrane and underlying lamina propria were isolated and harvested as previously described (Freytes, Badylak et al. 2004). Following peracetic acid, ethanol, deionized H_2O, and phosphate buffered saline treatment (Reing, Zhang et al. 2009), lyophilized sheets were comminuted and digested in pepsin and 0.01 N HCl for 48 hours prior to neutralization and dilution in PBS to yield a 5 mg/ml solution. The soluble protein concentration of *ex vivo* generated ECM degradation products was found to be 1.68 ± 0.17 μg/ml, and SDS-PAGE of these products in previous studies demonstrated a heterogeneous population of peptides (Brennan, Tang et al. 2008; Freytes, Martin et al. 2008).

2.2.2   Confirmation of Chemoactivity of ECM Degradation Products:

To confirm the chemotactic activity associated with ECM degradation products (Reing, Zhang et al. 2009), primary human perivascular stem cells (Crisan, Yap et al. 2008) were assayed for a chemotactic response in a Boyden chamber. Human perivasular stem cells were a gift from Dr. Bruno Peault, and these cells were isolated and prepared as previously described (Crisan, Yap et al. 2008). Perivascular stem cells were starved in high glucose Dulbecco's Modified Eagle Medium (DMEM) supplemented with 0.5% heat inactivated fetal bovine serum (FBS) for 16-18 hours at 37 ^{0}C and 5% CO_2 in a humidified incubator. After starvation, cells were resuspended in DMEM at a concentration of 6×10^5 cells/ml for 1 hour. Polycarbonate PFB filters (Neuro Probe,

Gaithersburg, MD) with 8 μm pores were coated with 0.05 m g/ml Collagen Type I (BD Biosciences, San Jose, CA). ECM degradation products were placed in the top and bottom chambers of Neuro Probe 48-well chemotaxis chambers (Neuro Proe, Gaithersburg, MD) at varying concentrations with $3x10^4$ cells in the top chamber, and incubated at 37 ^{0}C in 95% O_2 / 5% CO_2 for 3 hours. Migrated cells were fixed in methanol, stained with 500 nM DAPI (Sigma, D9564), imaged on a Nikon E600 microscope, and counted using ImageJ.

2.2.3   Flow Cytometry and Immunolabeling of Perivascular Stem Cells

Cells were detached from culture flasks using pre-warmed 15 mM sodium citrate for 5 minutes, centrifuged at 1500rpm for 5 minutes, resuspended, and filtered through a 70 μm filter prior to incubation with antibodies, all at a dilution of 1 μl per $1x10^7$ cells/ml, for 1 hr prior to extensive washing and resuspension with PBS for flow cytometric analysis. Antibodies included mouse monoclonal FITC-CD144 (clone 55-7H1, #560874), APC-CD34 (clone 581, #560940) , PE-CD146, and V450-CD45 (clone HI30, #560368) (BD Biosciences, San Diego, CA). For immunostaining, $1x10^5$ cells were cytospun onto slides and fixed for 30 s econds in ice cold methanol. Following permeablization in 0.1% TritonX and 0.1% Tween20 in PBS for 15 minutes, cells were blocked in 1% BSA diluted with 0.01% TritonX and 0.01% Tween20 in PBS for 1 hr. Cells were then stained for 1 hr with CD146 (clone P1H12) (Abcam, Cambridge, MA, ab24577), smooth muscle actin (clone 1A4) (Dako, Carpinteria, CA, M0851) or NG2 (Millipore, Billercia, MA, AB5320), each diluted 1:200 in blocking solution. Following extensive washing in PBS, cells were then incubated with donkey anti-rabbit IgG-Alexa Fluor 546 (Invitrogen, A10042) and donkey anti-mouse IgG-Alexa Fluor 488 (Invitrogen, A21202) diluted 1:400 in blocking buffer for 1 hour.

2.2.4 Animal Model of Digit Amputation:

All methods were approved by the Institutional Animal Care and Use Committee at the University of Pittsburgh and performed in compliance with NIH Guidelines for the Care and Use of Laboratory Animals. Adult female 6-8 week old C57/BL6 mice were obtained from Jackson Laboratories (Bar Harbor, ME). Following induction of surgical plane anesthesia with isofluorane (1-2%), each mouse was subjected to aseptic mid-second phalanx amputation of the third digit of the right hind foot (Figure 3). At 0, 24 and 96 hours post surgery 20 µg of chemotactic ECM degradation products were injected at the base of the amputated digit in group 1 animals via 30 gauge needle. Animals in group 2 were left untreated. Animals were sacrificed via cervical dislocation under deep isoflurane anesthesia (5-6%) at various time points following surgery. Digits were either fixed and sectioned for histologic analysis and immunolabeling, or harvested for cell isolation for subsequent flow cytometric analysis and cytospin.
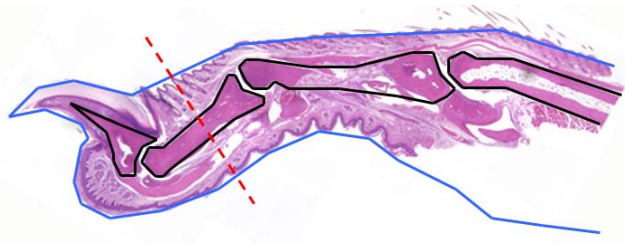
Figure 3. A schematic diagram overlaying an H&E image of an adult mouse digit. The red, dotted line depicts the site of amputation. Figure modified with permission from Scott A. Johnson, MS.

2.2.5 Fluorescein Labeling of ECM Degradation Products in a Digit Amputation Model

Degradation products of ECM were labeled with the fluorescein (FITC) fluorophore as per manufacturer's instructions (Thermo PierceNet, Pittsburgh, PA, #53027). Following mid-second

phalanx amputation under isoflurane anesthesia, FITC labeled ECM degradation products were injected at the base of the amputated digit. Following injection, animals were immediately sacrificed, and the entire foot was isolated and fixed in 4% paraformaldehyde prior to serial dehydration in 25%, 50%, 75%, 95%, and 100% acetone. Following dehydration, fixed digits were then incubated in Dent's fixative (1:4 DMSO:acetone) for 2 hours. Then, the digits were permeablized and bleached overnight in Dent's bleach (1:4:1 DMSO:acetone:H_2O_2). Digits were then equilibrated to a clearing solution consisting of 1:2 benzyl alcohol (Sigma, 402834) to benzyl benzoate (Sigma, B6630) (BABB) by serial 1 hour incubations in 1:3, 1:1, and 3:1 solutions of BABB:Dent's fixative. Afterwards, digits were then kept in 100% BABB until they were visibly optically cleared. Optically cleared digits were then imaged using a Nikon E600 epifluorescent microscope at 100x magnification, and images were taken with a Nuance camera. Images were deconvolved with a known FITC and tissue autofluorescence spectra and false colored as green and red, respectively.

2.2.6   Tissue Immunolabeling:

Harvested mouse digits were fixed in 10% neutral buffered formalin and decalcified for two weeks in 5% formic acid prior to being paraffin embedded and sectioned and stained for either Sox2, Rex1, or Sca1.

Sox2 staining utilized a primary antibody from Abcam ab15830 (Abcam, Cambridge, MA) or primary antibody from Millipore AB5603 (Millipore, Billerca, CA). Antigen retrieval was in 10 mM Citrate Buffer (Citrate: C1285, Spectrum, New Brunswick, NJ) for 20 minutes at 96°C. Following antigen retrieval, slides were placed in TBS + 0.05% Tween-20 for five minutes, rinsed in PBS for five minutes twice, blocked for 1 hour in 1.5% BSA / PBS, and

incubated overnight with primary antibody diluted in 1.5% BSA / PBS (1:100). Slides were then rinsed in PBS, treated with 3% hydrogen peroxide solution in methanol for 30 minutes, rerinsed in PBS and incubated with HRP conjugated secondary antibody for 1 hour (Rabbit anti-rat IgG-HRP (Dako, Carpinteria, CA, #P0450), r insed again in P BS, and developed with 3, 3' diaminobenzidine (DAB) (Vector Labs, Burlingame, CA).

Sca-1 staining utilized the primary antibody ab25196 (Abcam, Cambridge, MA). Antigen retrieval was for 10 m inutes at $93^{o}C$ in R&D Systems Antigen Retrieval Reagent Universal (R&D Systems #CTS015, Minneapolis, MN) following manufacturer's protocol. R&D Systems HRP-DAB Cell and Tissue Staining Kit for goat primary IgG antibodies (R&D Systems #CTS008, Minneapolis, MN) was used for subsequent staining, following manufacturer's instructions with the following three changes: (1) slides were blocked in 1.5% BSA/PBS, (2) primary antibody was diluted 1:1000 in 1.5% BSA/PBS and (3) incubations with biotinylated secondary antibody and subsequent washes were deleted since ab25196 is biotin-conjugated.

Rex1 staining utilized antigen retrieval with Antigen Unmasking Solution (Vector Laboratories, Burlingame, CA) by boiling under pressure for 2 min. Slides were then incubated in 3% hydrogen peroxide in methanol for 15 min to quench endogenous peroxidase activity. This was followed by incubation with the anti-mouse Rex1 primary antibody (affinity-purified, polyclonal rabbit antibody, custom-generated and supplied by Alpha Diagnostic, San Antonio, TX (project name: ZFP42-17, peptide#13209)) diluted 1:20 in 1.5% goat serum for 1 hour at room temperature. HRP conjugated goat anti-rabbit secondary antibody (Catalog No. 87-9263, SuperPicture, Zymed, San Francisco, CA) was added to each tissue section and incubated at room temperature for 30 min. Staining of the antigen (brown stain) was accomplished by incubation of the tissue sections with DAB chromogen substrate (SuperPicture, Zymed, San

Francisco, CA) for 8-10 min at 22°C. The negative control sections were treated identically to the adjacent sections except that 1.5% goat serum was used in place of primary Rex1 antibody.

After staining with DAB, all slides were counter-stained with Harris' hematoxylin, dehydrated, coverslipped with non-aqueous mounting medium, and imaged on a Nikon E600 microscope, Olympus Provis Microscope, or Olympus Fluoview 1000 Confocal Microscope. Images were taken at 40X magnification and 200X magnification. For quantification of the number of cells positive for markers, four images were taken in each sample: distal to the amputated edge of the second phalanx bone, proximal to the tip of the digit, and lateral to the cut edge of the second phalanx bone on either side. The number of positive cells in each image was counted by three independent investigators who were blinded to the treatment group. The mean number of positive cells was compared between various groups by a two-sided, unpaired student's t-test with unequal variance. Significance was determined at p = 0.05 level (α=0.05, β=0.2).

2.2.7 Cell Isolation

Following digit amputation and treatment, digits were harvested on day 14 post-amputation and placed into cold culture medium consisting of DMEM, 10% fetal bovine serum (Hyclone, Pittsburgh, PA), 100 U/ml penicillin, and 100 μg/ml streptomycin (Invitrogen, Carslbad, CA). Using a microdissection microscope under aseptic conditions, the epidermis and dermis were removed and the tissue distal to the amputated second phalanx bone was harvested into serum free DMEM containing 0.2% Collagenase Type II (Gibco Invitrogen, 17101-015) for 30 minutes at 37 ^{0}C. Cells were then centrifuged and reconstituted into warm culture medium, filtered

through a 70 μm filter, and counted on a hemocytometer prior to differentiation assays, cytopsin, or further immunolabeling for flow cytometric analysis.
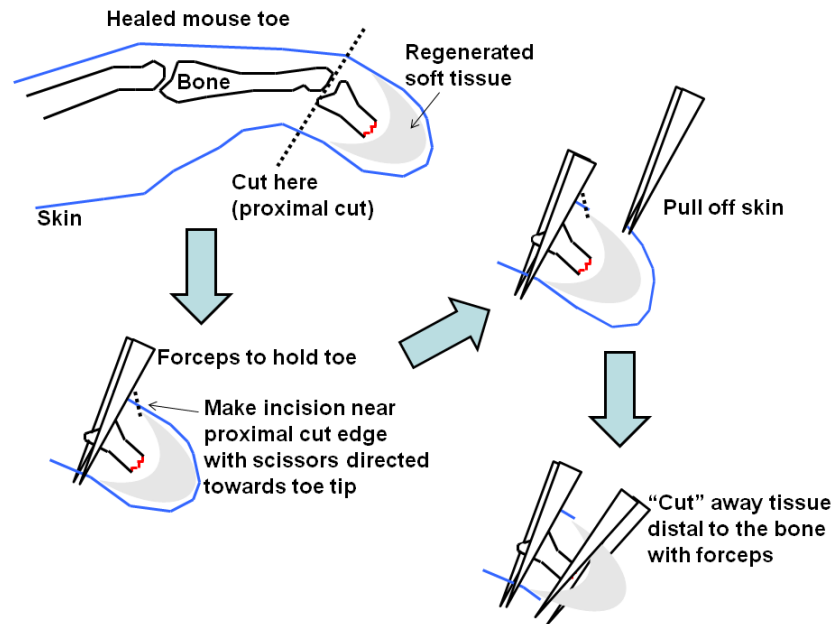
Figure 4. Schematic diagram showing the microdissection procedure by which cells are removed from amputated digits. Figure reproduced with permission from Scott A. Johnson, MS.

2.2.8 Differentiation Assays:

Mesodermal Differentiation: For adipogenic differentiation, cells were cultured in adipogenic differentiation medium (HyClone, Logan, UT, SH30886.02) for 14 days. Cells were then fixed in 10% neutral buffered formalin (NBF) and incubated in 0.5% Oil Red O (Alfa Aeasar, Ward Hill, MA) for 5 m inutes, extensively washed, and imaged for the presence of lipid vacuoles. For osteogenic differentiation, cells were cultured in osteogenic differentiation medium (HyClone, SH30881.02) for 21 da ys. After fixation in NBF, cells were incubated in 2% Alizarin Red solution to investigate for the presence of calcium.

26

Neuroectodermal Differentiation: Cells were cultured in DMEM supplemented with 10% FBS and 20 ng/ml bFGF (Sigma, St. Louis, MO, F0291) for 24 hours. Culture medium was then replaced with Neurobasal-A medium supplemented with 20 ng/ml bFGF, 20 ng/ml EGF (Sigma, E9644), and 2 μM all-trans retinoic acid (Sigma, R2625) for 7 days. After 7 days of culture, cells were fixed in 4% paraformaldehyde and prepared for staining. Cells were assessed for the presence of neuron and glial cell specific proteins β-tubulin III, NeuN, and glial fibrillary acidic protein (GFAP). The primary antibodies used were β-tubulin III ab7751 (Abcam), glial fibrillary acidic protein #Z0334 (DakoUSA), and NeuN #MAB377 (Millipore, Billerica, MA). Following fixation, slides were then washed, rehydrated in Tris Buffered Saline with 0.05% Tween20 (TBST), and incubated for 15 minutes in permeablization buffer (0.1% Triton X in TBST) at room temperature. Slides were then incubated in blocking solution (2% w/v bovine serum albumin (Sigma, A2153) in TBST) for one hour at room temperature, followed by incubation in primary antibody for one hour. All antibodies were used at a concentration of 1:100. After extensive washing, slides were then incubated in fluorophore conjugated secondary antibodies for 1 hour at room temperature. Secondary antibodies included Alexa Fluor 488 conjugated anti-rabbit IgG (Invitrogen, A-11008) and Alexa Flour 546 conjugated anti-mouse IgG (Invitrogen, A-11001), were used at a concentration of 1:250. Slides were counterstained with DAPI prior to mounting in fluorescent mounting medium (DakoUSA).

2.2.9   Flow Cytometric Analysis of Isolated Cells from Murine Digits

Following isolation of cells, cells were spun and resuspended in 200 μl in serum free DMEM prior to incubation with primary antibodies for 1 hour at 4 ^{0}C. Primary antibodies were FITC-Sca1 (clone D7) (Abcam, ab25031, Cambridge, MA), PE-CD133 (clone 13A4) (eBiosciences,

12-1331, San Diego, CA), e450NC-CD90.2 (clone 53-2.1) (eBiosciences, 48-0902), biotin-cKit (clone 2B8) (eBiosciences, 13-1171), and SAv-APC-Cy7 (BD Biosciences, 554063, San Diego, CA). Primary antibodies were incubated at a dilution of 1:200, and streptavidin conjugates were incubated at a dilution of 1:250 after washing away primary antibody. Cells were then fixed and labeled for APC-Sox2 by following the manufacturer's guidelines in the BD Mouse Pluripotent Stem Cell Transcription Factor Analysis Kit (BD Biosciences, 560585). Cells were then extensively washed, resuspended in PBS, and filtered through 70 μm filter prior to flow cytometric analysis.

2.2.10 Immunolabeling of Cytospins

Following cytospin of 1×10^4 isolated cells per slide, each slide was fixed in methanol for 30 seconds and stored at -20 ^{0}C. Prior to staining, slides were rehydrated in PBS for 5 minutes, and cells were permeablized in 0.1% TritonX/PBS for 15 minutes. Slides were blocked in 1% bovine serum albumin/PBS for 1 hour prior to overnight incubation with rabbit anti-Sox2 (1:100) and/or chicken anti-GFP (1:100) (Abcam, ab13970) diluted in blocking solution. Following two washes in PBS, slides were incubated for 1 hour with donkey anti-rabbit IgG-Alexa Fluor 488 (1:250) (Invitrogen, A21206), donkey anti-rabbit IgG-Alexa Fluor 546 (1:250) (Invitrogen, A10040) and/or donkey anti-chicken IgG-Alexa Fluor 488 (1:250) (Invitrogen, A11039) diluted in blocking solution. Following two washes in PBS, slides were counterstained with DRAQ5 (1:500) (Cell Signal, 4084, Danvers, MA) diluted in PBS for 30 seconds prior to three washes in PBS and coverslipping with fluorescent mounting medium (Dako, S3023). All images were taken at 200X magnification.

2.2.11 Nuclei to Collagen Ratio and Histomorphometric Analysis of Trichome Stained Sections

Following mid-second phalanx digit amputation and treatment with either ECM degradation products or corresponding control treatment, animals were euthanized at day 14 post-amputation and amputated digits were harvested, fixed in 10% neutral buffered formalin, decalcified, and sectioned for histologic analysis. Sections were stained with Masson's Trichrome stain to evaluate the ratio of cell to connective tissue at the site of amputation. Three images of the Trichrome stained sections were randomly taken at 32x magnification on an inverted microscope using AxioVision Rel 4.8 software. The relative cellularity and connective tissue in each image was calculated using a custom MATLAB script (version 7.11.0.584 R 2010b, MathWorks, Natick, MA). The MATLAB script is available upon request. Nuclei (purple) and connective tissue (blue) were isolated by hue histogram filtration and subsequent thresholding. Cellular density for each image was calculated as the ratio of the number of brown pixels to the number of blue pixels (Figure 5).
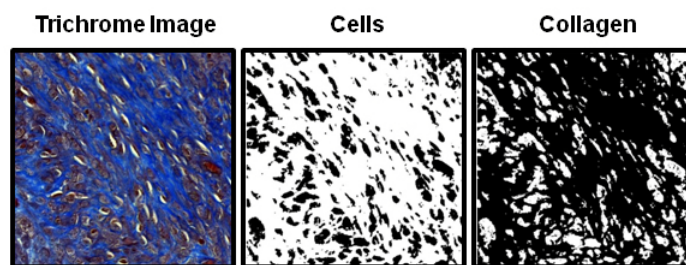
Figure 5. An example of the output of separation of nuclei from connective tissue in Trichrome stained samples.

Analysis of soft tissue area was found using ImageJ 1.44p (National Institutes of Health, USA). Blue soft tissue distal to the site of amputation was manually outlined and area of the complex object was analyzed (in pixels). Three width measurements (in pixels) of the second

29

phalanx were also taken at distal, mid, and proximal locations on the bone. Tissue growth was found as the area of blue soft tissue, as well as area of blue soft tissue normalized to the measured bone widths (Figure 6).
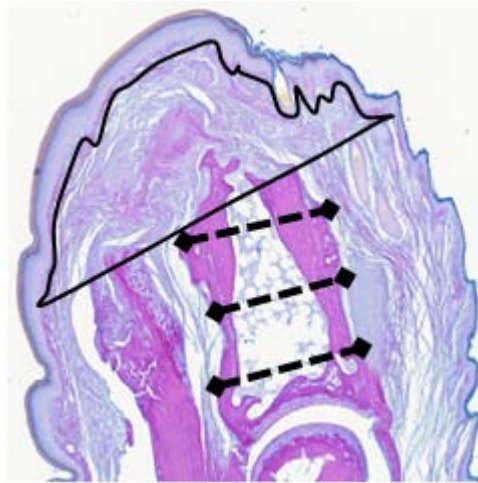
Figure 6. Schematic depiction of a Herovici stained digit section showing the measurement of area of soft tissue distal to the site of amputation as well as the measurement of bone width.

2.3   RESULTS

2.3.1   Confirmation of phenotype of human perivascular stem cells

The phenotype of human perivascular stem cells was confirmed *in vitro* by flow cytometric analysis for cell surface marker expression of perivascular stem cells. Perivascular stem cells expressed mesenchymal stem cell markers CD146, but they did not express endothelial cell marker CD144 (Figure 7). Additionally, as previously described (Crisan, Yap et al. 2008; Tottey, Corselli et al. 2011), perivascular stem cells did not express markers of blood lineage, CD34 and

CD45. Perivascular stem cells remained CD146+, CD144-, CD34-, CD45- through culture of passages 11-14 *in vitro* (Figure 7).
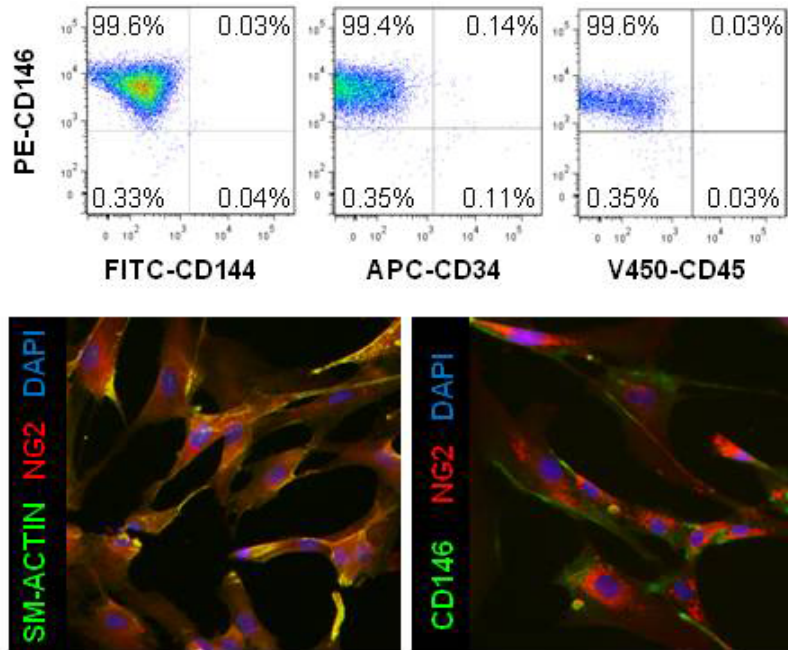
Figure 7. Perivascular stem cells express mesenchymal stem cell markers over multiple passages. In order to confirm that the perivascular stem cells did not alter phenotype after in vitro culture, cell surface expression of various markers was investigated by flow cytometry. Perivascular stem cells expressed mesenchymal stem cell marker CD146, sm-actin, and NG2, but they did not express endothelial cell marker CD144 or blood lineage markers CD34 and CD45.

2.3.2 Confirmation of chemotactic activity of ECM degradation products

Chemotactic activity of ECM degradation products was confirmed *in vitro* using human multipotent perivascular cells (Crisan, Yap et al. 2008) (Figure 8). Chemokinetic and haptotactic effects were ruled out by control wells which contained varying concentrations of the same ECM degradation products in both the top and bottom chambers. Results showed that cells selectively

migrated only when a concentration gradient was present (Figure 8), confirming the chemotactic

activity of the ECM degradation products.
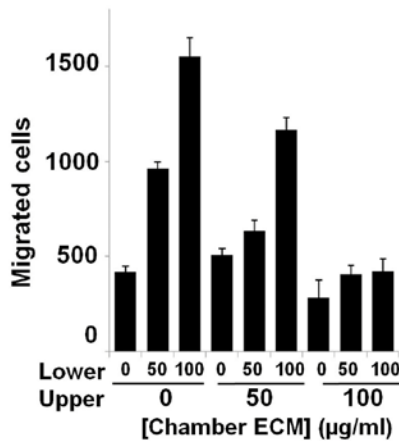
Figure 8. The *in vitro* migration of perivascular stem cells from the upper chamber of a Boyden assay to the lower chamber only in the presence of an ECM gradient confirms chemotactic and not chemokinetic activity of the degradation products. Error bars are S.D. between three wells, with a similar trend seen on three separate occasions.

2.3.3   Mid-second phalanx digit amputation does not regenerate

In order to confirm previous studies showing a completed wound healing response to murine mid-second phalanx digit amputation by day 14 post-amputation (Schotte and Smith 1959; Schotte and Smith 1961), a time course analysis of the default response to murine digit amputation was completed. At 4 da ys post-amputation, remnants of the immediate clotting response as well as local accumulation of inflammatory cells was observed. By day 7 pos t-amputation, the site of amputation was almost completely re-epithelialized, but the local immune response persisted. By day 14 post-amputation, the immune response had largely subsided. The site of amputation was replaced with a dense, connective tissue and thick, keratinized epithelium

with mature rete pegs, suggestive of a completed wound healing at the site of amputation. As far out as day 56 post-amputation, there was no observable growth of soft tissue or bone (Figure 9).
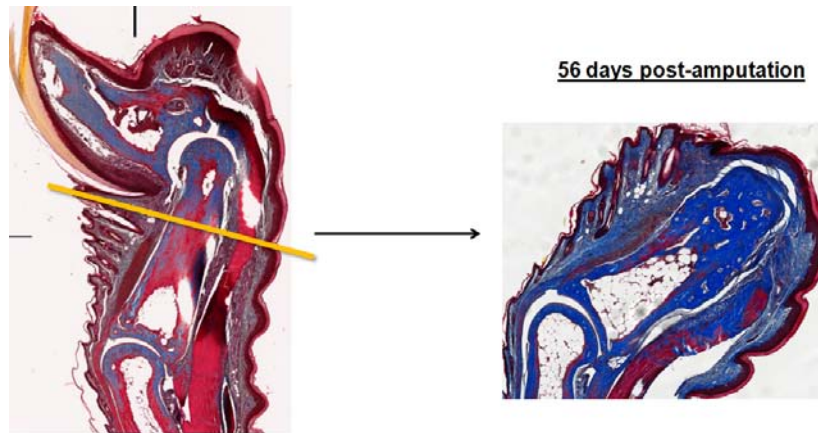
Figure 9. Trichome images of an unampuated digit (left) and amputated digit (right) show that amputation of the digit does not result in digit regrowth even as late as 56 days post-amputation, consistent with the overall goal of developing a non-regnerating model of composite tissue injury. The yellow line delineates the site of amputation.

2.3.4 Injection at the base of the footpad reaches the site of digit amputation

ECM degradation products were injected subcutaneously at the base of the amputated digit. Subcutaneous injection would theoretically serve as an endogenous repository of the ECM degradation products, and it would overcome the logistical limitations of local administration in this animal model. In order to confirm that regional administration of ECM treatments at the base of the footpad reach the site of amputation, India ink was injected at the base of the digit following mid-second phalanx amputation in mice (Figure 10). The injectate preferentially diffused along the amputated digit towards the site of amputation. Longitudinal sections of the amputated digit and transverse sections of the footpad confirmed anterograde and retrograde movement of injectate. A similar trend was observed on three separate occasions.
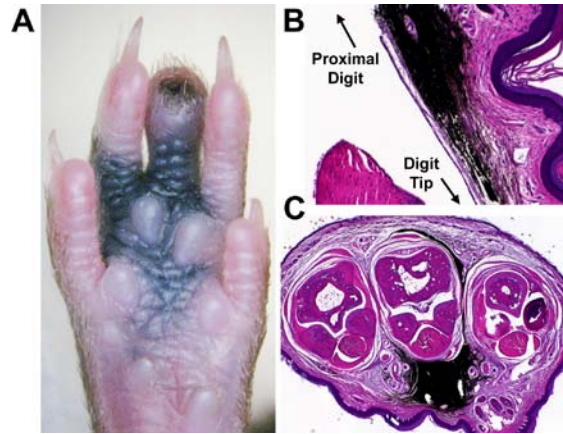
Figure 10. India ink injectate reaches the site of amputation *in vivo*. To investigate whether injections in the footpad reach the site of amputation, female adult C57/BL6 mice were subjected to mid-second phalanx amputation of the third digit bilaterally and injection of India ink at the base of the amputated digit. The injectate preferentially diffused along the amputated digit towards the site of amputation (A). Longitudinal sections of the amputated digit (B) and transverse sections of the footpad (C) confirmed anterograde and retrograde movement of injectate. A similar trend was observed on three separate occasions.

In order to directly assess whether ECM degradation products reach the site of amputation, a fluorescein (FITC) fluorophore was non-specifically covalently attached to the ECM degradation products. While the effect of FITC attachment upon the bioactivity of the ECM degradation products was not known, FITC attachment was still useful for assessing the regional distribution of ECM degradation products following administration at the base of the footpad. Immediately after injection, FITC labeled ECM degradation products were found at the site of injection and tracking along multiple digits, including the amputated digit (Figure 11).
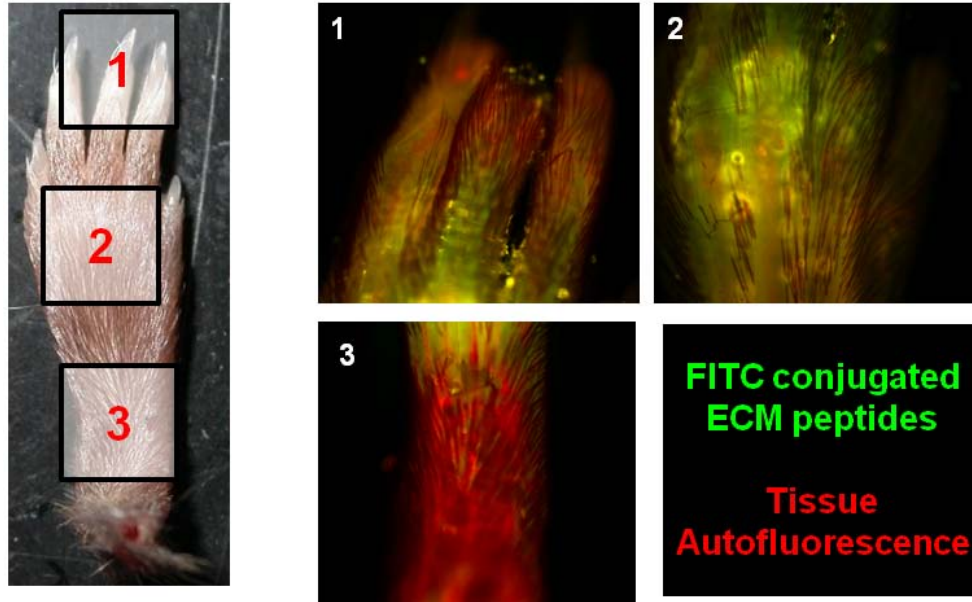
Figure 11. Following injection of FITC-conjugated ECM degradation products at base of the amputated digit, ECM degradation products were found diffusing along the amputated digit as well as adjacent unamputated digits.

2.3.5   ECM Degradation Products Promote the Accumulation of Mononuclear Cells *In Vivo*

Following mid-second phalanx amputation in C57/BL6 mice and treatment with ECM degradation products, phosphate buffered saline (PBS) carrier control, or no treatment (a clinical control), no macroscopic differences were observed between treatment groups prior to 14 days post-amputation.   However, Masson's trichrome stained sections of digits from ECM treated mice showed an accumulation of mononuclear cells distal to the site of amputation and a thin, keratinized epithelium (Figure 12). The number of accumulated cells varied between animals in the ECM-treated group, but the accumulation of cells was consistently limited to the soft tissue that began to develop at the cut end of the bone and extended to the digit tip. Mice from the PBS

and untreated control groups showed only scar tissue and an overlying thick keratinized epithelium at the digit amputation site (Figure 12).

Quantification of the relative ratio of cellularity to connective tissue on M asson's trichrome stained slides confirmed that treatment with ECM degradation products resulted in a more a cellular accumulation at the site of amputation (Figure 13). Quantification of the area over which the accumulated cells were found on the slide showed that there were no significant differences in the amount of soft tissue at the site of amputation between treatment groups, suggesting that the greater cellularity was due to an increased density of cells as opposed to more tissue growth (Figure 13).
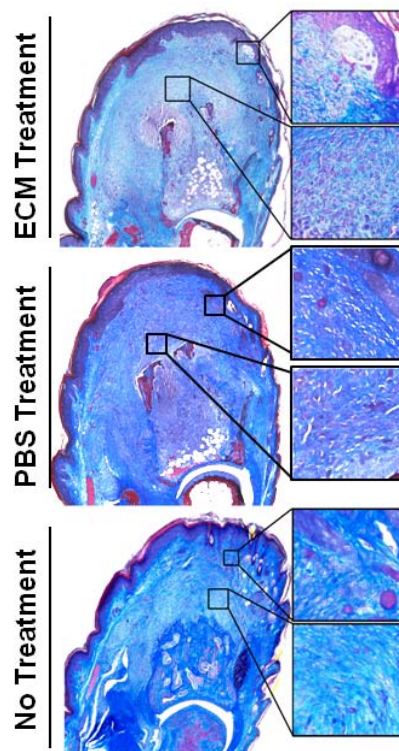
Figure 12. Masson's Trichrome stained slides of histologic sections of amputated digits treated with ECM degradation products, PBS control, and no treatment. Images were taken at 40x and 200x in the insets, respectively.
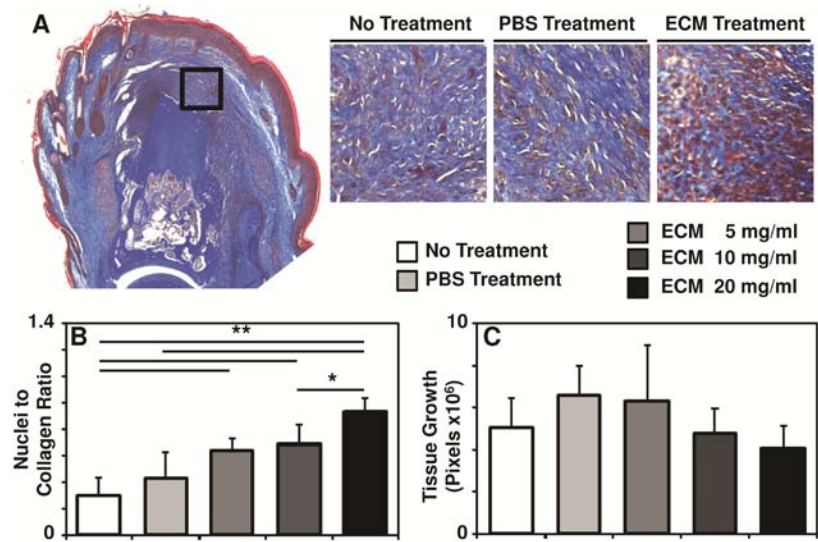
Figure 13. At day 14 post-amputation, treatment with ECM degradation products led to the accumulation of a heterogeneous population of cells at the site of amputation, whereas no treatment resulted in a less cellular accumulation concomitant with scar deposition at the site of amputation, consistent with a completed wound healing response to murine digit amputation (A) (Schotte and Smith 1959). Histologic appearance of a more densely cellular accumulation following ECM treatment was confirmed by quantification of the relative ratio of cellularity to connective tissue on Trichrome slides (B). Quantification of the area of growth distal to the site of amputation showed no difference between ECM treatment and no treatment, suggesting that the accumulated cells were more densely packed following ECM treatment (C). * $p < 0.05$. * $p < 0.01$. Errors bars represent Mean $\pm$ SEM (n=4).

2.3.6   Accumulated Mononuclear Cells Differentiate Along Neuroectodermal and Mesodermal Lineages

In order to identify the accumulation at the site of amputation, digits were harvested and the cellular accumulation was micro-dissected away from the digit. Cells were then plated and subjected to conditions of adipogenic, osteogenic, and neuroectodermal differentiation *in vitro*. Following culture in conditions of neuroectodermal differentiation, cells from ECM treated mice

showed heterogeneous morphologies including spindle-like cells with long processes that expressed β3-tubulin and NeuN, markers of differentiating neurons (Locatelli, Corti et al. 2003), and stellate shaped cells that expressed glial fibrillary acidic protein (GFAP), a marker of glial cells that is also expressed by some neural stem cells (Eng, Ghirnikar et al. 2000; Zhu and Dahlstrom 2007) (Figure 14). Cells from untreated mice cultured in conditions of neuroectodermal differentiation showed mainly spindle shaped cells consistent with a fibroblast or mesenchymal phenotype, and these cells did not give rise to cells expressing β3-tubulin, NeuN, or GFAP (Figure 14). However, when exposed to an adipogenic differentiation environment, cells from mice in both groups showed vacuoles that stained positive for Oil Red O, a s pecific stain for the presence of lipid accumulations (Figure 14). When subjected to conditions of osteogenic differentiation, cells from mice in both groups acquired a round morphology and stained positive for Alizarin Red, a stain that confirms the deposition of calcium by cells (Figure 14).
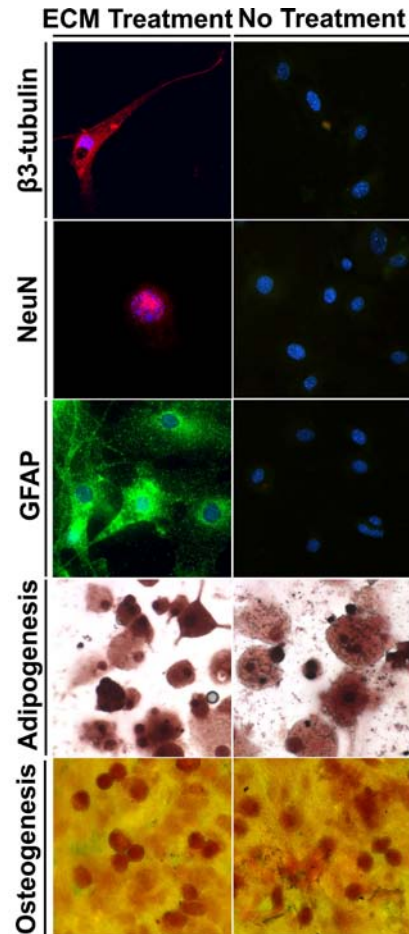
Figure 14. In vitro lineage differentiation potential of cell isolated distal to the site of amputation in digits of mice treated with ECM degradation products and untreated. Neuroectodermal differentiation was confirmed via expression for neuroectodermal markers (β-tubulin-III, NeuN, and GFAP). Adipogenic differentiation was confirmed via Oil Red O staining for the presence of lipid vacuoles. Osteogenic differentiation was confirmed via Alizarin Red staining for calcium deposition.

2.3.7 ECM Treatment Leads to a Heterogeneous Accumulation of Cells at Site of Amputation

Thus, at least a subset of the cells present at the site of amputation were capable of neuroectodermal and mesodermal differentiation *in vitro*, suggesting that a subset of the cells

present following digit amputation and treatment with ECM degradation products were progenitor cells. Flow cytometric analysis and immunolabeling studies were utilized to identify the phenotypes of the cells at the site of amputation, with a specific focus on determining the source of the progenitor cells at the site of amputation. Both local sources (bone marrow, periosteum, dermal hair follicles, perivascular) and circulating sources (hematopoietic) were considered.

Upon microdissection and dissociation of accumulated cells from amputated digits, a greater number of cells were present in ECM treateg digits as opposed to controls (Figure 15), consistent with the qualitative histologic appearance of Trichrome stained sections (Figure 13). Following plating and culture of the cells, cells acquired heterogeneous morphologies *in vitro* with separate subsets of cells showing roung, spindle, and triangular morphologies (Figure 15).
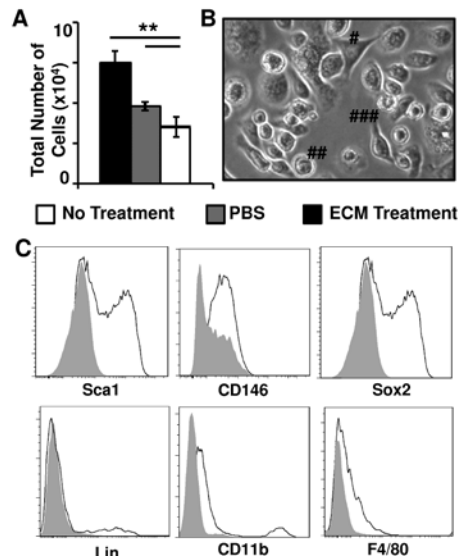
Figure 15. To further characterize the accumulation of cells at the site of amputation, the cellular accumulation was microdissected and dissociated for flow cytometric anaylsis . More cells were isolated from ECM treated digits as opposed to controls (A). Culture of the isolated cells over 2 weeks showed that the cells acquire heterogeneous morphologies including round, spindle, and triangular shaped morphologies, suggesting a heterogeneous population of cells (B). Flow cytometric analysis of the isolated cells confirmed a heterogeneous

accumulation of cells with subsets of cells that express stem cell markers Sca1, Sox2, and CD146 as well as subsets

that express differentiated markers CD11b, F4/80, and Lineage cocktail (C). * p < 0.05, ** p < 0.01. Errors

represent Mean $\pm$ SEM (n=4).

Flow cytometric analysis of the isolated cells confirmed a heterogeneous accumulation of cells with subsets of cells that express stem cell markers Sca1, Sox2, and CD146 as well as subsets that express differentiated markers CD11b, F4/80, and Lineage cocktail (Figure 15). To identify the phenotype of the accumulated cells, tissue sections were stained for markers of stem and progenitor cells, including Sox2 (Fauquier, Rizzoti et al. 2008), Rex1 (Mongan, Martin et al. 2006), and Sca1 (van de Rijn, Heimfeld et al. 1989). Mice treated with ECM degradation products accumulated a greater number of cells positive for stem cell markers Sox2 and Rex1 distal to the site of digit amputation compared to untreated mice and compared to normal, uninjured mice (Figure 16).
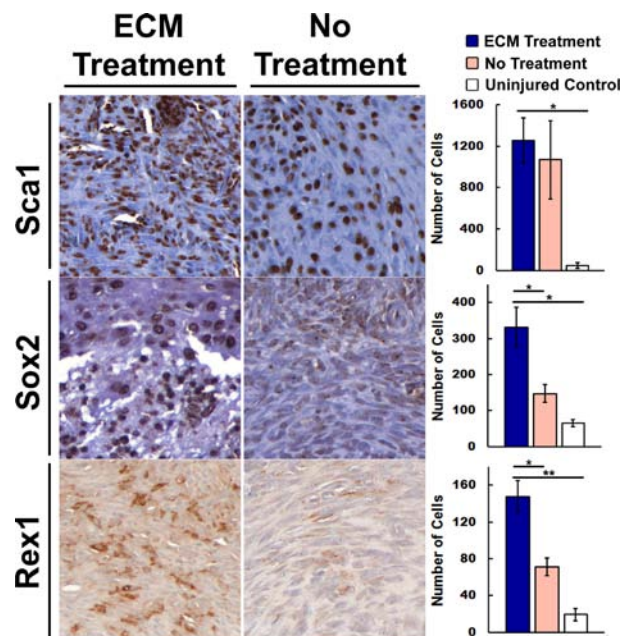
Figure 16. Histologic sections of cell accumulations distal to the site of amputation in mice 14 days post-amputation and injection of ECM degradation products or no treatment after staining for markers of multipotency.

41

All images were taken at a magnification of 400x. Cell counts are displayed in units of number of cells. * $p < 0.05$,
** $p < 0.005$ (between treatment and no treatment, or treatment and uninjured controls). Error bars represent Mean $\pm$
SEM (n=4).

2.3.8 ECM Treatment Results in Sox2+ Cell Accumulation at Site of Amputation

Sox2 is a transcription factor that plays an important role in the self-renewal of embryonic stem cells (Avilion, Nicolis et al. 2003) as well as adult progenitor cells including neural stem cells, dermal stem cells, neural crest derived stem cells, and osteogenic progenitors (Basu-Roy, Ambrosetti et al. ; Mansukhani, Ambrosetti et al. 2005; Biernaskie, Paris et al. 2009; Hutton and Pevny 2011). Thus, subsequent work focused on further characterizing the phenotype and source of the Sox2+ cells.

Following treatment with ECM degradation products, a greater number of Sox2+ cells were present at the site of amputation at days 10, 14 and 18 post-amputation as compared to PBS control (Figure 17). Expression of Sox2+ cells was confirmed by immunolabeling of cytospun slides (Figure 17) as well as flow cytometry (Figure 17). Flow cytometric analysis showed that the Sox2+ cells did not express dermal stem cell marker, CD133 (Biernaskie, Paris et al. 2009), or hematopoietic stem cell marker, c-kit (Spangrude, Heimfeld et al. 1988; Spangrude and Scollay 1990). Sox2+ cells did co-express markers Sca1 and CD90, known markers of bone marrow and periosteal derived mesenchymal stem cells (Zhang, Xie et al. 2005; De Bari, Dell'Accio et al. 2006) (Figure 17).
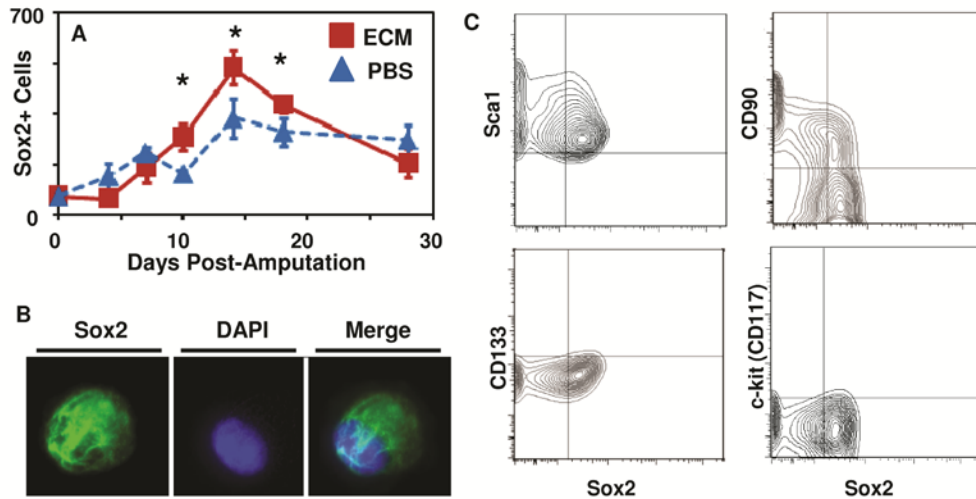
Figure 17. (A) Time course analysis of numbers of Sox2+ cells on histologic sections following digit amputation and treatment with either ECM degradation products or PBS control. (B) Confirmation of cytoplasmic and nuclear Sox2 expression in isolated cells cytospun to slides. (C) Flow cytometric analysis of Sox2+ cells. * $p <$ 0.05. Errors bars represent Mean $\pm$ SEM (n=4).

Immunolabeling of histologic sections of amputated digits showed that the majority of Sox2+ cells were found lateral to the amputated bone (Figure 18, 19). Following amputation of the proximal interphalangeal joint in which only soft tissue and no bone injury was induced, the accumulation of Sox2+ cells was markedly reduced (Figure 18, 19).
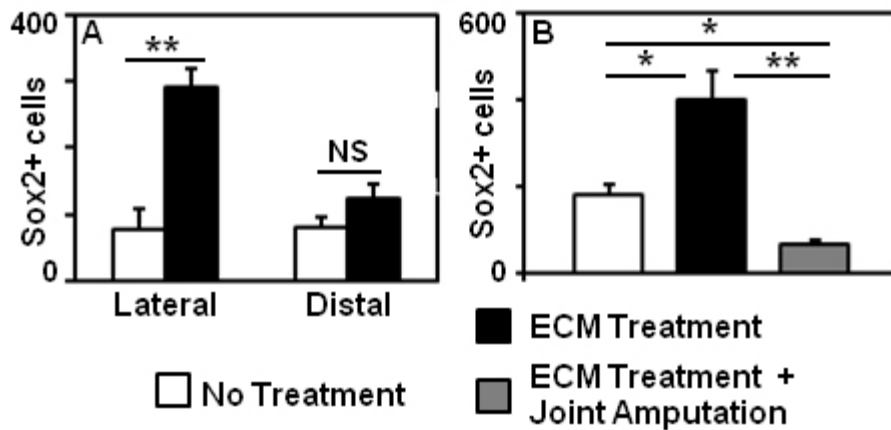
Figure 18. Sox2+ cell accumulation requires bone injury and is located lateral to the amputated bone.
(A) Immunolabeling of histologic sections of amputated digits showed that the majority of Sox2+ cells present at the

site of amputation following treatment with ECM degradation products were located lateral to the amputated P2 bone, consistent with a periosteal location. (B) Following digit amputation proximal to P2 bone at the joint such that no bone injury was induced, the accumulation of Sox2+ cells at the site of amputation following ECM degradation products was decreased. * p < 0.05. ** p < 0.01. Error bars are Mean $\pm$ SEM.
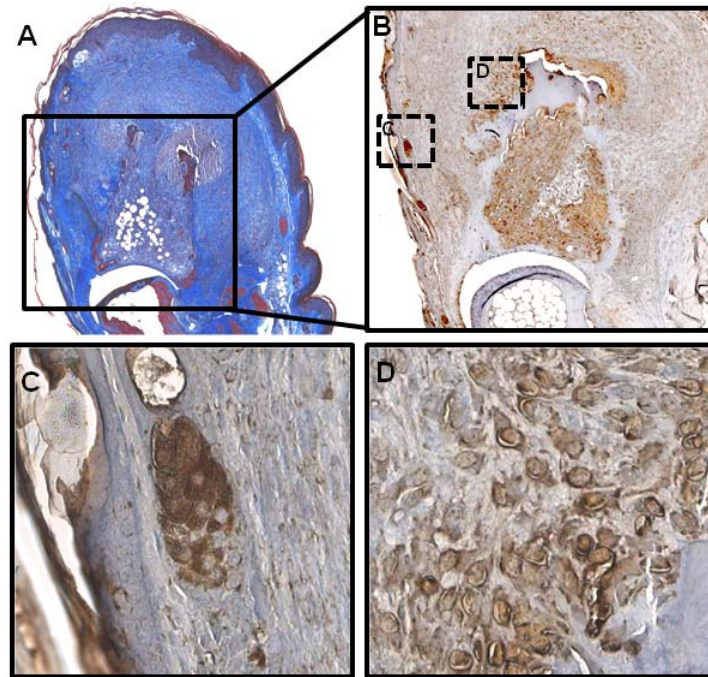
Figure 19. Representative images of immunohistochemical staining for the marker, Sox2. Unstained sections adjacent to Trichome stained sections (A) were stained with an antibody to the Sox2 antigen, and then counterstained with hematoxylin (B). Dermal stem cell staining at the base of hair follicles was used as a positive control (Avilion, Nicolis et al. 2003) (C). Sox2+ cells were found within and lateral to the amputated P2 bone of the digit. The cells showed predominantly cytoplasmic staining for Sox2 (D).

2.3.9 Sox2+ Cells are not Derived from Bone Marrow or Circulation

To distinguish between the bone marrow and the periosteum as the source of the Sox2+ cells, transgenic Sox2 eGFP/+ and wild type C57/BL6 mice transplanted with Sox2 eGFP/+ bone marrow were both subjected to mid-second phalanx amputation and treatment with ECM

degradation products. Bone marrow chimeric mice all displayed stable engraftment 4 weeks post-transplant with >80% of the blood expressing the Sox2-eGFP transgene. Expression of GFP in Sox2+ cells was confirmed in primary isolated subependymal neural stem cells from the mice (Figure 20). Cells were microdissected and isolated from digits of Sox2 eGFP/+ transgenic mice as well as bone marrow chimeric mice at day 14 post-amputation. Flow cytometric analysis confirmed GFP+ cells at the site of amputation in transgenic mice, but no GFP+ cells from amputated digits of bone marrow chimeric mice (Figure 21). GFP+ and GFP- populations were sorted by flow cytometry, cytospun, and immunolabeled for Sox2. All GFP+ cells co-expressed Sox2, whereas GFP- cells did not express Sox2 (Figure 21). GFP+ cells from β-actin-GFP/+ mice were used as a positive control.
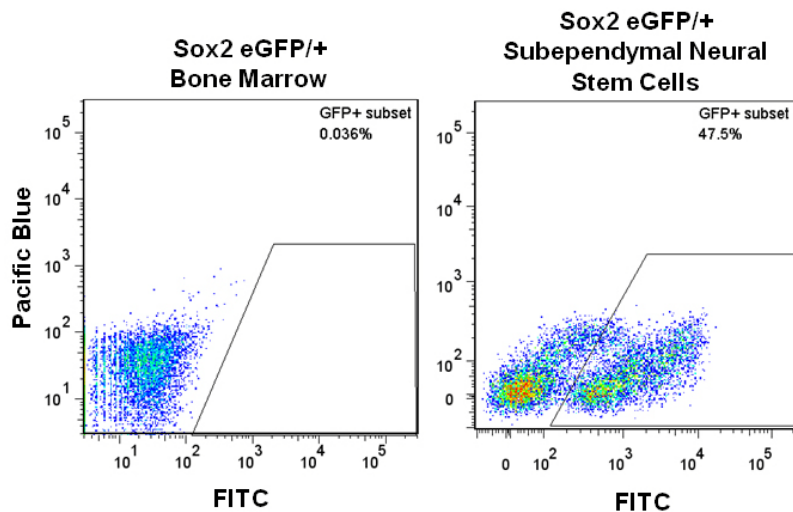
Figure 20. Sox2 eGFP/+ supendymal neural stem cells and bone marrow stromal cells were isolated from mice to serve as positive and negative controls, respectively, for eGFP expression. GFP expression was confirmed in subependymal neural stem cells, and the absence of GFP expression was confirmed in bone marrow stromal cells. These controls were used to gate for GFP+ expression in cells isolated from amputated digits (Figure 21).

45
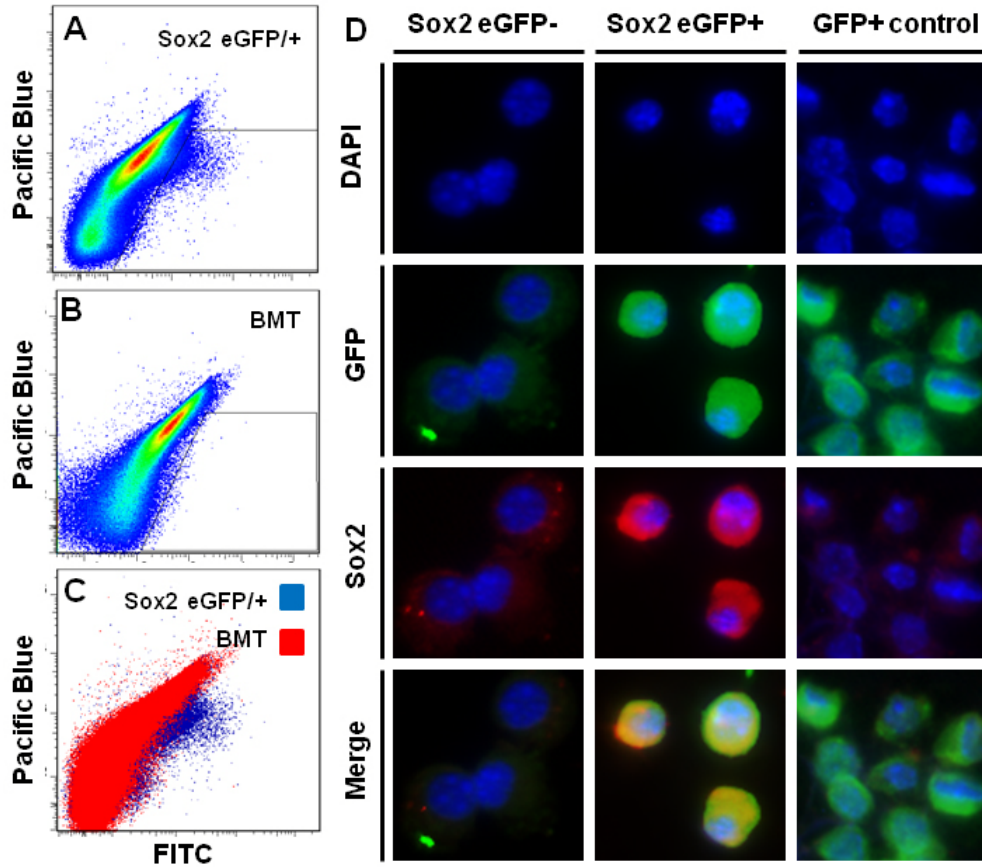
Figure 21. Sox2+ cells at the site of digit amputation are not derived from the bone marrow or circulation. Sox2 eGFP/+ transgenic mice and wild type C57/BL6 transplanted with Sox2 eGFP/+ bone marrow were subjected to mid-second phalanx digit amputation and treatment with ECM degradation products. At day 14 post-amputation, cells at the site of amputation were micro-dissected and dissociated for flow cytometric analysis for GFP expression. (A) GFP+ cells were found in cells isolated from Sox2 eGFP/+ transgenic mice. (B) A GFP+ population of cells was not found in cells isolated from bone marrow chimeric wild type mice. (C) Cells isolated from Sox2 eGFP/+ mice showed a population of cells by flow cytometric analysis that was not present in bone marrow chimeric wild type mice. (D) After sorting and cytospinning GFP+ and GFP- cell populations, immunolabeling confirmed that the GFP+ cells expressed Sox2 and GFP, whereas GFP- cells did not express Sox2 or GFP.

2.4   DISCUSSION

The findings of this chapter showed that degradation products of ECM promote the accumulation of a heterogeneous population of cells at a site of injury, a subset of which have the capacity to differentiate into ectodermal and mesodermal phenotypes *in vitro*. Additionally, a subset of the accumulated cells express Sca1, Sox2, and Rex1, all markers that have been associated with multipotential progenitor cells (van de Rijn, Heimfeld et al. 1989; Abdallah, Jensen et al. 2004; Mongan, Martin et al. 2006; Ceder, Jansson et al. 2008; Fauquier, Rizzoti et al. 2008). Further characterization of the Sox2+ subset of cells present at the site of amputation showed that the Sox2+ cells co-expressed surface antigens Sca1 and CD90, consistent with bone marrow mesenchymal stem cells. The periosteal location of Sox2+ cells, as well as the lack of bone marrow derived Sox2+ cells, suggest that the periosteum may be a source of the Sox2+ cells at the site of amputation.

2.4.1   ECM degradation products, matricryptic peptides, and progenitor cell recruitment

The generation of matricryptic peptides with biologic activity from ECM is not novel. Antimicrobial activity has been attributed to such peptides in the form of defensins (Ganz 2003), cecropins (Moore, Devine et al. 1994; Moore, Beazley et al. 1996), and magainins (Berkowitz, Bevins et al. 1990). Angiogenic and anti-angiogenic activity has been shown to be caused by maticryptic peptides derived from a variety of collagen molecules (Davis, Bayless et al. 2000; Li, Li et al. 2004). Peptides derived from extracellular matrix molecules have also been shown to modulate inflammation (Adair-Kirk and Senior 2008).

The mechanisms by which matricryptic peptides recruit stem cells *in vivo* are as of yet unknown. Additionally, the extent to which matricryptic peptides remain active *in vivo* is not known. Since ECM scaffolds consist of various molecules such as collagen and fibronectin, proteoglycans, glycoproteins, growth factors, and cytokines (Chun, Lim et al. 2007), degradation of these ECM scaffolds releases a heterogeneous set of molecules (Brennan, Tang et al. 2008; Freytes, Martin et al. 2008), each with varying biologic properties *in vivo*. Subsets of these peptides have been found to have different bioactive properties *in vitro* (Davis, Bayless et al. 2000; Sarikaya, Record et al. 2002; Brennan, Reing et al. 2006; Beattie, Gilbert et al. 2008; Brennan, Tang et al. 2008; Reing, Zhang et al. 2009). While a subset of generated peptides is clearly chemotactic for progenitor cells, the overall contribution of these peptides to progenitor cell recruitment *in vivo* is as of yet unknown. The contribution of otherwise inert proteins in this mixture to the chemotactic process is also not known with certainty, but further degradation of these inert molecules by local proteases at the site of injury may produce new, active matrcryptic residues (Lackie, Wilkinson et al. 1981; Davis, Bayless et al. 2000).

The present study focused upon the use of ECM degradation products generated *ex vivo* using a non-physiologic method of enzymatic digestion using the pepsin enzyme (Brennan, Tang et al. 2008; Freytes, Martin et al. 2008). However, other methods of degradation have also been utilized, including non-physiologic degradation via papain digestion (Reing, Zhang et al. 2009) and non-enzymatic degradation via acid digestion (Li, Li et al. 2004; Brennan, Reing et al. 2006). Pepsin was chosen as the singular method by which to degrade due to previous studies identifying chemotactic properties of the resulting ECM degradation products for progenitor cells (Brennan, Tang et al. 2008; Reing, Zhang et al. 2009). No published methods exist for robustly degrading ECM scaffolds *ex vivo* using physiologically relevant methods (e.g.

macrophage mediated degradation, MMP mediated degradation), and previous studies aiming to identifying the chemoattractive properties of endogenously created matricryptic peptides were not conclusive and open to multiple interpretations (Beattie, Gilbert et al. 2009). However, future studies may further investigate the chemoattractive properties of ECM degradation products resulting from more physiologic methods of degradation.

The present study focused only on the use of ECM derived from porcine urinary bladder. The ECM of porcine urinary bladder is a source of commercially available, FDA approved biologic scaffolds for tissue engineering applications. It has been widely studied for tissue engineering applications in a variety of soft tissues (Badylak, Vorp et al. 2005; Kochupura, Azeloglu et al. 2005; Nieponice, Gilbert et al. 2006; Gilbert, Gilbert et al. 2008; Kelly, Rosen et al. 2009; Nieponice, McGrath et al. 2009; Parekh, Mantle et al. 2009; Boruch, Nieponice et al. 2010; Medberry, Tottey et al. 2010; Davis, Callanan et al. 2011). In addition to studies investigating the surface ultrastructure (Brown, Lindberg et al. 2006; Brown, Barnes et al. 2010; Barnes, Brison et al. 2011) and composition (Chun, Lim et al. 2007) of urinary bladder matrix, the mechanisms of tissue remodeling by urinary bladder matrix have also been widely studied (Record, Hillegonds et al. 2001; Gilbert, Sacks et al. 2006; Valentin, Badylak et al. 2006; Gilbert, Stewart-Akers et al. 2007; Gilbert, Stewart-Akers et al. 2007; Gilbert, Stewart-Akers et al. 2007; Valentin, Stewart-Akers et al. 2009). While the ECM in scaffolds can be derived from multiple species and organs, it is unclear how much the source of the ECM affects the overall properties of the resulting ECM scaffold. Studies have shown *in vitro* that cells preferentially adhere, proliferate, and survive on ECM derived from the same organ as the cells (Petersen, Calle et al. ; Petersen, Calle et al. ; Sellaro, Ravindra et al. 2007). However, constructive remodeling has been observed following implantation of different sources of ECM *in vivo* in

certain injury models such as the rodent abdominal wall injury model (Valentin, Turner et al. ; Valentin, Badylak et al. 2006; Badylak, Valentin et al. 2008; Brown, Valentin et al. 2009; Valentin, Stewart-Akers et al. 2009). Additionally, *in vitro* studies with ECM degradation products have also shown that the post-natal age of the tissue from which the ECM is derived correlates more significantly with the chemoattractive properties of the resulting ECM degradation products (Brennan, Tang et al. 2008; Tottey, Johnson et al. 2010) than the actual tissue or organ source. Regardless, differences in the compositions between various sources of ECM (Brennan, Tang et al. 2008) may alter the *in vivo* effect of ECM degradation products upon progenitor cell accumulation. Future studies may directly compare ECM degradation products from different sources of ECM.

2.4.2   The Mid-second Phalanx Digit Amputation Model: Advantages, Disadvantages, and Implications

The present chapter utilized a mid-second phalanx amputation model to investigate the effect of ECM degradation products upon pr ogenitor cell recruitment *in vivo*. This model was chosen because the default response to injury in this model consists of tissue granulation, wound contraction, and complete re-epithelialization by 14 days post-amputation (Schotte and Smith 1959; Schotte and Smith 1961). Thus, as confirmed in the present chapter, mid-second phalanx amputation does not spontaneously result in tissue regeneration. This model differs from the more commonly studied model of distal phalanx amputation in neonatal (Fernando, Leininger et al. ; Yu, Han et al. ; Reginelli, Wang et al. 1995; Han, Yang et al. 2003; Han, Yang et al. 2008) and young mice (Borgens 1982; Neufeld and Zhao 1993; Neufeld and Zhao 1995; Mohammad and Neufeld 2000; Neufeld and Mohammad 2000). Because distal phalanx amputation results in

spontaneous regrowth of bone and soft tissue by 128 days post-amputation (Fernando, Leininger et al.), it is a useful model for understanding the basic mechanisms by which murine digits regrow functional tissue following distal amputation. In fact, bone morphogenic proteins (Yu, Han et al. ; Han, Yang et al. 2003), the Msx1 transcription factor (Reginelli, Wang et al. 1995; Han, Yang et al. 2003), and soluble factors released by the nearby nerves (Mohammad and Neufeld 2000) have all been identified as factors important for spontaneous distal phalanx regrowth following amputation.

However, the limitation of the model of distal phalanx amputation is that it is impossible to distinguish between whether a treatment fundamentally alters the default wound healing response or simply impedes/accelerates the host's natural ability to regenerate. Because adult mammals are not capable of regeneration of more proximal injuries, a treatment that simply only accelerates or decelerate's the host's natural regenerative response is not likely to be a viable therapeutic option for digit regeneration. However, the model of mid-second phalanx amputation utilized in the present chapter addresses this limitation, and the findings of the present study show that treatment with ECM degradation products results in a deviation from the default wound healing response of scar tissue deposition and instead causes a greater accumulation of cells that express markers of progenitor cells and show neuroectodermal and mesodermal differentiation potential *in vitro*. As discussed below, this response could be considered the initial phase of a non-blastemal epimorphic regenerative response to digit amputation.

2.4.3 Site Directed Accumulation of Progenitor Cells and Epimorphic Regeneration

The accumulation of cells expressing progenitor cell markers peaks at days 14 and 18 post-amputation, after which the number of cells progressively decreases. Since it is obvious that the

cells recruited to the site of injury following treatment with ECM degradation products do not spontaneously regenerate the missing body part, these cells do not fit the classic definition of a blastema. The response observed in the present study would be most consistent with the initial phase of a non-blastemal, epimorphic regenerative response (Morgan 1901; Sanchez Alvarado 2000). This type of regeneration is characterized by cell proliferation and subsequent regeneration of site appropriate tissue, the classic example of which in mammals is liver regeneration following acute liver injury (Ito, Hayashi et al. 1991; Michalopoulos 2007). Considered in this light, it is plausible that the recruitment of endogenous stem and progenitor cells to a site of injury that would not normally be populated by such cells, at least in such great numbers, could constitute the initial phase of a regenerative response.

Establishment of an optimal microenvironmental niche is critical for appropriate differentiation of multipotential cells. If the microenvironment could be controlled sufficiently by factors such as pH, state of hydration, electric field potential, and nutrient and growth factor availability among others, it may be possible to promote the development of site appropriate tissues in adult mammals. Thus, the logical next step is to identify strategies that can promote site appropriate differentiation, spatial organization, and patterning of these cells. In species such as the newt and salamander, the recruitment of multipotent stem cells to the site of amputation is only the first step of epimorphic regeneration (Kumar, Godwin et al. 2007). It is possible, and in fact likely, that the progenitor cells found at the site of amputation in our model are not pre-programmed to proliferate and differentiate into functional tissue. One possible explanation for this difference is that the recruited progenitor cells do not have the proper microenvironmental cues necessary to appropriately direct their proliferation, differentiation, and eventual patterning into functional tissue. If the concentrations and gradients of factors necessary to direct the cells

are known, then this may be possible by very precisely controlling the microenvironment at the site of amputation using a microfluidic device to cover the site of amputation (Hechavarria, Dewilde et al.) (see section 5.6.1)

2.4.4 Regional vs Local Treatment at the Site of Amputation

The work in the present study focused on using a regional subcutaneous injection as the primary method by which to provide a treatment at the site of amputation. While subcutaneous injection has logistical advantages with respect to animal compliance in an animal study, the critical limitation of such a method is the variable bioavailability and pharmacokinetics from treatment to treatment in this model. While fluorophore-labeled ECM degradation products were used to show that ECM degradation products can reach the site of amputation following treatment, the exact percentage of treatment or spatiotemporal distribution of ECM degradation products cannot be determined. As a result, it is not possible to distinguish between a regional effect and a local effect of ECM degradation product upon the outcome of progenitor cell accumulation. ECM degradation products are known to contain self-assembling peptides derived from structural ECM proteins that become highly viscous at physiologic pH and temperature (Freytes, Martin et al. 2008). Thus, the physical properties of the ECM degradation products likely affect the overall bioavailability and pharmacokinetics of the treatment *in vivo*.

An alternative method of treatment has been proposed in previous studies (Hechavarria, Dewilde et al.). Utilizing a microfluidic device at the site of amputation, it is possible to precisely control the localization and concentration of any given treatment option (section 5.6.1). Utilizing this device, known as the BIODOME (Biomechanical Interface for Optimized Delivery of MEMS Orchestrated Mammalian Epimorphosis), a previous study has shown that *local*

treatment with ECM degradation products in a similar proximal phalanx digit amputation model results in a similar heterogeneous accumulation of cells at the site of amputation (Hechavarria, Dewilde et al.), confirming that the ECM degradation products at least exert a local effect upon progenitor cell accumulation.

2.4.5   The importance of injury in ECM mediated progenitor cell recruitment

A surprising finding of the work in the present chapter was the dependency of progenitor cell accumulation upon the presence of injury. In the absence of a digit amputation, injection of ECM degradation products resulted in no c hange in number of progenitor cells as compared to untreated controls. Furthermore, additional work to identify the source of Sox2+ cells showed that bone injury was important for the accumulation of cells. Thus, some component of injury is important for the effect of ECM degradation products upon progenitor cell accumulation *in vivo*.

There is abundant evidence suggesting the importance of the innate immune response in overall remodeling of the ECM scaffold and subsequent constructive remodeling (Friedenstein, Piatetzky et al. 1966; Allman, McPherson et al. 2001; Badylak, Valentin et al. 2008; Brown, Valentin et al. 2009; Valentin, Stewart-Akers et al. 2009). Previous studies investigating the effect of the innate immune response upon progenitor cell recruitment have shown that polarized macrophages, both pro- and anti-inflammatory phenotypes, secrete paracrine factors that are chemotactic for adult progenitor cells (Lolmede, Campana et al. 2009). Consistent with this finding, the present study observed that injury alone increased the number of cells expressing markers of progenitor cells at the site of amputation *in vivo*. It is possible that ECM degradation products exert their effect upon progenitor cell recruitment by directly inducing paracrine release

of chemotactic factors from immune cells. It is also possible that ECM degradation products require a co-factor produced by immune cells in order to promote progenitor cell recruitment.

The time course of progenitor cell accumulation following digit amputation and treatment is consistent with this possibility that ECM degradation products act synergistically or secondarily through immune cells. While treatment with ECM degradation products is complete by day 4 post-amputation, peak accumulation of progenitor cells is not observed until days 14 and 18 pos t-amputation. While the present work cannot determine how long the ECM degradation products stay at the site of amputation, degradation products would still be present at the site of amputation within the first 4 days post-amputation during which the neutrophils and macrophages would be active at the site of amputation (i.e. the inflammatory phase of wound healing). Future studies are underway to address the effect of ECM degradation products upon macrophages *in vitro*, and this is discussed in greater detail in final discussions of the thesis in chapter 5. Preliminary work suggests that ECM degradation products potentiate the release of HMGB1 from macrophages, a known chemoattractant for progenitor cells (Porto, Palumbo et al. 2006; De Mori, Straino et al. 2007; Campana, Bosurgi et al. 2008; Lolmede, Campana et al. 2009; Ranzato, Patrone et al. 2009).

2.4.6   Site Directed Progenitor Cell Accumulation: Sources and Mechanisms

Recruitment and activation of a resident population of progenitor cells may be advantageous to the overall remodeling response. The use of bioactive factors for the site directed recruitment of progenitor cells can be thought of as a form of "endogenous stem cell therapy" (Kim, Xin et al. 2010; Lee, Cook et al. 2010). Stem cell therapy is a promising therapeutic approach to regenerative medicine, and numerous studies have shown efficacy following exogenous

introduction of stem cells at a site of injury (Horwitz, Gordon et al. 2002; Okamoto, Yajima et al. 2002; Chen, Fang et al. 2004; Bang, Lee et al. 2005; Janssens, Dubois et al. 2006; Janssens, Theunissen et al. 2006; Tyndall and Furst 2007). However, clinical translation of exogenous stem cell therapy has partially been limited by risks of immunorejection, infection, potential tumorigenesis, and difficulties in regulatory approval of exogenous stem cell therapy (Bongso, Fong et al. 2008). *In vivo* recruitment and differentiation of endogenous stem cells to a site of injury is an attractive alternative that may mitigate these risks. The present study further characterized ECM degradation products as a feasible therapy for promoting site directed recruitment of endogenous tissue progenitor cells *in vivo*.

However, previous studies have also shown that the mechanism of injury can directly dictate the relative contribution of various subsets of progenitor cells to the injury response (Majka, Jackson et al. 2003; Kienstra, Jackson et al. 2008). In addition to disrupting the stem cell niche of resident progenitor cells, the mechanism of injury can also affect the overall spatial and temporal composition of bioactive factors and cells within the injury microenvironment. Thus, understanding the phenotype and sources of the progenitor cells recruited following treatment with ECM degradation products is paramount to further directing these cells to proliferate and differentiate to recapitulate the missing digit.

Potential sources that contribute to the accumulation of progenitor cells at the site of amputation could include bone marrow derived cells, periosteal cells, perivascular cells, dermal stem cells, and circulating progenitor cells should all be considered (Friedenstein, Piatetzky et al. 1966; Friedenstein, Petrakova et al. 1968; Owen 1988; Crisan, Yap et al. 2008). Previous studies have shown that marrow derived cells participate in the constructive remodeling of tendon tissue (Zantop, Gilbert et al. 2006). However, the number of marrow derived cells in the reconstructed

tendon was relatively low compared to the number of cells observed at the amputation site in the present study. Transdifferentation or dedifferentiation are also plausible explanations for the presence of the multipotent cells, but these phenomena have not been shown to occur in large numbers *in vivo* in mammalian tissue (Shen, Slack et al. 2000; Frid, Kale et al. 2002; McKinney-Freeman, Jackson et al. 2002; Camargo, Green et al. 2003). The possibility that the observed multipotent cells were generated *in situ* following lineage reprogramming cannot be ruled out. However, few studies have demonstrated such a phenomenon *in vivo* and the mechanisms underlying such processes are not well understood (Zhou and Melton 2008).

In order to partially address potential mechanisms and sources of progenitor accumulation in this model of digit amputation, the work in the present chapter focused on further characterizing the Sox2+ cell population. The identification of a periosteal Sox2+ cell population at a site of injury following treatment with ECM degradation products that does not express markers of known Sox2+ adult progenitor cells (Biernaskie, Paris et al. 2009; Hutton and Pevny 2011) was an unexpected finding that warrants further study. Sox2 is a transcription factor that plays an important role in the maintenance of pluripotency (Avilion, Nicolis et al. 2003), and it has also been found to be expressed in a restricted set of adult progenitor cells such as neural stem cells, dermal stem cells, and neural crest derived stem cells (Biernaskie, Paris et al. 2009; Hutton and Pevny 2011). Recently, other studies have suggested that the Sox2 transcription factor plays a role in self-renewal of osteogenic progenitor cells (Basu-Roy, Ambrosetti et al. ; Mansukhani, Ambrosetti et al. 2005). The presence of periosteal Sox2+ cells in the present study is most consistent with activated osteogenic progenitors at the site of bone injury, but future studies are necessary to directly address this question.

Although Sox2 is most well studied as a nuclear transcription factor that mediates self-renewal of cells, the present study found Sox2 expression was not restricted to the nucleus but also found in the cytoplasm. Although the significance of cytoplasmic localization of Sox2 is not known with certainty, previous studies have shown that Sox2 activity can be regulated by shuttling of the Sox2 transcription factor in and out of the nucleus (Baltus, Kowalski et al. 2009). Export of Sox2 outside of the nucleus has been postulated to be an indicator of cell differentiation in Sox2+ progenitor cells (Li, Pan et al. 2007). Therefore, the cytoplasmic localization of Sox2 in cells may be a sign of these cells undergoing differentiation. Previous studies have also found that only a subset of Sox2+ cells at a site of amputation undergo mitosis, consistent with the hypothesis that heterogeneity amongst Sox2+ cells may be due to asymmetric division and differentiation. However, the present study did not directly determine the lineage differentiation potential of Sox2+ cells *in vitro* or *in vivo*, and future studies will investigate the phenotype and function of this Sox2+ population at the site of digit amputation.

Utilizing bone marrow chimeric mice, previous studies have shown that circulating progenitor cells contribute to remodeled tissue at the site of injury following implantation of an ECM scaffold (Badylak, Park et al. 2001; Zantop, Gilbert et al. 2006). In contrast, the present study shows for the first time that a subset of the progenitor cells recruited to a site of injury may not be derived from the bone marrow or circulation, but rather from resident progenitor cell populations near the site of injury (Zhang, Xie et al. 2005; De Bari, Dell'Accio et al. 2006). However, the present study does not rule out the possibility that circulating progenitor cells contribute to other subsets of Sca1+ and CD146+ progenitor cells also found at the site of amputation. In a complex injury microenvironment, certain types of progenitor cells such as lineage-restricted resident tissue progenitors may have a phenotype more optimal for survival,

proliferation, and eventually site specific differentiation into functional tissue at the site of injury. Thus, activation and recruitment of tissue resident progenitor cells may be advantageous for promoting the most optimal regenerative or constructive remodeling response to injury.

However, the present study did not directly determine the lineage differentiation potential of Sox2+ cells *in vitro* or *in vivo*, and future studies will investigate the phenotype and function of this Sox2+ population at the site of digit amputation. This is most convincingly done utilizing transgenic mice in which the Sox2+ cells can be tracked long-term *in vitro* and *in vivo* (Basu-Roy, Ambrosetti et al.).

2.4.7 Conclusions

Although questions remain that may serve as the basis for future studies, the work presented herein is the first set of studies to directly use ECM degradation products *in vivo* as a potential therapeutic option for tissue engineering of tissues. Not only has this body of work laid the foundations for future studies to address the importance of ECM degradation in a more controlled fashion (discussed in more detail in chapter 5), but it has also provided further insight into the mechanisms by which ECM scaffolds remodel. In addition to showing the degradation products of ECM scaffolds are biologically active at a site of injury *in vivo*, the findings of this chapter show for the first time that non-circulating progenitor cells also contribute to the cells that populate a site of injury and ECM implantation.

Even though the findings of this chapter did not result in constructive remodeling of the digit following amputation and treatment with ECM degradation products, the model is still very useful as a first-pass *in vivo* model for investigating bioactive properties of cryptic peptides. As discussed in future chapters, this model of digit amputation will be used to partially validate *in*

vivo the ability of a specific cryptic peptide to influence progenitor cell chemotaxis and

differentiation *in vitro*.

3.0 CHARACTERIZATION OF A SINGLE CRYPTIC PEPTIDE WITH CHEMOTACTIC PROPERTIES

3.1 INTRODUCTION

Sections of this chapter have been modified and adapted from (Agrawal, Tottey et al. 2011).

Biologic scaffolds composed of extracellular matrix (ECM) have been used successfully to promote site-specific, functional remodeling of soft tissue in both preclinical animal models (Badylak, Lantz et al. 1989; Lantz, Badylak et al. 1990; Cobb, Badylak et al. 1996; Hodde, Badylak et al. 1997; Badylak, Meurling et al. 2000; Caione, Capozza et al. 2006; Zalavras, Gardocki et al. 2006; Ott, Matthiesen et al. 2008; Ott, Clippinger et al. 2010; Uygun, Soto-Gutierrez et al. 2010) and human clinical applications (Metcalf, Savoie et al. 2002; Witteman, Foxwell et al. 2009; Derwin, Badylak et al. 2010; Mase, Hsu et al. 2010). Secreted by the cells of each tissue, ECM is highly conserved amongst many species and consists of molecules such as collagen, fibronectin, laminin, vitronectin, glycosaminoglycans, and growth factors oriented in a specific three dimensional structure and composition optimized for each tissue of origin (Badylak 2002; Sellaro, Ravindra et al. 2007). Although the mechanisms of ECM scaffold mediated constructive remodeling are not fully understood, stem cell recruitment (Badylak, Park et al. 2001; Zantop, Gilbert et al. 2006) and the release of bioactive peptides by protease mediated ECM degradation are thought to play a role in the constructive remodeling process

(Valentin, Badylak et al. 2006; Valentin, Stewart-Akers et al. 2009; Melman, Jenkins et al. 2011). In addition to possessing antimicrobial properties (Berkowitz, Bevins et al. 1990; Moore, Devine et al. 1994; Moore, Beazley et al. 1996; Ganz 2003), cryptic bioactive peptides derived from degradation of ECM components have been shown to be capable of initiating and potentiating constructive remodeling pathways such as angiogenesis, mitogenesis, and chemotaxis of site specific cells (Davis, Bayless et al. 2000; Li, Li et al. 2004; Agrawal, Brown et al. 2009). A number of specific fragments of ECM peptides have been identified, and these peptides are reviewed elsewhere (Davis, Bayless et al. 2000).

Work in the previous chapter focused on de termining the overall net effect of *ex vivo* generated ECM degradation products upon the site directed accumulation of progenitor cells at a site of injury in a murine model of mid-second phaland digit amputation. The findings suggested that degradation products of ECM may be a therapeutic option for promoting site directed recruitment of endogenous tissue progenitor cells for constructive remodeling of tissue following injury. However, to date, the specific peptides within the mix of ECM degradation products responsible for their net chemotactic effect have not been identified.

The objective of the work in the present chapter is to outline the prospective identification of a single cryptic peptide with chemotactic properties for adult stem cells of mesenchymal origin. Specifically, a single cryptic peptide derived from protease mediated degradation of an ECM bioscaffold derived from porcine urinary bladder was isolated that promotes *in vitro* migration of multiple cell types. Furthermore, the work in the present chapter shows that the isolated peptide was capable of promoting localized accumulation of progenitor populations to a site of injury *in vivo*, many of which express markers of multipotency.

3.2   MATERIALS AND METHODS

3.2.1   Overview of Experimental Design

The experimental methods were designed to systematically isolate a single matricryptic peptide that exhibits chemotactic potential for a well characterized population of human perivascular stem cells (Crisan, Yap et al. 2008) previously shown to migrate towards degradation products of ECM in low and high oxygen conditions (Tottey, Corselli et al. 2011). Matricryptic peptides were prepared by enzymatic degradation of biologic scaffolds derived from urinary bladder extracellular matrix, and subsequent serial fractionation of the resulting degradation products by ionic charge, size, and hydrophobicity. At each step, a transwell assay was utilized to determine the chemotactic potential of each eluted fraction for these stem cells. After isolation of a single cryptic peptide, the peptide was then synthesized and its chemotactic potential was evaluated for multiple types of progenitor cells and differentiated cells. Finally, an established model of adult murine digit amputation (Agrawal, Brown et al. 2009) was utilized to evaluate the ability of the cryptic peptide to promote the site-specific accumulation of progenitor cells *in vivo*. In all cases, statistical significance was determined by two-tailed student's t-test with $\alpha=0.05$ and $\beta=0.2$.

3.2.2   Decellularization of Tissue and Preparation of ECM Degradation Products:

Porcine urinary bladders were harvested from euthanized market weight (240-260 lb) pigs. The basement membrane and underlying lamina propria were isolated and harvested as previously described (Freytes, Badylak et al. 2004). Following peracetic acid, ethanol, deionized H_2O, and phosphate buffered saline treatment, lyophilized sheets were comminuted and digested in 0.1

mg/ml pepsin and 0.01 N HCl for 48 hours prior to neutralization and dilution in PBS to yield a 5 mg/ml solution (Reing, Zhang et al. 2009).

3.2.3   Isolation of Chemotactic Peptide:

Peptides of pepsin-digested UBM were fractionated via ammonium sulfate precipitation. Fractions were analyzed for protein content via BCA assay (Thermo) and chemotactic ability (as described below). Molecules in the 0-20% fraction of ammonium sulfate precipitation were discarded to remove the most gelatinous fractions and leave a solution suitable for subsequent chromatographic separation. The remaining 20-80% ammonium sulfate precipitant was isolated, dialyzed into PBS and concentrated using Amicon Ultra-4 (Millipore, MA, USA) devices. Concentrated protein was fractionated via two G3000SWXL HPLC size exclusion columns (Tosoh, Tokyo, Japan) in series at 0.5 ml/min in 10mM Tris, pH 7.4, 50 mM NaCl. Each fraction was analyzed for protein content and chemotactic ability.

Larger post size exclusion chromatography chemotactic fractions were pooled and adjusted to pH 8.8 in 50 mM Tris buffer and loaded onto a 1ml HiTrap Q ion exchange column at 0.5ml/min. Bound peptides were washed in buffer (50 mM Tris, pH 8.8) before fractionation using 0.2, 0.4, 0.5, 0.6, 0.7, 0.8, and 1.0 M salt concentrations in the same buffer. Fractions were dialyzed into PBS, and analyzed for protein concentration and chemotactic properties. Fractions showing chemotactic ability were concentrated via centrifugal filtration and injected onto an Octadecyl 4PW reverse phase column (Tosoh) and eluted over a 0-80% gradient of methanol in 10mM ammonium carbonate buffer at 0.5 ml/min. Fractions were concentrated via centrifugal evaporation, resuspended in H_2O, and analyzed for protein abundance and chemotactic properties. The peptide that revealed maximal chemotactic ability per mg of chemoattractant

was further characterized by mass spectrometry (NextGenSciences, Ann Arbor, MI) and then chemically synthesized (GenScript, Piscataway, NJ). A BLAST search (http://blast.ncbi.nlm.nih.gov/) for sequence homology was conducted using the non-redundant protein sequences (nr) database and Blastp algorithm. Parameters of the search were as follows: [1] max target sequences=100, [2] expect threshold=200000, [3] word size=2, [4] Matrix=PAM30, [5] gap cost existence=9 and extension=1, [6] no compositional adjustments.

3.2.4 Source of Cells and Culture Conditions

Human perivasular stem cells were a gift from Dr. Bruno Peault, and these cells were isolated and prepared as previously described (Crisan, Yap et al. 2008). Perivascular stem cells were cultured in high-glucose Dulbecco's modified Eagle's medium (DMEM, Invitrogen) containing 20% fetal bovine serum (FBS; Thermo), 100 U/mL penicillin, and 100 µg/ml streptomycin (Sigma) at 37°C in 5% CO_2. Human cortical neuroepithelium stem (CTX) cells were a gift from ReNeuron^{TM}. CTX cells were cultured in DMEM:F12 supplemented with 0.03% Human albumin solution, 100µg/ml human Apo-Transferrin, 16.2µg/ml Putrescine DiHCl, 5µg/ml Insulin, 60ng/ml Progesterone, 2mM L-Glutamine, 40ng/ml Sodium Selinite, 10ng/ml human bFGF, 20ng/ml human Epidermal growth factor, and 100nM 4-Hydroxytestosterone. Human adipose stem cells were isolated as previously described (Aksu, Rubin et al. 2008), and cultured in DMEM/F12 supplemented with 10% heat inactivated fetal bovine serum, 100 U/ml penicillin, and 100 µg/ml streptomycin. C2C12 muscle myoblast cells, IEC-6 intestinal epithelial cells, RT4-D6P2T rat Schwann cells, and HMEC human microvascular endothelial cells were obtained from ATCC and cultured following ATCC guidelines.

3.2.5   Transswell Cell Migration Assays

Chemotaxis assays were conducted in a transwell as described previously (Reing, Zhang et al. 2009). Perivascular stem cells were grown in culture medium to ~80% confluence and starved overnight in DMEM containing 0.5% heat inactivated serum. After starvation, cells were resuspended in DMEM at a concentration of $6x10^5$ cells/ml for 1 hour. Polycarbonate PFB filters (Neuro Probe, Gaithersburg, MD) with 8 µm pores were coated with 0.05 mg/ml Collagen Type I (BD Biosciences, San Jose, CA). The number of cells that migrated toward the lower chamber through 8 µm pore polycarbonate PFB filters (Neuro Probe, Gaithersburg, MD) was determined after 5h. The lower wells contained different amounts of the ECM peptide fraction of interest. Migrated cells were stained by 4',6-diamidino-2-phenylindole and quantified with ImageJ (NIH). All of the data are reported as the mean value of triplicate determinations with standard deviations. The assay was performed on three separate occasions. C2C12, IEC-6, RT4-D6P2T, and HMEC cells were grown to 80% confluence, and starved in serum free media overnight prior to placement in the transwell assay. CTX cells were grown to ~80% confluence were unstarved prior to resuspension and placement in the transwell assay. All other methods were identical for each cell type.

3.2.6   Animal Model of Digit Amputation:

All methods were approved by the Institutional Animal Care and Use Committee at the University of Pittsburgh and performed in compliance with NIH Guidelines for the Care and Use of Laboratory Animals. Mid-second phalanx digit amputation of the third digit on each hindfoot in adult 6-8 week old C57/BL6 mice (Jackson Laboratories, Bar Harbor, ME) was completed as

66

previously described (chapter 2). Following amputation, digits were either treated with a subcutaneous injection of $15\,\mu L$ of $10\,mM$ peptide, or the same volume of PBS as a carrier control (n=4 for each group). Treatments were administered at 0, 24 and 96 hours post surgery. Animals were sacrificed via cervical dislocation under deep isoflurane anesthesia (5-6%) at day 7 post-surgery. Digits were either fixed and sectioned for histologic analysis and immunolabeling (described below), or harvested for cell isolation for subsequent FACS analysis, cytospin, or immunolabeling (described below).

3.2.7   Tissue Immunolabeling

Harvested mouse digits were fixed in 10% neutral buffered formalin and decalcified for two weeks in 5% formic acid prior to being paraffin embedded, sectioned, and stained for Sox2 (Millipore, AB5603, Billerica, MA), Sca1 (Abcam, ab25196, Cambridge, MA) , o r Ki67 (Abcam, ab15580). Following deparaffinization, antigen retrieval in 10 mM citrate buffer (citrate: C1285, Spectrum, New Brunswick, NJ) was performed for 25 minutes at $95^{0}C$. Slides were blocked for 1 hour at room temperature in 1% bovine serum albumin (BSA) in phosphate buffered saline (PBS), and then incubated with primary antibody overnight at $4^{0}C$. Slides were then rinsed in PBS, treated with 3% hydrogen peroxide solution in PBS for 30 minutes, washed, and incubated for 1 hour with HRP conjugated anti-rat IgG (P0450, Dako, Carpinteria, CA) or anti-rabbit IgG (P0448, Dako) antibodies, washed, and developed with 3, 3' diaminobenzidine (DAB) (Vector Labs, Burlingame, CA). All primary antibodies were diluted 1:100 in blocking solution, and all secondary antibodies were diluted 1:200 in blocking solution.

After staining with DAB, all slides were counter-stained with Harris' hematoxylin, dehydrated, coverslipped with non-aqueous mounting medium, and imaged. Images were taken at 40X magnification and 200X magnification. For quantification of the number of cells positive for markers, three images were taken for each sample: distal to the amputated edge of the bone, and lateral to the cut edge of the bone on either side. The number of positive cells in each image was counted by three independent investigators who were blinded to the treatment group. The mean number of positive cells was compared between various groups by a two-sided, unpaired student's t-test with unequal variance. Significance was determined at p = 0.05 level (α=0.05, β=0.2).

3.2.8 Flow Cytometric Analysis:

Amputated digits were harvested and placed into cold culture medium consisting of DMEM, 10% mesenchymal stem cell grade fetal bovine serum (Invitrogen, Carlsbad, CA), 100 U/ml penicillin, 100 μg/ml streptomycin, and 0.1 mg/ml ciprofloxacin (USP, Rockville MD, 1134313). Using a microdissection microscope and aseptic technique, the epidermis and dermis were removed and the soft tissue distal to the amputated second phalanx bone was harvested into serum free DMEM containing 2% Collagenase Type II (Gibco Invitrogen, 17101-015) for 30 minutes at 37^0C, filtered through a 70 μm filter, counted, and prepared for flow cytometric analysis expression of Sca1 (Abcam, ab25031, Cambridge, MA) or markers of differentiated blood derived cells (Lineage cocktail, 559971, BD Biosciences, San Diego, CA). Cells were filtered through a 70 μm filter and incubated in primary antibody for 1 hour, washed, and then incubated in a streptavidin APC-Cy7 conjugated secondary antibody (554063, BD Biosciences) for 1 hour prior to washing and flow cytometric analysis.

3.2.9 Cytospin and Cell Immunolabeling

Following cytospin of 1×10^4 cells per slide, each slide was fixed in methanol for 30 seconds and stored at -20 ^{0}C. Prior to staining, slides were rehydrated in PBS for 5 minutes, and cells were permeablized in 0.1% TritonX/PBS for 15 minutes. Slides were blocked in 1% bovine serum albumin/PBS for 1 hour prior to overnight incubation with goat anti-Sox2 (1:50) (SantaCruz, Y-17, sc17320, Santa Cruz, CA), rabbit anti-Sox2 (1:100) (Millipore, AB5623), rat anti-Sca1-FITC (1:50) (Abcam, ab25031), or rabbit anti-phospho-Histone-H3 (1:100) (Abcam, ab32107) primary antibody diluted in blocking solution. Following two washes in PBS, slides were incubated for 1 hour with donkey anti-goat IgG-Alexa Fluor 350 (1:100) (Invitrogen, A21081, Carlsbad, CA) and/or donkey anti-rabbit IgG-Alexa Fluor 546 (1:250) (Invitrogen, A10040) diluted in blocking solution. Following two washes in PBS, slides were counterstained with DRAQ5 (1:500) (Cell Signal, 4084, Danvers, MA) diluted in PBS for 30 seconds prior to three washes in PBS and coverslipping with fluorescent mounting medium (Dako, S3023). All images were taken at 200X magnification.

3.2.10 Cell Adhesion Assays

The cell adhesion assay was completed as previously described (Humphries 2009). Briefly, wells were either left uncoated or coated with 10% fetal bovine serum, collagen type I (a known pro-adhesive substrate), or the isolated cryptic peptide. Non-specific binding was blocked with heat denatured 10% bovine serum albumin. Five thousand human perivascular stem cells were seeded into each well and allowed to attach for 20 minutes. After 20 minutes, unattached cells and media were removed from each well. The attached cells were fixed in 10% neutral buffered

formalin overnight, and then stained in 0.05% w/v crystal violet solution for 10 minutes and destained until optimal staining had occurred. Each well was then destained with 10% (v/v) acetic acid, and absorbance was measured at 570 nm on a spectrophotometer as a surrogate for cell number.

3.3   RESULTS

3.3.1   Isolation, Identification and Synthesis of Chemotactic Cryptic Peptide

The various protein fractions following ammonium sulfate precipitation were dialyzed against phosphate buffered saline (PBS) and all fractions showed chemotactic activity (migration of the perivascular stem cells to the bottom well of the transwell chambers) compared to the PBS control (Figure 22 a,b).   The fractions were pooled, concentrated and further fractionated via size exclusion chromatography (Figure 22c). Protein quantification showed that the peptide fragments distributed into two peaks, with a long tail of small size molecules. Analysis of each fraction showed that the chemotactic effect was also distributed into two peaks. However, these chemotactic peaks were not aligned with the protein peaks. Chemotactic activity of each fraction did not correlate with the total amount of protein, but rather was a net effect of the distribution of specific molecules with the UBM peptide mix.

Analysis of the second chemotactic peak showed these molecules to be too small to bind to ion exchange beads carrying either a positive or negative charge resulted in very little capture. Thus, the most chemotactic fractions from the first size exclusion peak were pooled and refractionated via ion exchange chromatography (Figure 22d). After adjustment to pH 8.8, the

70

remaining peptides were bound to a HiTrap Q ion exchange column, washed in salt free buffer and eluted over a series of increasing concentrations of salt. The fractions were adjusted to a biological buffering condition and analyzed for chemotactic activity (Figure 22e). The fraction with the greatest chemoactivity per mg/ml of protein was chosen for further study.   The fraction with the greatest chemotactic activity per mg/ml of protein was the 0.6 M fraction. The 0.6 M fraction was further fractionated by reverse phase chromatography (Figure 22f). Unbound peptides (peak 1) and bound peptides were eluted over a 0-80% methanol gradient and analyzed for protein concentration. Protein peaks were then evaluated for chemotactic activity (Figure 22g). Fractions 2 and 4 showed the greatest amount of chemotactic activity, and lesser chemotactic activity was also shown in the unbound fraction. Because Fraction 2 showed the greatest chemoactivity per mg of protein, this fraction was isolated for sequence analysis by mass spectrometry. Analysis showed that the fraction consisted predominantly of a single peptide with the amino acid sequence of IAGVGGEKSGGF, a sequence identical to a string of amino acids from the C-terminal telopeptide of collagen IIIα. The peptide was chemically synthesized and evaluated in the same transwell chemotactic assay over a range of concentrations (Figure 22h, 23). Chemokinetic activity as a cause of the cell migration was ruled out by varying the relative concentrations of the peptide in the upper and lower wells of the transwell chambers (Figure 22h). A BLAST search of the isolated peptide sequence showed that the peptide sequence was highly conserved in collagen IIIα amongst eight mammalian species including human (Figure 22i). A hydropathy plot showed that the IAGVGGEKSGGF sequence was derived from the most hydrophobic region of the collagen type IIIα C-terminal telopeptide (Figure 24).
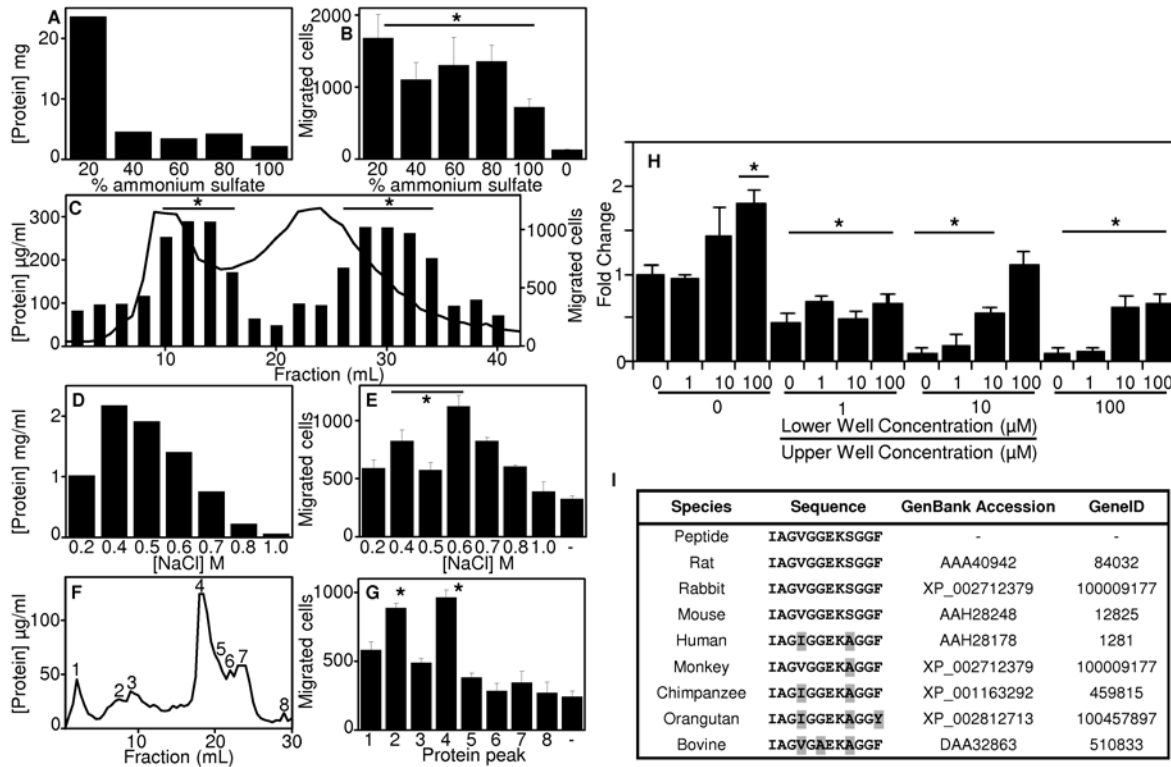
Figure 22. Identification of chemotactic peptide. UBM digest was fractionated and chemotactic ability quantified against perivascular stem cells by ammonium sulfate (a, b), size exclusion (c), ion exchange (d, e), and reverse phase (f, g) chromatography. Peptide was identified via mass spectroscopy and synthesized to assay for chemotactic potential for human perivascular stem cells (h). A BLAST search for the isolated peptide sequence showed over 75% homology with the Collagen IIIα molecule over eight separate species. Error bars are Mean $\pm$ SD. * $p < 0.05$ as compared to negative control.
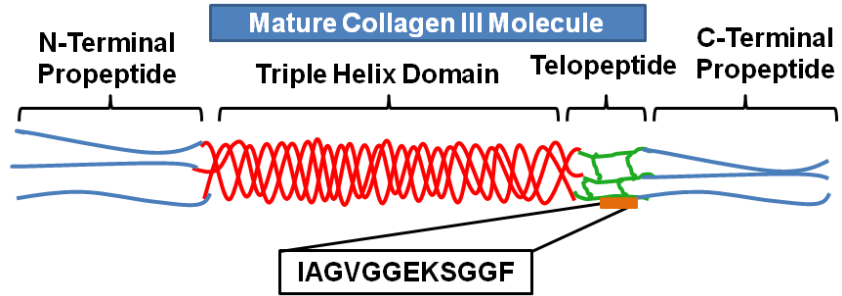
Figure 23.. A schematic diagram of the collagen type IIIα molecule and the region that the isolated cryptic

peptide is derived from.
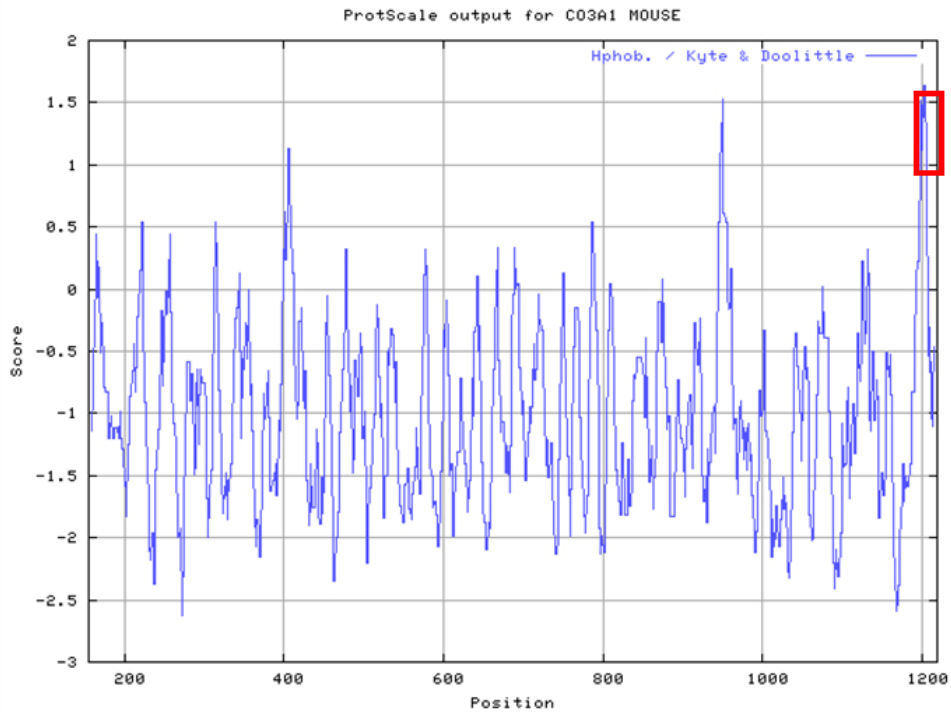
Figure 24. A hydropathy plot showed that the isolated cryptic peptide (red box) was derived from the most

hydrophobic region of the collagen type IIIα C-terminal telopeptide. Hydropathy plot was completed at

http://expasy.org/cgi-bin/protscale.pl using the Kyte & Dolittle scale.

3.3.2 Cryptic Peptide Shows In-vitro Chemotactic Activity Toward Several Cell Types

In order to test whether the isolated cryptic peptide affected migration of other cell types, the migration of various cell types was assessed in response to the isolated cryptic peptide. The synthesized peptide showed positive chemotactic activity toward human neuroepithelial cells (Figure 25a), human adipose stem cells (Figure 25b), C2C12 mouse myoblast cells (Figure 25c), the RT4-D6P2T rat Schwann cell line (Figure 25d), and human microvascular endothelial cells (HMEC) (Figure 25e). The rat intestinal cell IEC-6 line (Figure 25f) was unresponsive to the peptide.
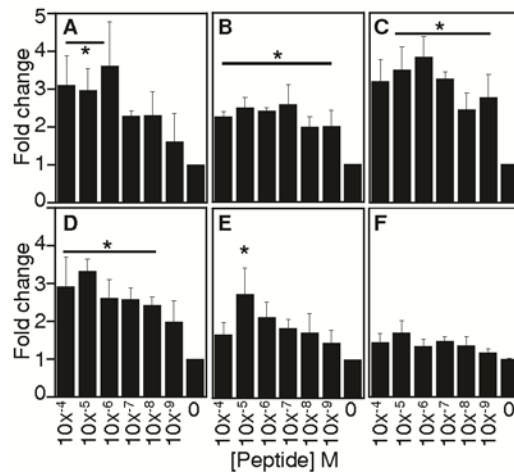
Figure 25. Peptide promotes migration of multiple cell types *in vitro*. The chemotactic ability of the peptide was tested over six orders of magnitude concentration against human neuroepithelial cortical (CTX) stem cells (a), human adipose stem cells (b), mouse myoblast (C2C12) cells (c), rat Schwann (RT4-D6P2T) cells (d), human microvascular endothelial (HMEC) cells (e), and rat intestinal epithelial (IEC6) cells (f). Error bars are Mean $\pm$ SD. * $p < 0.05$ as compared to negative control.

3.3.3 Cryptic Peptide Shows In vivo Recruitment of Sox2+, Sca1+, Lin- cells

Histologic examination of peptide treated digits at day 7 pos t-amputation showed a dense, cellular infiltrate both lateral and distal to the site of amputation, concomitant with an invaginating epithelium and incomplete basement membrane (Figure 26a). The PBS treated digits showed a less dense cellular infiltrate concomitant with scar tissue deposition and a mature epithelium consistent with a typical wound healing response in the murine digit (Figure 26b) (Schotte and Smith 1959). Immunolabeling studies showed a 6.6 fold increase in Sox2+ cells and a 1.6 f old increase in Sca1+ cells at the site of amputation following peptide treatment as compared to PBS treatment (Figure 26c). FACS analysis of the Sca1+ cells showed that the Sca1+ cells did not co-express markers of differentiated blood lineage (Figure 26d). Isolated cells that were co-immunolabeled for both Sox2+ and Sca1+ confirmed co-expression of Sca1 and Sox2 in a subset of cells (Figure 26e).
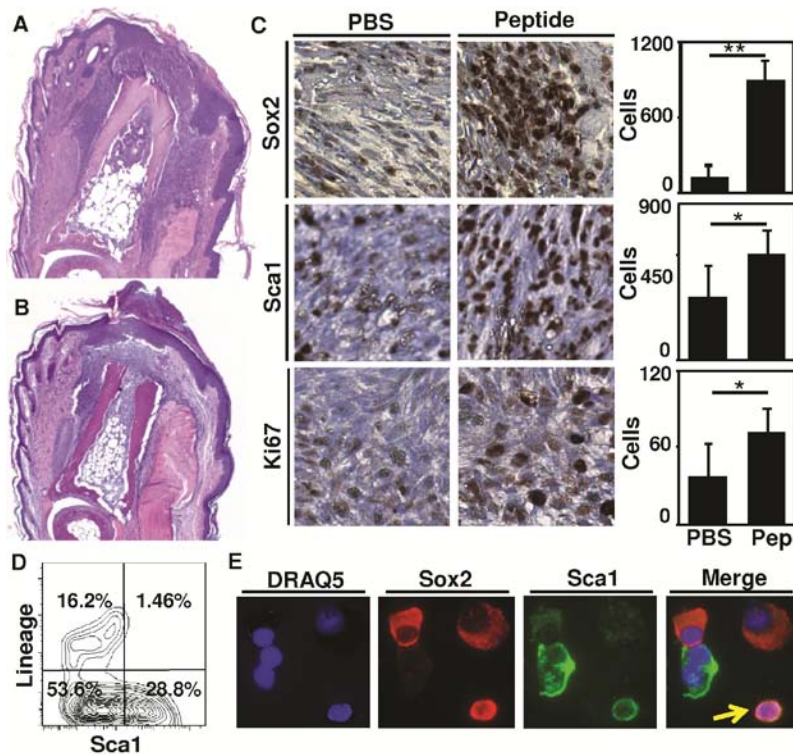
Figure 26. Peptide results in greater numbers of progenitor cells *in vivo*. Adult mouse hind foot digits were amputated at the mid-second phalanx and treated with 15μL of either PBS or peptide. Histologic examination by hematoxylin and eosin staining showed a thinner, invaginating epithelium concomitant with a denser cellular response following peptide treatment (a) as compared to PBS carrier control treatment (b). Histologic sections showed that peptide treatment led a greater number of Sox2, Sca1, and Ki67 positive cells at the site of amputation (c). Flow cytometric analysis confirmed that Sca1+ cells did not express markers of differentiated blood lineage (d). Co-expression of Sca1 and Sox2 was observed in subsets of cells following cytospin and co-immunolabeling (arrow) (e). Images were taken at 40x magnification (a, b), 630x magnification (a,b), or 400x magnification (c,e). Error bars are Mean $\pm$ SD. * $p < 0.05$. ** $p < 0.01$.

Histologic sections from peptide treated and PBS treated digits were also stained for Ki67 to evaluate cell proliferation. At day 7 post-amputation, peptide treatment led to a 1.9 fold increase in Ki67+ cells at the site of amputation (Figure 26c). Cells were located both lateral and

distal to the plane of amputation. To confirm that Sox2+ and Sca1+ cells were undergoing mitosis, accumulated cells were isolated and co-immunolabeled for phosphorylated Histone H3 (Hans and Dimitrov 2001) and either Sox2 or Sca1. Subsets of both Sox2+ cells and Sca1+ cells also showed pan-nuclear expression of phosphorylated Histone H3 (Figure 27), consistent with ongoing mitosis (Hans and Dimitrov 2001).
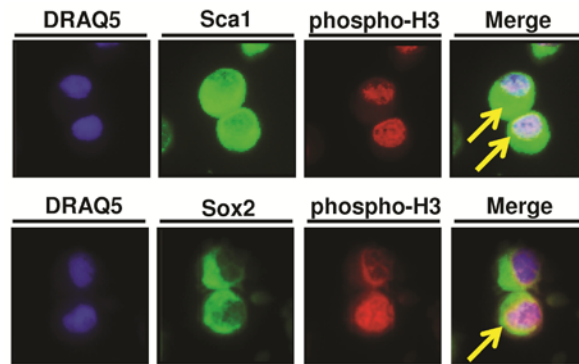
Figure 27. A subset of Sox2 and Sca1+ cells are mitotic. To confirm that Sca1+ and Sox2+ cells were actively proliferating, isolated cells were cytospun and co-immunolabeled for either Sca1 or Sox2 and a marker of cells in the M phase of the cell cycle, phosphorylated Histone H3 (Hans and Dimitrov 2001). Subsets of Sca1+ and Sox2+ co-expressed nuclear Histone H3 (arrows). Images were taken at 400x magnification.

3.3.4 Chemotactic Activity of Peptide is Specific to the Peptide Composition, but not the sequence

The work thus far in the present chapter outlined the chemotactic activity of the peptide to a carrier control for multiple cell types *in vitro*, and it showed the ability of the peptide to cause the site-directed accumulation of Sox2+, Sca1+, Lin- cells at a site of digit amputation. However, the relative chemoattractive properties as compared to a known chemoattractant was not been

investigated thus far. Thus, *in vitro* migration assays were completed with human perivascular stem cells to compare the chemotactic potential of the isolated cryptic peptide to the chemotactic potential of unfractionated ECM degradation products and fetal bovine serum, both known chemoattractants *in vitro*. At each concentration *in vitro*, unfractionated ECM degradation products resulted in more migration of human perivascular stem cells compared to the single cryptic peptide. The only exception was at the highest concentration of 1 mg/ml, which is likely due to the spontaneous gelation of the ECM degradation at such high concentrations (Freytes, Martin et al. 2008) (Figure 28).
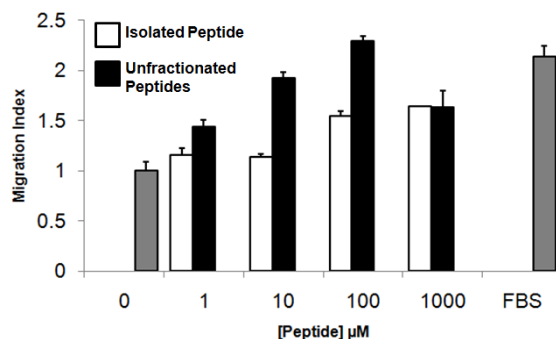
Figure 28. Migration of human perivascular cells towards the isolated cryptic peptide, IAGVGGEKSGGF, compared to the unfractionated ECM degradation products showed that the isolated cryptic peptide showed 50-75% of the activity that the unfractionated ECM degradation products showed. PBS and 10% FBS were used as negative and positive controls.

In order to investigate the importance of the peptide sequence for its chemotactic activity, a scrambled peptide, GIAEGVGKGFGS, was created (Table 1). The scrambled peptide was designed to scramble the non-polar amino acids in the cryptic peptide. It was theorized that any receptor interacting with the peptide would do s o via hydrogen bonding between non-polar amino acids in the peptide and the receptor. Although variation in the migration of human perivascular stem cells towards the scrambled peptide was greater, there was no significant

difference between the effect of the original and scrambled cryptic peptides *in vitro* (Figure 29). This suggests that perhaps the sequence of the peptide itself is not the primary determinant of the peptide's chemoattractive effect.

Table 1. Sequences of peptides utilized for migration assay studies.

Peptide	Sequence
Cryptic Peptide	IAGVGGEKGSGGF
Scrambled Peptide	GIAEGVGKGFGS
Hydrophobic Peptide	CCGGGAAAIAGV
Hydrophilic Peptide	RGAPGPQGPRGD
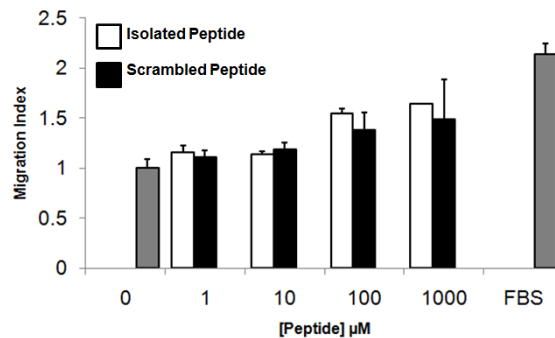
Figure 29. Migration of human perivascular stem cells towards the isolated cryptic peptide, IAGVGGEKSGGF, or a scrambled peptide, GIAEGVGKGFGS, showed that there was no significant difference in migration towards the unscrambled or scrambled peptide. PBS and 10% FBS were used as negative and positive controls.

Because the peptide was derived from one of the most hydrophobic regions of the collagen type IIIα molecule, it was possible that the chemotactic effect of the cryptic peptide was due to a physical propery of the peptide such as hydrophobicity. To test this possibility, the chemotactic activity of the peptide was compared to the most hydrophobic 12 amino-acid sequence in collagen type III, CCGGGAAAIAGV, as well the most hydrophilic region of

79

collagen type III, RGAPGPQGPRGD (Table 1). The more hydrophobic peptide showed no chemotactic effects at any concentration tested when compared to a negative control, but the hydrophilic peptide caused a greater amount of migration at every concentration tested when compared to the cryptic peptide (Figure 30). Thus, the physical property of hydrophobicity did not correlate directly with chemotactic potential.
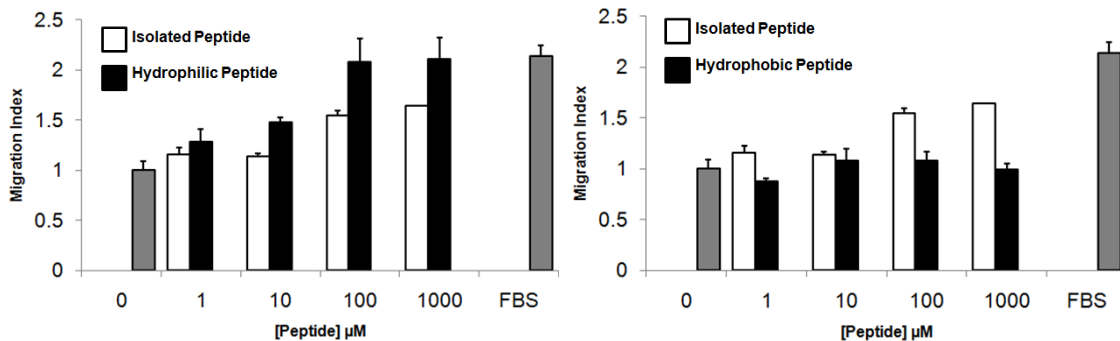
Figure 30. Migration of human perivascular stem cells towards the isolated cryptic peptide, IAGVGGEKSGGF, a more hydrophobic peptide, CCGGGAAAIAGV, or a more hydrophilic peptide, RGAPGPQGPRGD, showed that peptide hydrophobicity did not correlate with perivascular stem cell migration.

3.3.5   Effect of Peptide upon Adhesion of Human Perivascular Stem Cells

Because the peptide was derived from collagen type III, and because integrin receptors are abundant on mesenchymal stem cells such as the human perivascular stem cell, integrins were suggested as a potential target receptor of the peptide. A hallmark of integrin receptors is that their ligands, when immobilized or adsorbed to a surface, cause a dose dependent increase in cell adhesion (Humphries 2009). Thus, the adhesion of human perivascular stem cells to surfaces coated with the cryptic peptide was tested. The peptide caused increased cell adhesion compared to uncoated controls. Compared to a known adhesion protein, collagen type I, the peptide caused less cell adhesion (Figure 31).
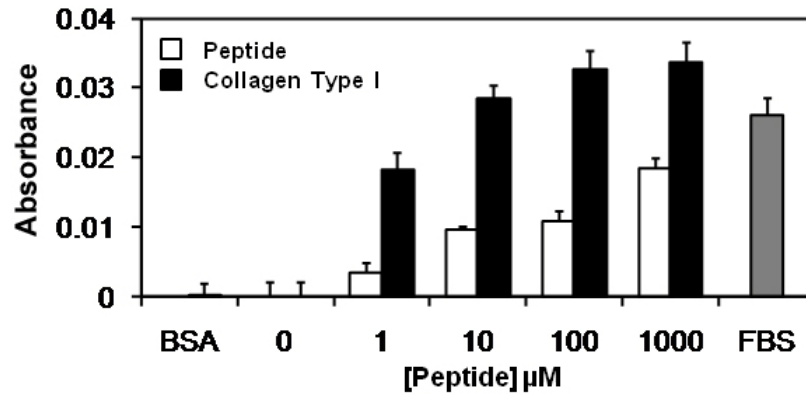
Figure 31. A cell adhesion assay for human perivascular stem cells showed that the isolated cryptic can increase cell adhesion, but less so than known positive controls Collagen type I and 10% FBS.

3.4   DISCUSSION

The present chapter identifies a novel matricryptic peptide with *in vitro* chemotactic activity for several types of progenitor cells and differentiated cells. This peptide is also associated with the increased presence of Sox2+ and Sca1+,Lin- cells at the site of experimentally induced injury in a mouse model. As a short twelve amino acid oligopeptide derived from the C-terminal telopeptide region of the collagen IIIα molecule, the sequence of this molecule is highly conserved amongst at least eight mammalian species.

3.4.1   The chemotactic cryptic peptide

The cryptic peptide identified in the present study was derived from the C-terminal telopeptide region of the collagen type IIIα molecule. The C-terminal telopeptide region of fibrillar collagen is known to be a site of interchain cross-linking of cysteine residues that ultimately stabilize the

triple helix structure of collagen (Barth, Kyrieleis et al. 2003). Thus, in the absence of injury and protease mediated degradation, it is unlikely that such a sequence would actively interact with cells due to extensive cross-linking. However, protease mediated matrix degradation at a site of injury would not only destabilize and release peptides from the triple helical domain of collagen, but also expose and cleave the telopeptide regions of collagen to release cryptic peptides similar in sequence to the isolated peptide in the present study. Previous studies have shown that telopeptide sequences can be isolated in the circulating blood following turnover of collagen and soft tissue remodeling in a clinical setting (Kitahara, Takeishi et al. 2007; Banfi, Lombardi et al. 2010; Kanoupakis, Manios et al. 2010). Thus, while the cryptic peptide in the present study was isolated by non-physiologic methods of degradation, it is likely that a similar peptide can and would be released *in vivo* at a site of injury.

The present chapter identified a single peptide derived from a mixture of matricryptic peptides that can recruit stem, progenitor, and differentiated cells *in vitro* and is associated with an increased accumulation of such cells at sites of injury *in vivo*. However, the findings of the present study do not preclude the existence of other pro- and anti-chemotactic matricryptic peptides. It is likely that degradation of ECM leads to release of a large mixture of anti- and pro-chemotactic peptides that yields an overall net effect *in vivo*. Indeed, certain fractions of the ammonium sulfate precipitated peptides in the present study showed inhibited migration of progenitor cells; a finding that suggests degradation products of ECM contain chemotactically positive, negative, and likely also neutral peptides. Isolation of these peptides was not pursued. Although an active peptide described in the present study was isolated from a mix of mammalian matricryptic peptides, the naturally occurring contribution of this particular peptide to the host response to injury was not determined. The present study also showed the efficacy of the isolated

oligopeptide in an adult mammalian model of digit amputation via local accumulation of progenitor cells at the site of injury. While the present study cannot determine whether the efficacy of the isolated peptide is dependent on the type of injury, future studies will further investigate the potential role of the peptide in progenitor cell recruitment in various other types of injury.

Additionally, the present chapter focused on identifying a bioactive cryptic fragment of one source of extracellular matrix. Extracellular matrix derived from the porcine urinary bladder has been used in multiple pre-clinical applications for site-specific remodeling of a variety of soft tissues (Badylak, Vorp et al. 2005; Kochupura, Azeloglu et al. 2005; Nieponice, Gilbert et al. 2006; Gilbert, Gilbert et al. 2008; Kelly, Rosen et al. 2009; Nieponice, McGrath et al. 2009; Parekh, Mantle et al. 2009; Boruch, Nieponice et al. 2010; Medberry, Tottey et al. 2010; Davis, Callanan et al. 2011). However, commercially available biologic scaffolds composed of extracellular matrix are derived from a number of species and organs (Crapo, Gilbert et al. 2011). It is possible that a similar cryptic peptide would be found in ECMs from other sources. Collagen III is a common constituent of many soft tissues from which ECM scaffolds are made, and its sequence is highly conserved from species to species. The present study found that the isolated cryptic peptide's sequence is also highly conserved amongst over eight species, many of which are already used as sources of ECM for commercial applications. Thus, it is likely and expected that the isolated cryptic peptide, or a similar derivative of such a peptide, would qualitatively possess the same bioactive properties in multiple mammalian species and commercially available extracellular matrix scaffolds.

The work presented in the present chapter focused on understanding the single cryptic peptide. Thus, there is no data that evaluates the overall contribution of this peptide to the net

chemotactic properties of the unfractionated ECM degradation products from which the peptide was isolated. Ideally, this would be measurable by supplementation of the peptide to degradation products mix as well as depletion of the peptide from the ECM degradation products, presumably by an antibody or column-mediated depletion method. While supplementation of ECM degradation products *in vitro* and *in vivo* is possible for future studies, depletion may be logistically difficult. The short length of the peptide and its similarity in sequence to other structural protein components within the degradation products does not allow for specific depletion (i.e. antibody mediated) of the cryptic peptide from the unfractionated ECM degradation products. The work presented herein will serve as the future basis for studies to more directly address the contribution of the cryptic peptide towards the net chemotactic properties of ECM degradation products.

3.4.2   Mechanisms of action of the chemotactic cryptic peptide

The findings of the present chapter show that the identified cryptic is most active at concentrations of 0.1mM and 1 mM *in vitro*. By pharmacological standards, these concentrations are fairly high, especially considering the possibility of a single ligand, receptor interaction. Most chemotactic peptides that act via a known ligand/receptor interaction are active in the nanomolar and picomolar concentrations, approximately 10^6 fold more potent than the peptide identified in the present study.

However, the findings of the present chapter also suggest that there is something specific about the cryptic peptide that contributes to its chemotactic effect, however weak the effect may be when normalized to concentration. Although a randomly scrambled peptide showed approximately the same chemotactic effect *in vitro*, a similar 12 amino acid peptide derived from

the collagen type IIIα C-terminal telopeptide (CCGGGAAAIAGV) showed no chemoactivity at the same concentrations. This confirms that the effect of the isolated cryptic peptide is not purely due to the presence of a high concentration of protein or peptide.

The finding that a scrambled peptide showed effectively the same chemotactic effect that the cryptic peptide showed *in vitro* was a surprising finding with multiple potential explanations. Scrambling of the peptide is meant to disrupt any specific combination of amino acids in the peptide that may bind to a specific receptor on a cell, for example. Because scrambling of the peptide did not affect overall migration of perivascular stem cells, one potential explanation for the findings is that the mechanism of action of the cryptic peptide is not via a direct receptor/ligand interaction. However, it is possible that the scrambled peptide and cryptic peptide both promote migration via separate mechanisms. Ideally, multiple scrambled sequences would be used to address this question fully.

The derivation of the cryptic peptide from one of the most hydrophobic regions of collagen type III suggests that potentially a biophysical property of the peptide is the primary determinant of its chemotactic properties. The most logical biophysical property would be hydrophobicity. However, the more hydrophobic 12 amino acid peptide also derived from the telopeptide region of collagen type III showed very little activity.

It is possible that the effect of the peptide is actually a hybrid of a receptor/ligand interaction and a biophysical property. The biophysical properties of the peptide would allow for it to non-specifically bind receptors or other proteins on a cell surface. If the concentration of the non-specifically bound peptides on the cell surface is high enough, it is possible that the peptides may then actually induce signaling through the receptors that are bound. Although the present

study does not address this potential mechanism directly, it is possible to do so through a number of focused experiments.

Labeling of the peptide either a fluorophore or a radiolabel would allow for the tracking of the peptide when supplemented into a culture flask containing cells. Following fixation of the cells, it would be possible to localize the peptides to either on the cell surface or within the cell itself. A cell surface localization would support the theory of a hybrid mechanism of action of the peptide. If the peptide could then be attached to biotin, it would be possible to either use immunoprecipitation or use a column in order to find and identify proteins that attach to the peptide. While this approach does not require *a priori* identification of candidate proteins that bind the peptide, it may not be a feasible approach given the low affinity of the peptide for any receptor that would exist. The last potential approach is a hypothesis driven approach in which specific signaling pathways would be targeted systematically in order to identify which pathways are important for exerting the peptide's effect *in vitro* and *in vivo*.

An attractive target of action of the cryptic peptide is via modulation of integrin signaling pathways (Agrez, Bates et al. 1991; Horton, Spragg et al. 1994; Xia and Zhu 2010). Integrins are important in stem cell chemotaxis (Chavakis, Aicher et al. 2005), and the cryptic peptide identified in the present chapter is derived from the collagen type III molecule, a protein known to bind to integrins (Humphries, Byron et al. 2006). Although the sequence of the cryptic peptide does not contain any known integrin binding motifs (Humphries, Byron et al. 2006), it is still possible that non-specific binding of integrins by the peptide may promote signaling through the integrin receptors. Future studies may investigate integrin mediated pathways.

3.4.3 *In vivo* Progenitor Cell Recruitment by the Cryptic Peptide

The recruitment of various cell types such as stem and progenitor cells, endothelial cells, and muscle precursor cells to sites of tissue injury represents a plausible host response to support tissue reconstruction. The mechanisms underlying such a recruitment process are largely unknown, but it is feasible that cryptic peptide-mediated recruitment represents one such strategy. The manner in which the oligopeptide described herein was generated was non-physiologic but a previous study has shown naturally occurring degradation products following ECM mediated tissue reconstruction have similar properties (Beattie, Gilbert et al. 2009). In fact, degradation products of ECM have been shown to regulate the site directed recruitment of differentiated (Davis, Bayless et al. 2000; Li, Li et al. 2004; Agrawal, Brown et al. 2009) and progenitor cells (Brennan, Tang et al. 2008; Reing, Zhang et al. 2009) *in vivo*.

However, the work in the present chapter focused upon a single cryptic peptide that is derived from a mixture of ECM degradation products. Both the single cryptic peptide and the mixture of ECM degradation products show chemotactic activity *in vitro*, and the work in the present chapter utilized a murine model of digit amputation to assess the *in vivo* ability of the peptide promote the site directed accumulation of progenitor cells. Although the outcomes in the present chapter focused only identification of progenitor cells by their expression of transcription factors and cell surface antigens associated with multipotent stem cells, work in chapter 2 showed that a subset of cells found at the site of amputation are capable of mesodermal and neuroectodermal differentiation *in vitro*. The work in the present chapter expanded upon the previous characterization of the Sca1+ population of cells by confirming that they did not express markers of differentiated cells found within the blood. Additionally, the work in the

present chapter confirmed that a subset of Sca1+ cells also co-expressed the progenitor cell marker Sox2, consistent with flow cytometric findings in the previous chapter.

Although treatment with the single cryptic resulted in the accumulation of the same population of Sca1+, Sox2+, Lin- cells that were found following treatment with unfractionated ECM degradation products, there was a marked difference in the time course of accumulation of these cells following peptide treatment. A peak in Sca1+ and Sox2+ cells was observed at day 14 post-amputation following treatment with unfractionated ECM degradation products, whereas the peak of accumulation of cells following treatment with the single cryptic peptide occurred at day 7 post-amputation. This difference is not due just to differences in the potency of the treatments because the peak numbers of Sox2+ and Sca1+ cells found at the site of amputation did not differ between the two treatments. As discussed in chapter 2, a critical difference between these two treatments may be their physical properties. Due to the presence of self-assembling collagen derived peptides in the unfractionated mixture, physiologic pH and temperature induced geleation of the ECM degradation products. However, the single purified cryptic peptide diluted to same protein concentration *in vitro* remained completely aqueous at physiologic pH and temperature. This differing physical property between the two treatments would likely result in a difference in bioavailability *in vivo*.

As discussed in chapter 2, a critical limitation of the digit amputation model of injury utilized is the method of treatment. Limited by a regional administration of treatment by subcutaneous injection at the base of amputated digit, a true assessment of the spatiotemporal concentration of any treatment has not been feasible. Thus, differing physical properties such as viscosity could affect both the spatial and temporal bioavailability of any treatment without any way of actually monitoring it. For example, an aqueous solution such as the single cryptic

peptide would likely diffuse faster as well as be excreted from the system quicker. Thus, any bioactive effect such as site directed accumulation of progenitor cells may occur earlier post-treatment, and the effect of peptide treatment would also be diminished that much more quickly. This is consistent with the findings of the present chapter.

Future studies will aim to mitigate this confounding factor by utilizing the BIODOME device discussed in Chapter whereby any treatment's spatiotemporal concentration can locally be controlled at the site of amputation.

3.4.4 Clinical Relevance of a Purified Chemotactic Peptide

Site specific recruitment of multipotent progenitor cells in response to limb amputation is a prerequisite for blastemal based epimorphic regeneration in species such as newts and axolotls (Kragl, Knapp et al. 2009). Soluble factors are present that can recruit selected cell types and selected genetic programs are activated to participate in the regeneration process that results in a perfect phenocopy of the missing tissue structure (Kumar, Godwin et al. 2007; Kragl, Knapp et al. 2009; Monaghan, Epp et al. 2009). While blastema formation does not occur following injury in adult mammalian species, recruitment to and/or directed differentiation of tissue specific progenitor cells at the site of injury has the potential to alter the default scar tissue wound healing response toward a more constructive tissue remodeling response (Lee, Cook et al. ; Kim, Xin et al. 2010). In organs such as the liver, bone marrow, and intestinal lining that are capable of mounting a regenerative response to injury, activation and recruitment of progenitor cell compartments is an important prerequisite to site appropriate tissue regeneration (Lewis and Trobaugh 1964; Lagasse, Connors et al. 2000; Barker, van Es et al. 2007). Thus, recruitment of multipotent progenitor cells to a site of injury in response to placement of a chemotactic peptide

may be considered as a form of endogenous stem or progenitor cell therapy. The clinical efficacy of such therapies, however, remains to be determined. However, while the previous chapter focused on using a less characterized mixture of peptides for treatment *in vitro* and *in vivo*, the present chapter's work focused on a single peptide. The potential for further characterization and understanding of the mechanisms of a single purified peptide subsequently also increases the translational potential of such a therapy.

4.0 ACCELERATION OF OSTEOGENESIS BY AN ISOLATED CRYPTIC PEPTIDE IN VITRO AND IN VIVO

4.1 INTRODUCTION

Sections of this chapter have been modified and adapted from (Agrawal, Kelly et al. 2011)

Biologic scaffolds composed of extracellular matrix (ECM) have been used to promote site-specific, functional remodeling of tissue in both preclinical animal models (Badylak, Lantz et al. 1989; Lantz, Badylak et al. 1990; Cobb, Badylak et al. 1996; Hodde, Badylak et al. 1997; Badylak, Meurling et al. 2000; Caione, Capozza et al. 2006; Zalavras, Gardocki et al. 2006; Ott, Matthiesen et al. 2008; Ott, Clippinger et al. 2010; Uygun, Soto-Gutierrez et al. 2010) and human clinical applications (Metcalf, Savoie et al. 2002; Witteman, Foxwell et al. 2009; Derwin, Badylak et al. 2010; Mase, Hsu et al. 2010). Following implantation of a non-crosslinked ECM scaffold at a site of injury, a dense mononuclear infiltrate (Valentin, Badylak et al. 2006; Badylak, Valentin et al. 2008) degrades the scaffold over the course of 60-90 days (Record, Hillegonds et al. 2001; Gilbert, Stewart-Akers et al. 2007). The degradation of the ECM scaffolds results in the release of small cryptic peptides with novel bioactivity not present in the parent ECM proteins (Davis, Bayless et al. 2000; Davis 2010). These cryptic fragments have been shown to possess antimicrobial, immunomodulatory, angiogenic and anti-angiogenic, mitogenic, and chemotactic properties, among others (Berkowitz, Bevins et al. 1990; Moore,

Devine et al. 1994; Moore, Beazley et al. 1996; Davis, Bayless et al. 2000; Ganz 2003; Li, Li et al. 2004; Adair-Kirk and Senior 2008; Agrawal, Brown et al. 2009). Additionally, cryptic fragments of ECM proteins have also been shown to be able to regulate the chemotaxis of a variety of progenitor cell populations *in vitro* and *in vivo* (Brennan, Tang et al. 2008; Crisan, Yap et al. 2008; Reing, Zhang et al. 2009; Tottey, Corselli et al. 2011).

To date, no studies have investigated the differentiation potential of cryptic peptides derived from degradation of ECM proteins. Findings of the previous chapter characterized a single cryptic peptide derived from the C-terminal telopeptide region of the collagen IIIα subunit, IAGVGGEKSGGF. Specifically, the work showed that the peptide had *in vitro* and *in vivo* chemotactic activity for multiple progenitor cells including human perivascular stem cells. An unexpected finding of the previous chapter was that the same peptide then repeatedly caused a bone nodule formation at the site of amputation. Although this was not discussed in the previous chapter, this finding is the subject of the present chapter. Specifically, the present chapter will show data that this cryptic peptide accelerates osteogenesis of mesenchymal stem cells *in vitro* and promotes the formation of a bone nodule at a site of digit amputation consistent with the presence of Sox2+, Sca1+, Lin- mesodermal progenitor cells identified in the previous chapters.

4.2   MATERIALS AND METHODS

4.2.1   Overview of Experimental Design

The experimental methods were designed to address the hypothesis that an isolated cryptic peptide, IAGVGGEKSGGF, alters osteogenesis *in vitro* and *in vivo*. Osteogenesis *in vitro* was assessed by measuring calcium deposition, alkaline phosphatase activity, and mRNA expression of osteogenic markers via quantitative RT-PCR. Osteogenesis was investigated *in vivo* in an established adult mammalian model of digit amputation (Schotte and Smith 1959; Schotte and Smith 1961). The deposition of calcium was determined by histologic examination as well as by injection of calcium dyes.

4.2.2   Peptide Synthesis

The cryptic peptide, IAGVGGEKSGGF, was chemically synthesized (GenScript, Piscataway, NJ). The peptide was reconstituted at a stock concentration concentration of 10 mM in sterile filtered calcium and magnesium free phosphate buffered saline.

4.2.3   Source of Cells and Culture Conditions

Human perivasular stem (PSC) cells, a perivascular progenitor cell population (Crisan, Yap et al. 2008), were isolated and prepared as previously described (Tottey, Corselli et al. ; Crisan, Yap et al. 2008). PSCs were cultured in high-glucose Dulbecco's modified Eagle's medium (DMEM, Invitrogen, Carlsbad, CA) containing 20% fetal bovine serum (FBS; Thermo, Pittsburgh, PA),

100 U/mL penicillin, and 100 μg/ml streptomycin (Invitrogen) at 37°C in 5% CO_2. PSCs were characterized by immunolabeling and flow cytometry. Human cortical neuroepithelium stem (CTX) cells and human spinal cord neural stem (SPC) cells were a gift from ReNeuron[TM]. CTX cells were cultured in DMEM:F12 supplemented with 0.03% human albumin solution, 100μg/ml human apo-transferrin, 16.2μg/ml putrescine DiHCl, 5μg/ml insulin, 60ng/ml progesterone, 2mM L-glutamine, 40ng/ml sodium selinite, 10ng/ml human bFGF, 20ng/ml human epidermal growth factor, and 100nM 4-hydroxytestosterone.

4.2.4 *In vitro* osteogenic differentiation and Alizarin red stain

PSC, CTX, or SPC cells were seeded at a density of 2×10^4 cells/well in 24 well plates. Following attachment, cells were cultured in either normal culture medium or osteogenic differentiation medium, consisting of DMEM containing 10% FBS, 100 U /ml penicillin, 100 μ g/ml streptomycin, 10 mM β-glycerophosphate (Sigma, St. Louis, MO, G9422), and 50 μ g/ml ascorbic acid (Sigma, A4544). Wells were supplemented to a final concentration of 0, 1, 10, or 100 μM of the cryptic peptide. At days 4, 7, 14, and 21, wells were fixed in 10% neutral buffered formalin and stained with 40 mM Alizarin red at pH 4.1 (Sigma, A5533). Semi-quantitative analysis of alizarin red staining was completed as previously described (Gregory, Gunn et al. 2004). Briefly, wells were stained for 20 minutes with 40 mM alizarin red and then washed twice with distilled H_2O. Following washing, wells were incubated in 400 μl of 10% acetic acid until complete destaining was achieved. Each well was then neutralized with 160 μ l of 10% ammonium hydroxide. The optical density of each sample to 405 nm wavelength light was then read measured on a spectrophotometer.

4.2.5   Alkaline Phosphatase staining

PSCs were seeded at a density of 2×10^4 cells/well in 24 well plates. At day 7 post-culture in either normal growth medium or osteogenic differentiation medium supplemented with 0, 1, 10, or 100 µM of peptide, cells were fixed for 2 minutes in 10% neutral buffered formalin. A subset of wells were stained with alkaline phosphatase substrate (Vector Labs, Burlingame, CA, SK-5100) and imaged. Semi-quantitative analysis of alkaline phosphatase activity was completed by incubating the second subset of wells in 0.5 mg/ml p-Nitrophenyl Phosphate (Thermo, Pittsburgh, PA, #37620) for 30 minutes at 37 ^{0}C in the dark prior to measuring the optical density of each sample to 405 nm light using a spectrophotometer.

4.2.6   Adipogenic Differentiation

PSCs were seeded in wells at a density of 2×10^4 cells/well in 24 well plates. Following cell attachment, cells were cultured in normal culture medium or adipogenic differentiation medium (Hyclone, Pittsburgh, PA, SH30886.02). Cells were fixed at days 7 and 14 in 10% neutral buffered formalin prior to staining with 0.5% Oil Red O solution (Alfa Aeasar, Ward Hill, MA) in 3:2 isopropanol:distilled H_2O for 30 minutes. Following washing twice with distilled H_2O. Semi-quantitative analysis of Oil Red O staining was completed as previously described (Trouba, Wauson et al. 2000). Briefly, wells were destained in 100% isopropanol for 30 minutes. Aliquots of each well were then read on a spectrophotometer for absorbance at 490 nm wavelength.

4.2.7 PCR studies

Following culture of PSCs in culture medium or osteogenic medium supplemented with either 0 or 100 µM peptide, cells were cultured for 4, 7, or 14 days. Cells were then incubated in Trizol solution (Invitrogen, 11596-018) for 15 minutes at room temperature. RNA was extracted from Trizol solutions using phenol-chloroform extraction, and RNA was converted to cDNA using DNA Superscript Assay (Invitrogen, 18080). Real time quantitative PCR was then carried out using SYBR green dye (Applied Biosystems, Carlsbad, CA, 4385614) on a BioRad iCycler iQ5 PCR machine. After initial denaturation at 95 ^{0}C for 3 minutes, PCR was run for 45 cycles, with each cycle consisting of: (1) melting at 95 ^{0}C for 10 seconds, (2) annealing for 30 seconds, and (3) extension at 72 ^{0}C for 30 seconds. PCR was carried out for osteogenic, chondrogenic, adipogenic, and housekeeping genes (Table 2). The annealing temperature for Col1, SPP1, LPL, and 1HAT was 60 ^{0}C, and the annealing temperature for ABCB1 and Runx2 was 62 ^{0}C. A housekeeping gene control, 23s, was run simultaneously for each gene marker at each annealing temperature.

Table 2. A list of primers used in the present chapter along with Accession Number and predicted product size.

Marker	Forward (5'-3')	Reverse (5'-3')	Accession Number	Size (bp)
SPP1	CTCCATTGACTCGAACGACTC	CAGGTCTGCGAAACTTCTTAGAT	NM_000582	230
Col1	ATGGATTCCAGTTCGAGTATGGC	CATCGACAGTGACGCTGTAGG	NM_000088	246
1HAT	AACTGCTTTTGGTTACAAGGGT	GAAGTAAGGTTCCGAATGGCTT	NM_003642	239
ABCB1	GGGAGCTTAACACCCGACTTA	GCCAAAATCACAAGGGTTAGCTT	NM_000927	154
Runx2	AGATGATGACACTGCCACCTCTG	GGGATGAAATGCTTGGGAACTGC	NM_001024630	125
LPL	AGGAGCATTACCCAGTGTCC	GGCTGTATCCCAAGAGATGGA	NM_000237	126
23s	GCACAGCCCTAAAGGCCAACCC	TCACCAACAGCATGACCTTTGCG	NM_001025	243

4.2.8 Animal Model of Digit Amputation

All methods were approved by the Institutional Animal Care and Use Committee at the University of Pittsburgh and performed in compliance with NIH Guidelines for the Care and Use of Laboratory Animals. Mid-second phalanx digit amputation of the third digit on each hindfoot in adult 6-8 week old C57/BL6 mice (Jackson Laboratories, Bar Harbor, ME) was completed as previously described (chapter 2). Following amputation, digits were either treated with a subcutaneous injection of 15 µL of 10 mM peptide, or the same volume of PBS as a carrier control (n=4 for each group). Treatments were administered at 0, 24 and 96 hours post surgery. Animals were sacrificed via cervical dislocation under deep isoflurane anesthesia (5-6%) at day 7, 14, 18, or 28 post-surgery. Digits were fixed in 10% neutral buffered formalin, decalcified for 2 weeks in 10% formic acid, and then sectioned at 5 µm thickness on to slides for further staining. Slides were either stained with Masson's trichrome stain or Alcian blue stain.

4.2.9 Calcium Dye Studies and Optical Clearance of Tissue

Analysis of *in vivo* calcium deposition was adapted from previous studies (Neufeld and Zhao 1995; Zhao and Neufeld 1995). Three days prior to digit amputation, mice were injected IP with 3.5 mg/kg green calcein dye (Invitrogen, C481). Mice then were subjected to digit amputation and treatment. One day prior to harvest, mice were injected IP with 50 mg/kg alizarin red calcium dye (Sigma, A5533). Animals were sacrificed on day 14 post-amputation via cervical dislocation under deep isoflurane anesthesia (5-6%). Isolated digits were then fixed in 4%

paraformaldehyde prior to serial dehydration in 25%, 50%, 75%, 95%, and 100% acetone. Following dehydration, fixed digits were then incubated in Dent's fixative (1:4 DMSO:acetone) for 2 hours. Then, the digits were permeablized and bleached overnight in Dent's bleach (1:4:1 DMSO:acetone:H_2O_2). Digits were then equilibrated to a clearing solution consisting of 1:2 benzyl alcohol (Sigma, 402834) to benzyl benzoate (Sigma, B6630) (BABB) by serial 1 hour incubations in 1:3, 1:1, and 3:1 solutions of BABB:Dent's fixative. Afterwards, digits were then kept in 100% BABB until they were visibly optically cleared. Optically cleared digits were then imaged using a Nikon E600 epifluorescent microscope at 100x magnification, and images were taken with a Nuance camera. Images were deconvolved with known spectra for alizarin red and calcein dye to identify new versus old depositions of calcium.

4.3   RESULTS

4.3.1   Peptide promotes bone formation *in vivo*.

Work in the previous chapter had shown that treatment with the single cryptic peptide in an established model of murine digit amputation (Schotte and Smith 1959; Schotte and Smith 1961) resulted in the accumulation of Sox2+, Sca1+, Lin- cells at day 7 post-amputation. An unexpected finding of the work was that a bone nodule was observed at the site of amputation at day 14 post-amputation that was not present in PBS or untreated amputated digits (Figure 32a). Differential calcium dye stains were to determine whether there was new calcium deposition at the site of amputation utilized (Neufeld and Zhao 1995; Zhao and Neufeld 1995) following peptide treatment. Following initial injection with a green calcein dye to label all bones green,

mice were subjected to mid-second phalanx amputation and treatment. On day 14 post-amputation, mice were injected with a second dye, Alizarin red, to label all new deposited calcium red. Following peptide treatment, more new calcium deposition was noted in the amputated P2 bone (Figure 32a). Additionally, Alcian blue and Trichrome staining showed that the bone-like nodule progressed from a glycosaminoglycan-rich structure with at day 14 post-amputation towards a collagenous nodule devoid of glycosaminoglycans at day 28 post-amputation, suggesting endochondral ossification as the primary mechanism of osteogenesis in *in vivo* (Figure 32b).
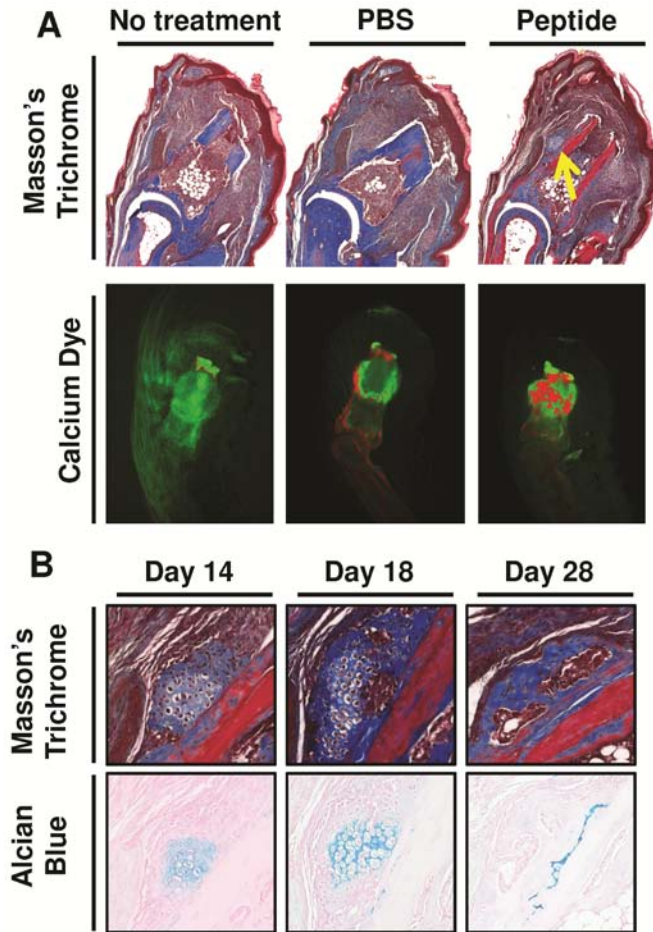
Figure 32. Cryptic peptide promotes bone deposition in an adult mammalian model of digit amputation. To determine whether the isolated cryptic peptide promotes osteogenesis *in vivo*, adult C57/BL6 mice were subjected to mid-second phalanx amputation and either left untreated, treated with PBS carrier control, or treated with the isolated cryptic peptide. (A) At day 14 post-amputation, histologic analysis revealed a bone-like nodule present at the site of amputation in the peptide treated group. Differential calcium dye injections showed that peptide treatment increases calcium deposition at the site of amputation. (B) Alcian blue stain showed that the bone nodule stained positive for glycosaminoglycans at early time points, suggesting that the nodule underwent endochrondral ossification. Images are representative of n=4 animals in each treatment group.

Work in the previous chapter had determined that the cellular accumulation seen at the site of amputation lateral to the amputated expressed Sox2 and Sca1, both markers of multipotent progenitor cells. The same site where these cells were found on d ay 7 post-amputation

100

histologically showed a bone nodule at day 14 post-amputation (Figure 33). Additionally, a time course analysis of Sox2+ cell expression and histomorphometric analysis of bone nodule growth showed that the growth of the bone nodule coincided with a decrease in Sox2+ cells (Figure 34). Thus, while not conclusively the only mechanism by which the bone nodule may form, one plausible hypothesis was that the mesodermal progenitor cells present lateral to the site of amputation eventually underwent osteogenic differentiation to give rise to the bone nodule. Thus, the remainder of the *in vitro* work aimed to determine the *in vitro* effect of peptide treatment upon osteogenic differentiation of a model mesenchymal stem cell, the human perivascular stem cell (Crisan, Yap et al. 2008).

Figure 33. Cellular accumulation correlates with bone nodule formation. Representative Trichrome images from day 7 post-amputation and day 14 post-amputation digits treated with the isolated cryptic peptide show that the accumulation of cells at the site of amputation spatially correlates with the bone nodule formation.
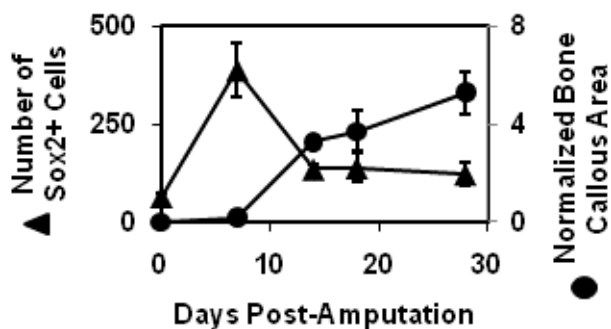
Figure 34. Immunohistochemical staining of Sox2 staining as well as histomorphometric analysis of bone growth showed that the increase in bone growth coincided with a decrease in Sox2+ cells, suggesting that Sox2+ cells may play a role in osteogenesis.

4.3.2   Peptide accelerates osteogenesis *in vitro*.

Following culture of human perivascular stem (PSC) cells in either normal growth medium or osteogenic differentiation medium supplemented with 0, 1, 10, or 100 μM peptide, calcium deposition by the cells was measured by Alizarin red staining. There was a dose-dependent increase in Alizarin red staining at days 7 and 14 post-treatment (Figure 35). By day 21 post-treatment, no significant difference in Alizarin red staining was noted between treatment groups. Culture of PSCs in normal growth medium supplemented with 0, 1, 10, or 100 μM peptide did not result in any changes in Alizarin red staining at any time point (Figure 35), suggesting that the isolated cryptic peptide accelerates osteogenesis only in conditions of osteogenic differentiation. Concomitant with increased calcium deposition, a dose dependent increase in alkaline phosphatase activity was observed on day 7 post-treatment with peptide in conditions of osteogenic differentiation (Figure 36).
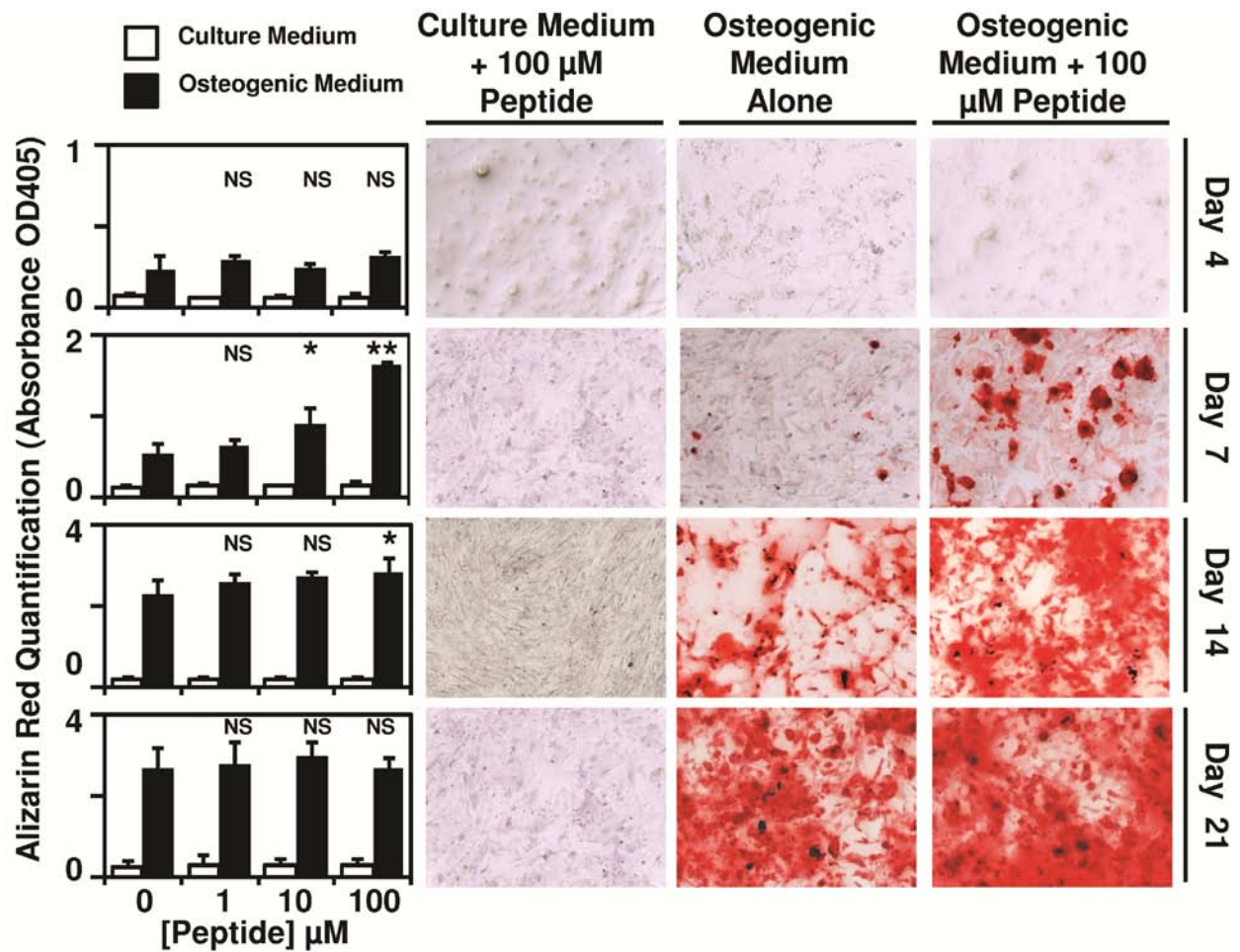
Figure 35. Cryptic peptide accelerates osteogenesis of perivascular stem cells. Human perivascular stem cells were cultured in either culture medium or osteogenic differentiation medium. Following supplementation of medium with 0, 1, 10, 100 µM of the isolated cryptic peptide, osteogenic differentiation was determined by Alizarin red stain of the cells. At 7 and 14 days post-differentiation, the isolated cryptic peptide accelerated osteogenesis of perivascular stem cells. *p < 0.05, ** p <0.01 as compared to the 0 µM osteogenic differentiation group. Error bars represent Mean ± SEM of experiments in triplicate (n=3).
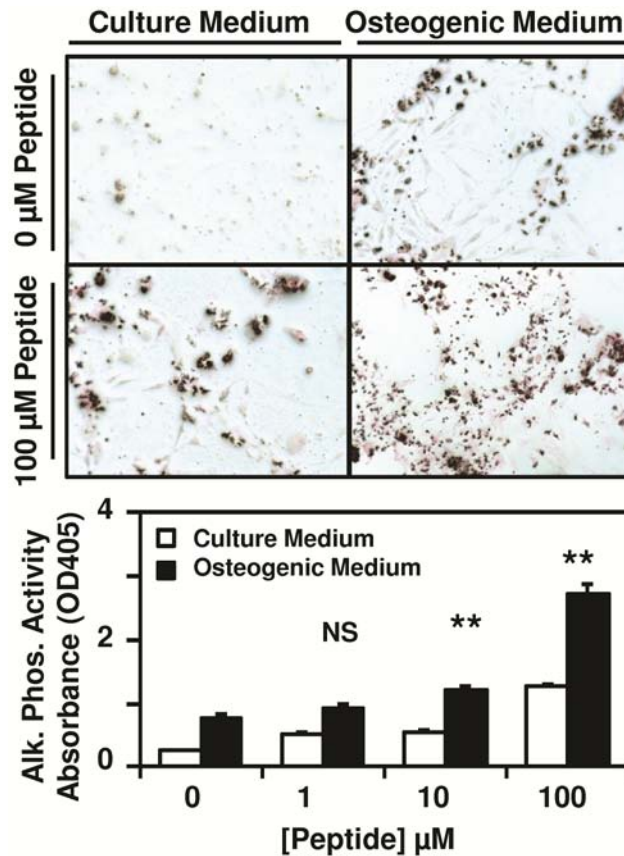
Figure 36. Cryptic peptide increases alkaline phosphatase activity. Human perivascular stem cells were cultured in either culture medium or osteogenic differentiation medium. Following supplementation of medium with 0, 1, 10, 100 μM of the isolated cryptic peptide, alkaline phosphatase activity was measured by PNPP substrate reaction and staining. At 7 days post-differentiation and treatment, the isolated cryptic peptide resulted in increased alkaline phosphatase activity. *p < 0.05, ** p <0.01 as compared to the 0 μM osteogenic differentiation group. Error bars represent Mean ± SEM of experiments in triplicate (n=3).

To determine whether the peptide promotes osteogenesis in stem cells not known to show osteogenic differentiation potential, human cortical neuroepithelial stem cells (CTX) and spinal cord neural stem cells (SPC) were cultured in normal growth medium or osteogenic differentiation medium supplemented with 0, 1, 10, or 100 μM peptide. PSCs cultured in osteogenic differentiation medium with no supplement was used as a positive control. At day 7

post-treatment, peptide treatment in normal growth medium or osteogenic differentiation medium did not result in calcium deposition and Alizarin red staining of CTX and SPC cells (Figure 37).
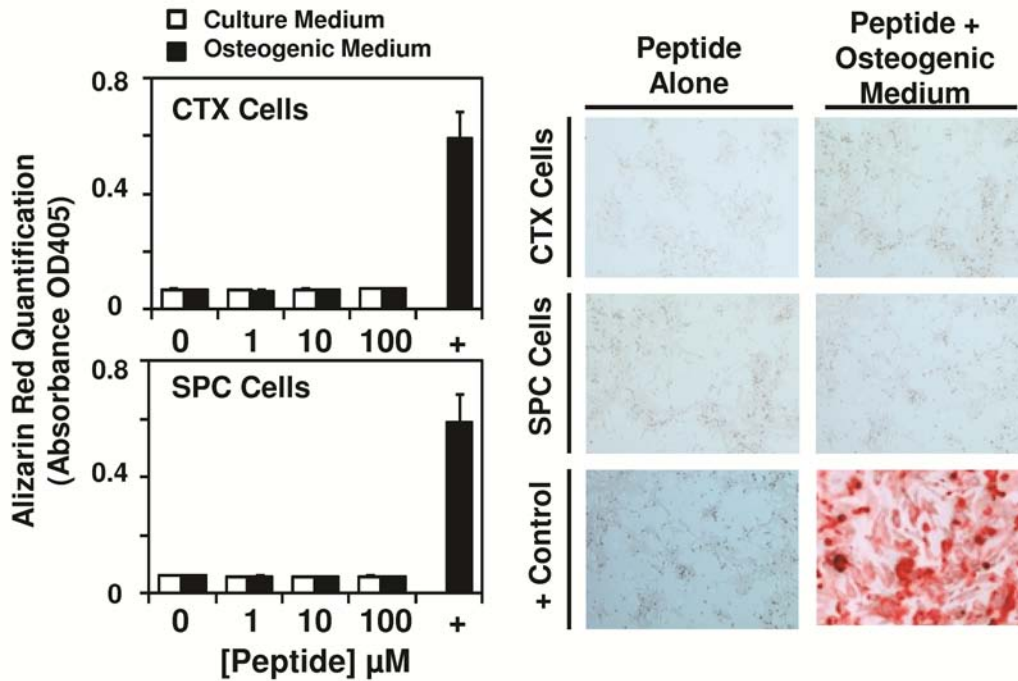
Figure 37. To determine whether the isolated cryptic peptide promotes osteogenic differentiation of non-mesenchymal stem cells, human cortical neuroepithelial stem cells and human spinal cord neural stem cells were cultured in normal culture medium or osteogenic differentiation medium in the presence of 0, 1, 10, or 100 μM of the isolated cryptic peptide. The isolated peptide did not promote osteogenic differentiation of the neural stem cells. Error bars represent Mean $\pm$ SEM of experiments in triplicate (n=3).

To confirm that the observed *in vitro* calcium deposition was due to true osteogenesis and not secondary to necrotic ossification from overgrowth of cells, the ability of the peptide to induce proliferation in human perivascular stem cells was assessed. Although unfractionated ECM degradation products induced mitogenesis of PSCs, consistent with previous studies (Tottey, Corselli et al. 2011), no change in PSC proliferation was observed in response to treatment with the cryptic peptide (Figure 38). Because no differences were noted in cell number

between peptide treated groups and negative controls, the calcium deposition observed in response to peptide treatment cannot be secondary to selective overgrowth in peptide treated groups.
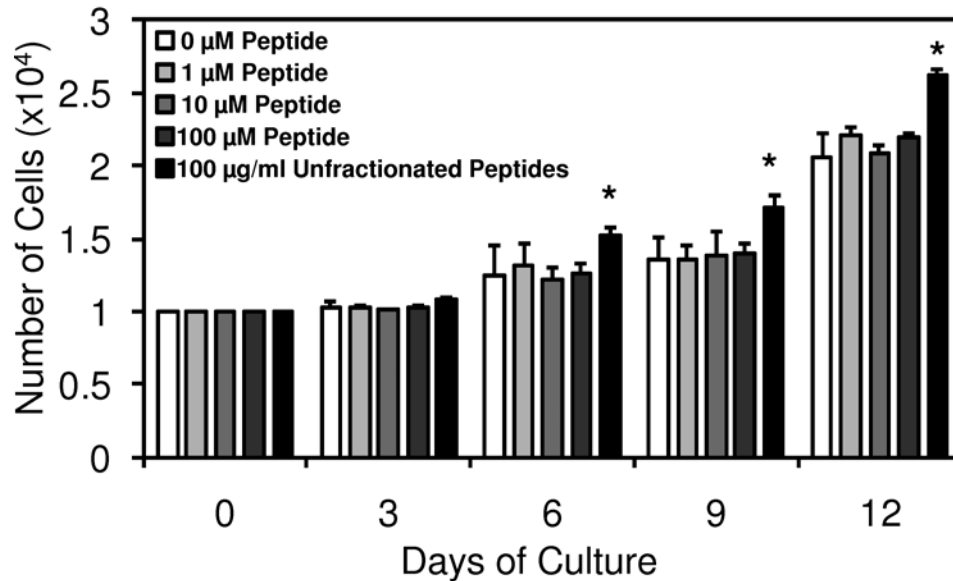
Figure 38. Cryptic peptide does not alter proliferation of perivascular stem cells. To determine whether the peptide induced osteogenesis by increasing proliferation of cells, perivascular stem cells were supplemented in normal growth medium supplemented with 0, 1, 10, or 100 µM peptide, or 100 µg/ml of unfractionated cryptic peptides as a positive control (Tottey, Corselli et al. 2011). Over the course of 12 days, no change in cell number was observed following culture in any concentration of cryptic peptide. *$p < 0.05$ as compared to normal growth medium at each time point. Error bars represent Mean $\pm$ SEM of experiments in triplicate (n=3).

4.3.3   Peptide does not alter adipogenesis *in vitro*.

To determine whether the peptide alters the differentiation of PSCs along other mesenchymal lineages in addition to osteogenesis, PSCs were cultured in normal growth medium or adipogenic differentiation medium supplemented with 0, 1, 10, or 100 µM peptide. Although an increase in

Oil Red O staining was noted in conditions of adipogenic differentiation at days 7 and 14 post-treatment, peptide treatment did not alter the rate of adipogenesis (Figure 39).
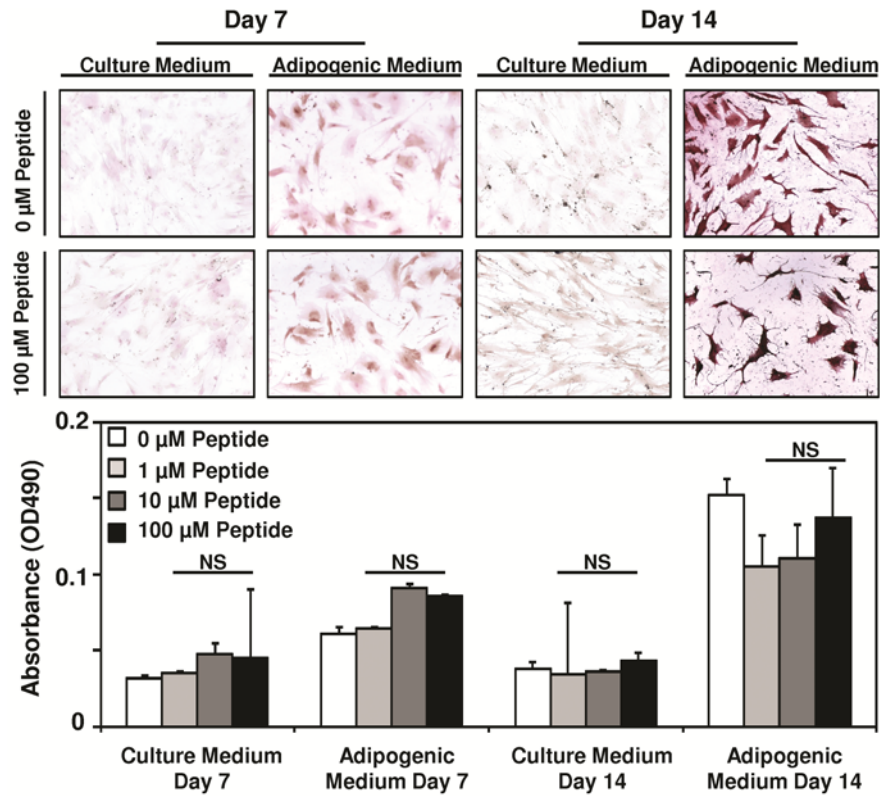
Figure 39. Cryptic peptide does not alter adipogenesis of perivascular stem cells. Human perivascular stem cells were cultured in either culture medium or adipogenic differentiation medium. Following supplementation of medium with 0, 1, 10, 100 μM of the isolated cryptic peptide, differentiation was determined by Oil Red O stain. No differences were noted between treatment groups at any time point. Error bars represent Mean ± SEM of experiments in triplicate (n=3).

4.3.4   Peptide promotes expression of osteogenic and chondrogenic markers in human perivascular stem cells.

To determine whether the cryptic peptide accelerates osteogenesis by increasing mRNA expression of osteogenic genes, PSCs were cultured in either normal growth medium, growth

medium supplemented with 100 µM cryptic peptide, osteogenic differentiation medium alone, or osteogenic medium supplemented with 100 µM cryptic peptide. At 4 days post-culture, peptide treatment did not significantly change the expression of osteogenesis-related genes Collagen I, Runx2, or Osteopontin (SPP1). However, supplementation of the peptide in osteogenic medium resulted in a significant increase in Collagen I and Osteopontin expression in PSCs (Figure 40). Peptide treatment alone also resulted in a significant increase in the expression of the chondrogenic gene, ABCB1, and peptide supplementation of osteogenic medium resulted in a significant increase in expression of both chondrogenic genes, ABCB1 and 1HAT (Figure 40). No mRNA expression of lipoprotein lipase, a marker of adipogenesis, was observed through 45 cycles of qRT-PCR.
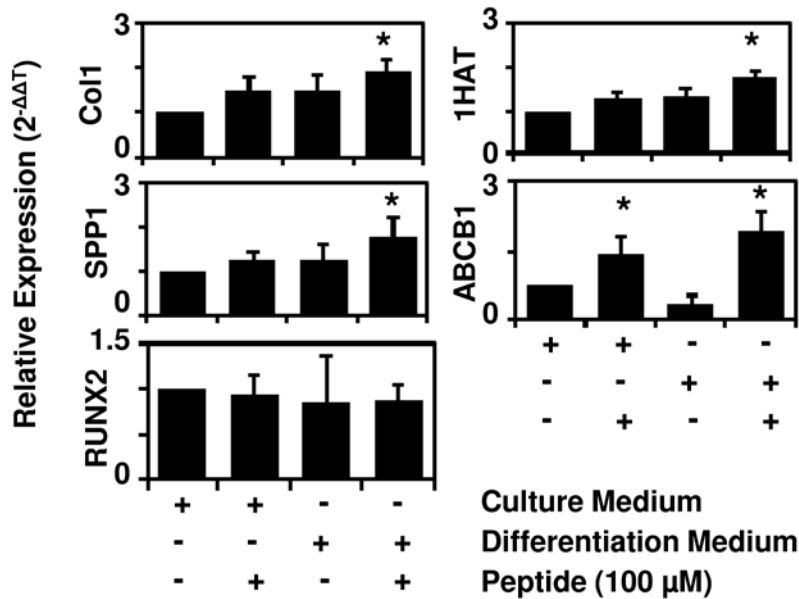
Figure 40. Cryptic peptide increases expression of osteogenic and chondrogenic genes *in vitro*. To determine whether the cryptic peptide accelerates osteogenesis by increasing mRNA expression of osteogenic genes, perivascular stem cells were cultured for 4 days in normal growth medium or osteogenic medium unsupplemented or supplemented with 100 µM cryptic peptide. Osteogenic medium supplemented with peptide resulted in a significant increase in Collagen I, Osteopontin (SPP1), 1HAT, and ABCB1 expression. No expression of LPL was

observed over 45 cycles of RT-qPCR. * p < 0.05 as compared to normal growth medium for each gene. Error bars represent Mean $\pm$ SEM of six experiments (n=6).

4.4 DISCUSSION

4.4.1 Osteogenic Activity of Cryptic Peptides

The work of the present chapter identified a novel property of a cryptic peptide previously shown to possess chemotactic activity in chapter 3. The cryptic peptide accelerated osteogenic differentiation of human perivascular stem cells (PSC), and treatment with the cryptic peptide at a site of digit amputation *in vivo* resulted in formation of calcified bone at the site of amputation. An increasing body of literature has begun to recognize the importance of cryptic fragments of proteins that contain novel activity not associated with their parent molecules. Collectively referred to as the "cryptome" (Davis, Bayless et al. 2000; Autelitano, Rajic et al. 2006; Ng and Ilag 2006; Pimenta and Lebrun 2007; Mukai, Hokari et al. 2008; Mukai, Seki et al. 2009; Davis 2010), various peptides have been identified to show bioactive properties including antimicrobial, pro- and anti-angiogenic, chemotactic, and mitogenic activity (Berkowitz, Bevins et al. 1990; Moore, Devine et al. 1994; Moore, Beazley et al. 1996; Davis, Bayless et al. 2000; Ganz 2003; Li, Li et al. 2004; Adair-Kirk and Senior 2008; Agrawal, Brown et al. 2009). The present study shows that such cryptic peptides may also be able to affect the differentiation of stem cells. Since stem cell are known to home to sites of inflammation and participate in the injury response, the release of cryptic peptides with the ability to alter stem cell differentiation at

the site of injury may be a conserved, desirable response to promote tissue reconstruction following injury.

The cryptic peptide used in the present study is derived from the C-terminal telopeptide of collagen III, a region known to be enzymatically cleaved and released into the circulation following soft tissue injury (Kitahara, Takeishi et al. 2007; Banfi, Lombardi et al. 2010; Kanoupakis, Manios et al. 2010). However, most trauma does not lead to spontaneous bone formation at the site of injury secondary to the release of cryptic peptides such as the one identified in the present study. Following an injury, there are likely thousands of peptides released from wound sites, and the cryptic peptide in the present study would only be one of many peptides that exert an overall *net* effect upon differentiation of local stem cells. It is likely that cryptic peptides exist which can not only promote differentiation of stem cells, as shown in the present study, but also can inhibit differentiation. The present study investigated the activity of a single cryptic peptide by injecting supra-physiologic concentrations *in vivo*, many orders of magnitude greater than the concentrations of other cryptic peptides that would be expected to be released from a site of digit amputation.

4.4.2 Injury Dependence of Peptide's Osteogenic Activity: Implications and Clinical Relevance

The findings of the present chapter show that the cryptic peptide depends on an osteogenic microenvironment in order to promote osteogenesis *in vitro* and *in vivo*. The dependence of the cryptic peptide's osteogenic activity upon the microenvironment is an interesting property with potential therapeutic implications. There are many well known osteogenic growth factors such as bone morphogenic protein that have been used with varying degrees of success to induce and/or

110

promote bone growth *in vivo* (Dickinson, Ashley et al. 2008; Rogozinski, Rogozinski et al. 2009). However, in many cases, these growth factors also promote heterotopic ossification at sites where osteogenesis is not desired, in addition to other side effects (Mannion, Nowitzke et al. 2010). The cryptic peptide in the present study only enhanced osteogenesis of perivascular stem cells *in vitro* when cultured in the presence of osteogenic differentiation medium. Additionally, peptide treatment only resulted in the formation of a bone nodule lateral to the amputated bone at the site of amputation, i.e. an active site of periosteal injury/inflammation. Bone injury *in vivo* locally activates pathways of bone deposition and osteogenesis (Ai-Aql, Alagl et al. 2008). Furthermore, injury to the periosteum that surrounds the bone activates latent PSCs within the periosteum (De Bari, Dell'Accio et al. 2006) to promote osteogenesis (Zhang, Xie et al. 2005). The present study found bone nodule formation *in vivo* only lateral to the bone, consistent with a l ocation where activated periosteal mesenchymal stem cells (MSC) would likely promote osteogenesis.

The microenvironmental niche at a site of injury is a complex, important determinant of a host response to injury (Lutton and Goss 2008). Previous studies have extensively examined the role of the microenvironmental niche in controlling stem cell adhesion, migration, and differentiation (Watt and Hogan 2000). In addition to cues from nearby cells (Chow, Lucas et al. 2011) and biophysical cues from the environment (Keung, Kumar et al. 2010), extracellular cues are thought to regulate stem cell behavior in an injury microenvironment (Jackson, Majka et al. 2001; Majka, Jackson et al. 2003; Kienstra, Jackson et al. 2008; Discher, Mooney et al. 2009). While the present study shows a novel property of cryptic peptides that may contribute to the regulation of stem cell behavior at a site of injury, it also shows that the microenvironment itself plays a reciprocal role in altering the activity of cryptic peptides. In the absence of osteogenic

differentiation conditions, the cryptic peptide utilized in the present study shows no osteogenic activity. Additionally, the peptide only induces bone formation at a site of amputation *in vivo*. It is possible that a co-stimulatory growth factor or molecule is present in an osteogenic microenvironment that is necessary for the peptide's mode of action. It is also possible that the cryptic peptide activates a signaling pathway that acts in synergy with existing activated osteogenic signaling pathways to enhance osteogenesis. An attractive target of action of the cryptic peptide in the present study is via modulation of integrin signaling pathways (Agrez, Bates et al. 1991; Horton, Spragg et al. 1994; Xia and Zhu 2010). Integrins are important in both osteogenesis (Shih, Tseng et al. 2011) and stem cell chemotaxis (Chavakis, Aicher et al. 2005), both properties of the cryptic peptide in the present study. Future studies will further investigate these mechanisms.

4.4.3   Future Studies

In addition to studies investigating the mechanism by which the peptide accelerates osteogenesis of mesenchymal stem cells *in vitro* (potential approaches to elucidating a mechanism were discussed in Chapter 3), a number of future studies can further investigate the osteogenic activity of the single cryptic peptide.

The present study only administered peptide at a site of injury where a basal amount of ostoegenesis would be expected following bone injury. Although *in vitro* studies suggest that the the effect of the peptide is specific to osteogenesis and requires an osteogenic microenvironment to be effective, this could be tested *in vivo* by administrering the same peptide in a non-osteogenic environment. For example, the peptide could be injected subcutaneously in an injured muscle as well at a site of muscle injury to determine the injury-dependent and injury-

independent osteogenic properties of the cryptic peptide. The effect of peptide treatment in these cases may not only confirm the *in vitro* findings of the present chapter, but also may offer more clues as to the mechanisms by which the peptide exerts its effect.

In summary, the present study identified a novel property of a cryptic peptide derived from C-terminal telopeptide region of the collagen IIIα molecule. The cryptic peptide selectively enhanced osteogenesis *in vitro*, and treatment with the peptide resulted in the formation of a bone nodule lateral to the amputated bone in a mouse model of digit amputation. While further work is necessary to identify the mechanisms of action of the cryptic peptide, the identification of cryptic peptides capable of altering stem cell differentiation is a novel property not previously attributed to cryptic peptides. In addition to potential therapeutic implications for the treatment of bone injuries and chronic diseases, cryptic peptides with the ability to alter stem cell recruitment and differentiation at a site of injury may serve as powerful new tools for influencing stem cell fate in the local microenvironmental niche.

5.0   DISSERTATION SYNOPSIS, GENERAL DISCUSSIONS, AND FUTURE DIRECTIONS

The findings of the present thesis aimed to establish a link between the *in vitro* and *in vivo* chemoattractive properties of degradation products of ECM scaffolds for progenitor cells, with a long term goal of using ECM degradation products as a potential therapy for site directed recruitment of progenitor cells and constructive remodeling of more complex tissues such as limbs and digits. Because species capable of limb regeneration do so via local recruitment of multipotent stem cells (Kragl, Knapp et al. 2009), the use of ECM degradation products in adult mammals following digit amputation might serve as a form of "endogenous stem cell therapy" to alter the default wound healing response of scar tissue deposition at a site of amputation.

In order to understand the *in vivo* bioactive properties of ECM degradation products, the work in the present thesis specifically addressed three aims. It showed that *ex vivo* generated ECM degradation products were chemotactic for progenitor cells *in vitro* and promoted the site directed recruitment of progenitor cells *in vivo*. Additionally, a single cryptic peptide was isolated from the mixture of ECM degradation products with similar *in vitro* and *in vivo* properties for progenitor cells. Although the contribution of this single peptide to the net chemotactic effects of ECM degradation products was not elucidated and the mechanisms by which the single cryptic peptide exerts its effect were not determined, the identification of a single ECM cryptic peptide with chemotactic potential for progenitor cells is the first to be

reported in the literature. Finally, the work in the present thesis also identified a new property of ECM cryptic peptides by showing that a single cryptic peptide had the potential to alter progenitor cell differentiation *in vitro* and *in vivo*, specifically along an osteogenic lineage.

Nevertheless, the results of the present thesis identified a number of questions that remain. As such, these are potential future avenues of investigation that will not only serve to further confirm the findings of the present thesis, but also give new insight into the biological basis for ECM scaffold mediated constructive remodeling at a site of injury. Additionally, these future avenues of investigation may identify new therapeutic strategies as well as molecular targets by which to further influence a site of injury and alter the default wound healing response from scar tissue deposition towards more of a regenerative response.

One of the predominant themes in the discussion that follows is the establishment of links between the various known mechanisms by which ECM scaffolds remodel. As discussed in the introduction of the present thesis, the mechanisms by which ECM scaffolds exert their constructive remodeling effect *in vivo* are only partially understood. However, based on previous studies, four potential mechanisms have been identified: [1] rapid degradation of the ECM scaffold, [2] site directed recruitment of differentiated and progenitor cells, [3] mechanotransduction through the implanted scaffold, and [4] polarization of the local immune cells at the site of scaffold implantation. Although previous have studies have focused on understanding these phenomena separately, the present thesis attempted to establish a link between two of these mechanisms. Specifically, the present thesis showed that ECM degradation products may be responsible for site directed recruitment of progenitor cell recruitment to a site of ECM scaffold implantation that has previously been observed.

Previous studies have unequivocally showed that rapid degradation of ECM is an essential prerequisite for constructive remodeling of tissue to occur at a site of ECM implantation (Valentin, Stewart-Akers et al. 2009). Thus, the proceeding discussion focuses on future studies that either directly or indirectly addresses a global hypothesis that the existence of ECM degradation products and cryptic peptides may be the precipitating factor for other downstream events of constructive remodeling: immune cell polarization, rapid angiogenesis, and site directed recruitment of differentiated and progenitor cells.

The findings of the present thesis showed that the existence of injury was an essential prerequisite to accumulation of progenitor cells, potentially suggesting that ECM degradation products may interact with the immune system. While mechanotransduction itself was not investigated in the present thesis, the findings of the present thesis highlight the importance of the local injury microenvironment in dictating the response to injury. Finally, if in fact ECM degradation products are the unifying link between all of the proposed mechanisms by which ECM scaffolds exert their constructive remodeling effect, then molecular signaling pathways that are common to all mechanisms discussed may be responsible for mediating the effect of ECM degradation products upon cells.

5.1 DIRECT ASSESSMENT OF THE ROLE OF ECM DEGRADATION IN CONSTRUCTIVE REMODELING AFTER SCAFOLD IMPLANTATION

Although the present attempted to establish a link between bioactive cryptic peptide released from ECM degradation and the subsequent site-directed accumulation of progenitor cells that has been observed in previous studies (Badylak, Park et al. 2001; Zantop, Gilbert et al. 2006), the

116

work of the present thesis did not directly address the necessity of ECM degradation for subsequent progenitor cell recruitment. Two critical limitations of the digit amputation model utilized in the present work were the type of treatment used and the lack of regeneration following treatment. Previous studies that have shown that ECM scaffolds promote constructive remodeling generally utilized a sheet or compacted form of ECM scaffolds (Badylak, Hoppo et al. ; Mase, Hsu et al. ; Badylak, Lantz et al. 1989; Lantz, Badylak et al. 1990; Lantz, Badylak et al. 1992; Kropp, Eppley et al. 1995; Prevel, Eppley et al. 1995; Clarke, Lantz et al. 1996; Kropp, Rippy et al. 1996; Pope, Davis et al. 1997; Badylak, Meurling et al. 2000; Badylak, Kokini et al. 2001; Record, Hillegonds et al. 2001; Badylak, Kokini et al. 2002; Badylak, Vorp et al. 2005; Kochupura, Azeloglu et al. 2005; Robinson, Li et al. 2005; Badylak, Kochupura et al. 2006; Lopes, Cabrita et al. 2006; Ota, Gilbert et al. 2007). While other studies have also shown that inhibition of ECM degradation (Valentin, Stewart-Akers et al. 2009), studies thus far have not directly investigated the importance of degradation of the scaffold upon subsequent progenitor cell recruitment. In the studies that have tried to alter scaffold degradation, the methods used to inhibit degradation (cross-linking and macrophage depletion) may have other confounding effects *in vivo* besides inhibition of ECM degradation. Cross-linking not only alters the degradation of the scaffold, but also then affects surface topology and macromolecular composition of the scaffold. Macrophage depletion not only inhibits phagocyte mediated degradation of the scaffold, but also eliminates the contribution of the innate immune response to injury and remodeling (both positive and negative contributions).

Thus, it is necessary to utilize a more versatile model of injury where ECM implantation results in the formation of functionally appropriate tissue and no treatment results in a poor outcome. To partially address these questions, preliminary work in the laboratory has resulted in

the development of a murine model of volumetric muscle injury (section 5.6.3). In such a model, it is possible to fill the defect with a powdered ECM construct that then facilitates constructive remodeling of the muscle tissue. The advantage of such a model, though, is that the volumetric defect can be filled with any of a number of scaffolds. To directly address the importance of ECM degradation upon subsequent constructive remodeling, the defect could be filled with: [1] ECM degradation products, [2] a normal ECM construct, [3] a cross-linked ECM construct, [4] normal ECM construct with macrophage depletion, and [5] a normal ECM construct with protease inhibitors within the scaffold. The use of these four treatments groups spans the spectrum of ECM degradation by using a treatment method where ECM is completely degraded as well as three separate methods where ECM degradation is inhibited. The volumetric construct allows for the inclusion of protease inhibitors in the three dimensional ECM construct, and this treatment option theoretically accounts for many of the confounding factors in previously utilized methods of inhibiting ECM degradation (Valentin, Stewart-Akers et al. 2009). It is possible that the protease inhibitors themselves may interact with the innate host response to injury and/or have other undesirable side effects, but this would be addressable with control untreated mice that are only locally administered protease inhibitors.

Such a model would be very powerful for addressing the effect of ECM degradation and/or subsequent cryptic peptide release upon any of the mechanisms by which ECM scaffolds remodel. It would be possible to determine a correlation between ECM scaffold degradation and immune cell polarization, rapid angiogenesis, mechanotransduction, or progenitor cell recruitment. More importantly, any alterations could then be causally linked to overall constructive remodeling and restoration of functional muscular tissue. Future studies may investigate this.

118

5.2 THE IMPORTANCE OF INJURY IN ECM-MEDIATED RECRUITMENT OF PROGENITOR CELLS *IN VIVO*: PARACRINE EFFECTS OF IMMUNE CELLS

A key finding of the present thesis that was not further discussed was the importance of the injury in ECM degradation product mediated progenitor cell recruitment *in vivo*. In the absence of any injury, and specifically in the absence of a bone type of injury, there was a severe reduction in the number of cells expressing markers of progenitor cells at a site of digit amputation. These findings suggest that some component of the injury is critical for ECM-mediated recruitment of progenitor cells.

As discussed in chapter 1, one possible explanation for this dependence on injury is that the effect of ECM degradation products upon progenitor cell recruitment occurs through a immune system derived secondary mediator. Given the peak accumulation of progenitor cells at 14 days post-amputation, even though treatment with ECM degradation products ceased after 4 days post-amputation, it is likely that the direct of ECM degradation products is on another cell present at the site of injury at the time. Within the context of the time course of immune cell infiltration at a wound site, macrophages would be abundant at the site of injury when ECM degradation products were locally administered. Furthermore, given the abundant evidence showing the importance of macrophages in tissue regeneration (Valentin, Stewart-Akers et al. 2009), and specifically given the importance of local macrophages in ECM scaffold mediated constructive remodeling at a site of injury,. (Friedenstein, Piatetzky et al. 1966; Allman, McPherson et al. 2001; Badylak, Valentin et al. 2008; Brown, Valentin et al. 2009; Valentin, Stewart-Akers et al. 2009), it is plausible that macrophages may be the secondary mediator by which ECM degradation exert their effect upon progenitor cells *in vivo*.

Although the present thesis did not directly address this question, preliminary evidence suggests that macrophages may, in fact, play a role in promoting progenitor cell recruitment (section 5.6.2). Expanding upon previous studies showing that activated macrophages can have a paracrine effect upon progenitor cell migration *in vitro* (Lolmede, Campana et al. 2009), preliminary studies conducted *in vitro* with a human monocyte/macrophage THP-1 cell line suggest that paracrine factors released by macrophages in response to ECM degradation products may be chemotactic for multiple progenitor cell populations (section 5.6.2). In fact, one of the potential molecules released by the macrophages has been identified as HMGB1, a high mobility group protein that plays reciprocal roles in both tissue regeneration and septic shock (Bianchi 2007; Campana, Bosurgi et al. 2008). In fact, in regenerative conditions, HMGB1 is known to possess chemotactic properties for multiple differentiated and progenitor cell types (Porto, Palumbo et al. 2006; De Mori, Straino et al. 2007; Lolmede, Campana et al. 2009; Ranzato, Patrone et al. 2009).

Although it ma y seem surprising that HMGB1 may play a role in ECM mediated progenitor cell recruitment, there are many reasons that ECM scaffolds may exert their effect at least partially through molecules such as HMGB1. HMGB1 has increasingly been recognized as a part of a family of proteins known as damage associated molecular patterns (DAMPs), proteins that are released systemically following injury to cells to signal that damage has occurred (Bianchi 2007). Because the methods u tilized to create ECM scaffold require mechanical, chemical, and enzymatic methods of removal of cellular components (Crapo, Gilbert et al. 2011), clearly many components of cell debris may be left over in the resulting scaffold (Gilbert, Freund et al. 2009) which could exhibit properties of DAMPs. Unpublished data from our laboratory suggests that HMGB1 is one of these DAMPs that can be found in scaffolds even after

decellularization has been completed to meet well accepted standards (Crapo, Gilbert et al. 2011).

Thus, the role of DAMPs within the scaffold as well as other DAMPs known to be released by local inflammatory cells at a site of injury may be an important mechanism by which ECM scaffolds exert their constructive remodeling effect *in vivo*. As such, the role of DAMPs in the host response to biomaterials, and the subsequent effect of this interaction upon the overall remodeling response, is an area of research that requires further study.

5.3   THE BIODOME AND THE ABILITY TO CONTROL THE MICROENVIRONMENT OF THE SITE OF AMPUTATION

As discussed throughout the thesis, one of the main limitations of the approach undertaken in the present thesis to recruit multipotent stem cells to a site of injury was the lack of constructive remodeling in the digit following amputation, treatment, and progenitor cell recruitment. As such, the findings of the present thesis are most consistent with the initial phase of non-blastemal epimorphic regeneration. The next step in non-blastemal epimorphic regeneration is spatiotemporally appropriate proliferation, self-renewal, and differentiation of the recruited multipotent progenitor cells, a process that is dependent on the microenvironment of the injury (Watt and Hogan 2000; Kumar, Godwin et al. 2007; Lutton and Goss 2008; Kragl, Knapp et al. 2009; Monaghan, Epp et al. 2009; Keung, Kumar et al. 2010; Tottey, Corselli et al. 2011).

Thus, progress in tissue engineering of more complex and composite tissues may require a more precise ability to control the microenvironment of the site of injury. As discussed in previous chapters, one approach to more precisely controlling the injury microenvironment may

121

be through the use of a microfluidic device that covering the site of amputation and is capable of controlling various properties of the injury microenvironment including hydration, pH, temperature, electrical potential, and concentrations of bioactive factors (Hechavarria, Dewilde et al.). In collaboration with the Automation & Robotics Research Institute (ARRI) at the University of Texas Arlington, a prototype device designated as the BIODOME (Biomechanical Interface for Optimized Delivery of MEMS Orchestrated Mammalian Epimorphosis) has been developed for an adult mouse model of digit amputation (section 5.6.1). Preliminary evidence suggests that treatment with the isolated cryptic peptide used in the present thesis results in a similar accumulation of heterogeneous cells at the site of amputation, but the cells are only capable of osteogenic differentiation potential (section 5.6.1). This finding is consistent with the unexpected finding that the peptide altered osteogenesis of progenitor cells *in vitro*.

Future studies will further investigate the use of the BIODOME for both therapeutic purposes as well as a scientific tool to better understand the role of various components of the injury microenvironment in constructive remodeling.

5.4   ECM DEGRADATION AND THE IDENTIFICATION OF OTHER CRYPTIC PEPTIDES

In the present thesis, ECM degradation products were created *ex vivo* utilizing pepsin mediated digestion of ECM scaffolds. The resulting soluble solution was considered a model of ECM degradation products. While not similar to the type of ECM degradation that would be expected at a site of injury following implantation of an ECM scaffold, previous studies have shown that the peptide mixture of pepsin-digested ECM scaffolds does show repeatable bioactivity for

multiple cells *in vitro* (Brennan, Reing et al. 2006; Crisan, Yap et al. 2008; Agrawal, Brown et al. 2009; Reing, Zhang et al. 2009; Tottey, Johnson et al. 2010). The work in the present thesis focused specifically on its net chemotactic effect upon multiple progenitor cells *in vitro* (Brennan, Tang et al. 2008; Crisan, Yap et al. 2008; Reing, Zhang et al. 2009; Tottey, Johnson et al. 2010; Tottey, Corselli et al. 2011). The work in the present thesis identified a specific cryptic peptide from this mixture that can partially recapitulate the net effect of the unfractionated ECM degradation products.

Given the framework provided in the present thesis for isolation of a specific peptide from a mixture of peptides with a net bioactive effect, a very tangible future direction is the further identification of peptides from the pepsin-digested ECM degradation products. Because the effect of the mixture is a *net* effect, it is likely that both pro- and anti-chemotactic peptides exist within the mixture of ECM degradation products. Given the low potency of the isolated cryptic peptide in the present thesis, it is likely that there are many other peptides that exist within the ECM degradation product mixture that contribute to the *net* chemotactic effect that is seen *in vitro* and *in vivo*. Identification of these peptides could result in the creation of an optimal mixture of specific peptides that is chemotactic for progenitor cells *in vitro* and *in vivo*.

Additionally, utilizing the same methods for fractionation and isolation of a peptide, future studies can purify a peptide with other bioactive properties. Previous studies have shown that degradation products of ECM have both mitogenic (Reing, Zhang et al. 2009) and antibacterial properties (Brennan, Reing et al. 2006) in addition to the chemotactic properties that were the focus of the present thesis. The present thesis also showed that at least a subset of the ECM degradation products is able to alter the rate of progenitor cell differentiation *in vitro*. Fractionation of the ECM degradation products and further fractionation based on an assay other

than a Boyden chamber migration assay might allow for the purification and identification of other bioactive peptides with these properties.

Of specific interest to the work in the present thesis is the identification of peptides and treatments that can influence the differentiation of progenitor cells. Serendipitously, the cryptic peptide isolated in the present thesis altered the rate of osteogenic differentiation of human perivascular stem cells *in vitro*. However, because the fractionation scheme was meant to purify a peptide based on human perivascular stem cell chemotaxis and not based on osteogenic differentiation, it is not known whether other peptides exists that would more potently promote osteogenic differentiation. Additionally, it is possible that peptides also exist that would inhibit osteogenic differentiation. Finally, cryptic peptides may exist that might accelerate or decelerate the rate of differentiation of stem cells along other lineages such as chondrogenesis, adipogenesis, and myogenesis. Identification of such peptides would result in a library of peptides that could be utilized to influence and/or control the differentiation of progenitor cells *in vitro* or *in vivo* at a site of injury.

5.5   DIFFERENTIAL SIGNALING THROUGH INTEGRINS: A POTENTIAL STRATEGY FOR CONTROLLING STEM CELL FATE *IN VITRO* AND *IN VIVO*

The findings of the present thesis suggest that ECM degradation products may play an important role in the ECM mediated constructive remodeling response. While multiple ECM cryptic peptides have been identified with novel abilities to modulate and initiate pathways such as angiogenesis, mitogenesis, and chemotaxis that are not associated with the parent ECM

molecules from which the peptides are derived, the mechanisms underlying these novel bioactive properties are not well understood (Davis, Bayless et al. 2000; Hocking and Kowalski 2002).

Most of the literature investigating the biology of degradation products of ECM focuses on the new epitopes that are exposed following enzymatic digestion of fibrillar, structural ECM proteins (Davis, Bayless et al. 2000). The ECM of any given tissue has a highly ordered structure. Because the fibrillar proteins formed tightly packed structures in which many motifs are not generally available to bind to cells, degradation of the structural proteins of ECM may uncover hidden epitopes within the structural proteins that can influence cell behavior and phenotype. However, relatively fewer studies have investigated whether the existing integrin-binding epitopes also still play a role within the ECM degradation products.

In cells interacting with an ECM scaffold, the cell is polarized with respect to integrin signaling because only one side of the cell actually interacts with the scaffold itself [citation]. During ECM degradation, the highly ordered structure of the ECM scaffold is lost. Thus, while the cell cannot bind to the highly ordered ECM scaffold in a tightly coordinated fashion, it may still be able to the bind the soluble integrin-binding ligands (i.e. ECM degradation products) that are released from the degrading ECM scaffold. The spatial distribution of integrin signaling within a cell may potentially contribute to differences in cell phenotype or function, and these differences may be one explanation as to why degradation products of ECM scaffolds exhibit novel bioactive properties such as osteogenic differentiation.

Integrins have been shown to play important roles in stem cell biology. Not only have integrins been found to be reliable and specific cell surface markers for multiple adult tissue stem cells (Zheng and Taniguchi 2003; Tsuchiya, Heike et al. 2007; Kamiya, Kakinuma et al. 2009), but other studies have also shown that integrin signaling can influence various responses of stem

125

cells. For example, previous studies have shown that ECM proteins partially regulate embryonic stem cell fate (Suzuki, Iwama et al. 2003; Flaim, Chien et al. 2005). Additionally, integrins are thought to regulate proliferation, migration, and differentiation of adult neural stem cells (Weaver, Yoshida et al. 1995; Anton, Kreidberg et al. 1999; Vogelezang, Liu et al. 2001; Nakamoto, Kain et al. 2004; Leone, Relvas et al. 2005). In multiple other adult stem cell populations including hematopoietic, mammary, crypt, satellite, and spermatogonial stem cells, expression of specific subsets of integrin receptors has been shown to regulate their localization to and function within their respective stem cell niches (reviewed in (Ellis and Tanentzapf) and (Raymond, Deugnier et al. 2009)). A recent study has also shown that integrin receptor expression on stem cells is predictive of their ability to home to various sites within the body (Kanatsu-Shinohara, Takehashi et al. 2008).

A recent study has also shown that differential signaling through integrin receptors may be a useful approach for directing the differentiation of stem cells for tissue engineering applications (Lee, Yun et al. 2011). By utilizing a combination of ligands for various integrin receptors, Lee *et al* showed that they can not only maintain the pluripotency of embryonic stem cells but also control the lineage along which the embryonic stem cells differentiate depending on the exact combination of integrin ligands utilized (Lee, Yun et al. 2011). While the referenced study focused on *in vitro* manipulation of embryonic stem cells, the findings of the present thesis suggest that ECM degradation products may be identified that could recapitulate this process for adult stem cells *in vitro* and *in vivo*.

5.6   FUTURE DIRECTIONS

5.6.1   Control of the digit amputation microenvironment with a BIODOME

In collaboration with the Automation & Robotics Research Institute (ARRI) at the University of Texas Arlington, a prototype device designated as the BIODOME (Biomechanical Interface for Optimized Delivery of MEMS Orchestrated Mammalian Epimorphosis) has been developed for an adult mouse model of digit amputation (Figure 41). Consisting of a septum and two one-way valves for easy access to the fluid reservoir, testing of this device is currently under way in the Badylak laboratory.
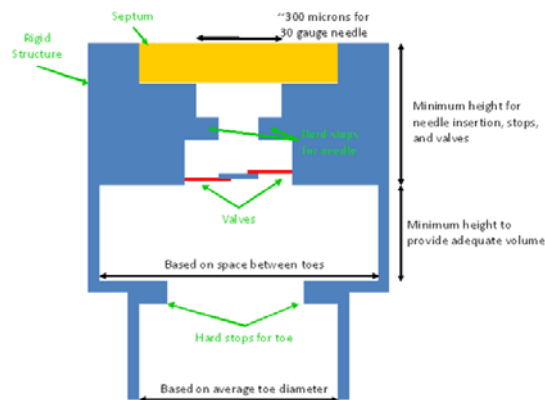
Figure 41. Prototype of a microfluidic device capable of controlling the microenvironment of the site of amputation, designated as the BIODOME (Biomechanical Interface for Optimized Delivery of MEMS Orchestrated Mammalian Epimorphosis).

Following mid-second phalanx digit amputation on the right hind foot of adult female C57/BL6 mice, a BIODOME device was surgically attached and fastened via Locktite glue at the tip of the amputated digit (Figure 42). The BIODOME device was filled with the same bioactive ECM homing signals that were used without a BIODOME to recruit a multipotential cell cluster

(MCC) at the site of amputation. In order to determine whether a more long term, continuous treatment of the amputated digit with bioactive ECM peptides would result in a greater accumulation, the peptides were left in the BIODOME for 2 da ys post-amputation. E-collars were placed around the neck of each mouse to prevent chewing and the BIODOMES were left on for 2 days and then removed with acetone to dissolve the glue. Mice were then euthanized at day 14 post-amputation (12 days post-removal of placed BIODOME) and toes were submitted for histology.
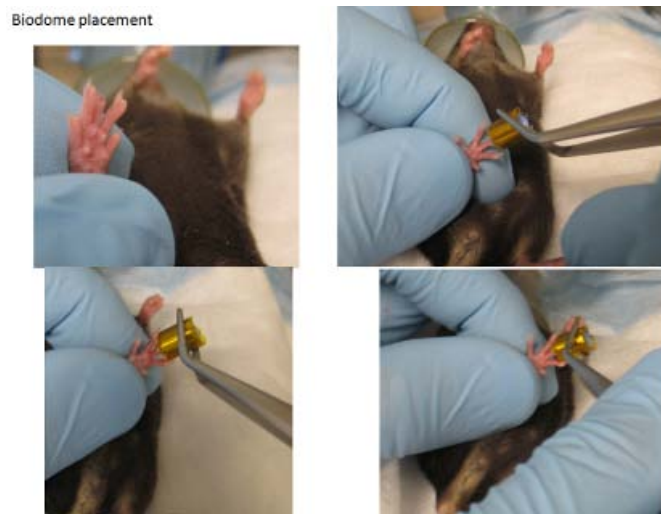
Figure 42. Placement of a BIODOME device.

At 14 days post-amputation (12 days post-BIODOME removal), gross examination of the amputated digits showed that treatment with bioactive ECM peptides in the BIODOME resulted in larger, more bulbous structure at the site of amputation as compared to treatment with phosphate buffered saline (PBS) (Figure 43). Microscopic, histologic examination showed that, indeed this bulbous accumulation consisted of a heterogeneous cellular accumulation distal to the site of amputation (Figure 43).
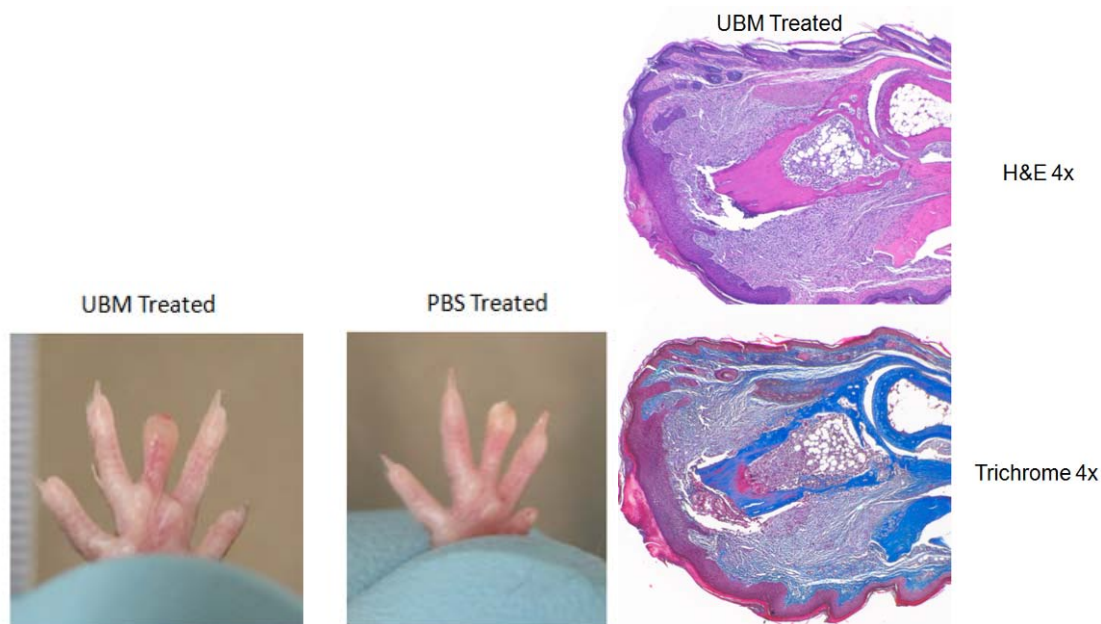
Figure 43. Gross examination and histologic examination of the amputated digits fitted with a BIDOME and treated with bioactive ECM homing signals (UBM) or phosphate buffered saline (PBS).

In order to further characterize the cellular accumulation at the site of amputation, the cells were microdissected from the site of amputation. Previous work has showed that treatment with bioactive ECM peptides resulted in the accumulation of a population of cells with osteogenic, adipogenic, and neuroectodermal lineage differentiation potential. Preliminary work completed in collaboration with Dr. Susan Braunhut's group shows that continuous treatment for 2 days of bioactive ECM homing peptides within a BIODOME results in a similar accumulation of cells. At day 21 post-amputation and treatment with bioactive peptides, microdissected cells were isolated, filtered, and plated into a culture flask. Treatment with bioactive ECM peptides resulted in a more cellular accumulation. Upon microdissection, approximately 8 times as many cells were isolated from digits treated with bioactive ECM peptides as compared to PBS (Figure 44). After culturing the cells for 5 days, equal numbers of cells from PBS and peptide treated groups were subjected to conditions of adipogenic differentiation and osteogenic differentiation.

After 3 weeks of culture in adipogenic or osteogenic differentiation, cells isolated from peptide treated digits were capable of osteogenic differentiation, whereas PBS treated digits showed no differentiation potential (Figure 45).
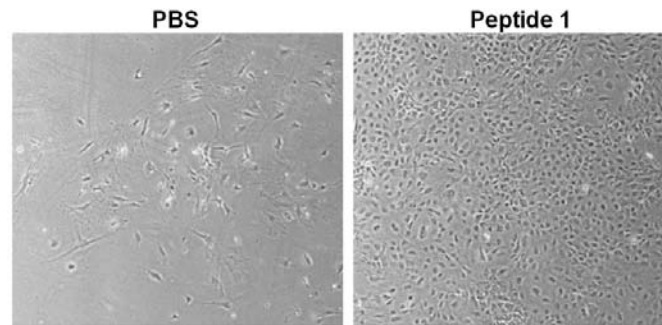
Figure 44. Treatment with an ECM bioactive peptide resulted in a greater cellular accumulation at the site of amputation, as shown by isolating and culturing the cells (31,111 cells in the peptide treated group vs 4,444 cells in the PBS treated group).
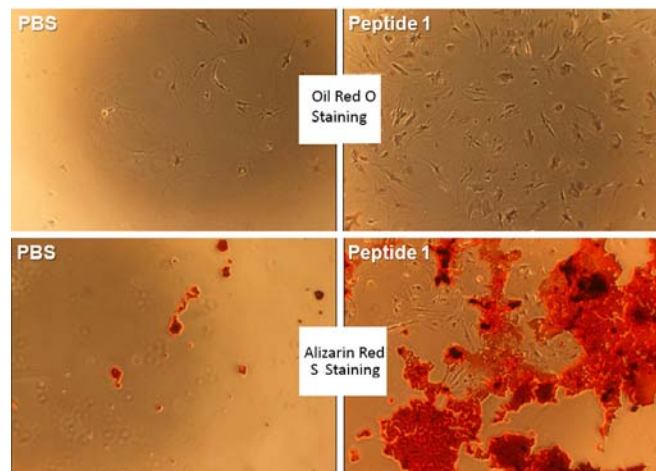
Figure 45. Treatment with an ECM bioactive peptide resulted in a cellular accumulation capable of osteogenic differentiation, whereas PBS treatment as a control yielded cells with no differentiation potential.

5.6.2 The importance of injury in ECM-mediated progenitor cell recruitment: a role for macrophage derived HMGB1

To investigate the effect that ECM degradation products may have upon macrophages as well as the subsequent effect of the macrophage conditioned medium upon migration of human perivascular stem cells *in vitro*. Following the culture of THP-1 cells in the presence of various concentrations of ECM degradation products, the resulting conditioned medium was harvested for Boyden chamber migration assays (Figure 46).

Media Supplemented with:
- 0 µg/ml UBM pepsin digest
- 100 µg/ml UBM
- 200 µg/ml UBM
- 500 µg/ml UBM

Collect media supernatant after 7 days

Perivascular stem cell migration assay in boyden chamber

Media Supplemented with:
- 0 µg/ml UBM pepsin digest
- 100 µg/ml UBM
- 200 µg/ml UBM
- 500 µg/ml UBM
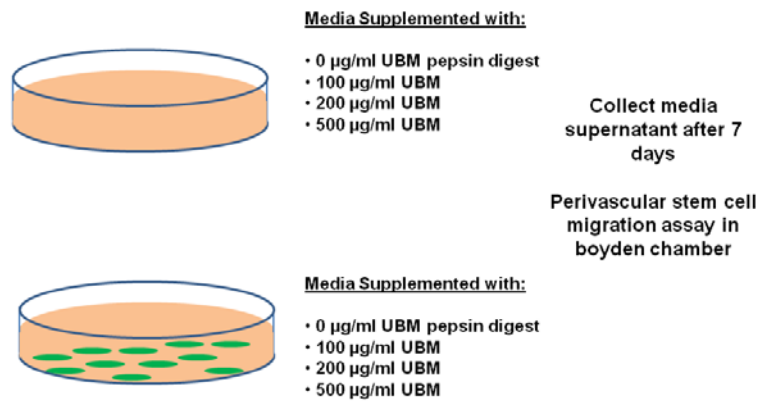
Figure 46. Schematic diagram showing the experimental outline for studies with THP-1 cells.

Preliminary data suggested that, as compared to the same ECM supplemented medium, THP-1 cell conditioned medium causes a dose-dependent increase in perivascular stem cell migration *in vitro*. Notably, supplementation of culture medium with the same concentration of ECM degradation products did not result in the same level of migration, suggesting that either the THP-1 cells release a soluble factor or they act upon the ECM degradation products to create a more pro-chemotactic product (Figure 47).

131
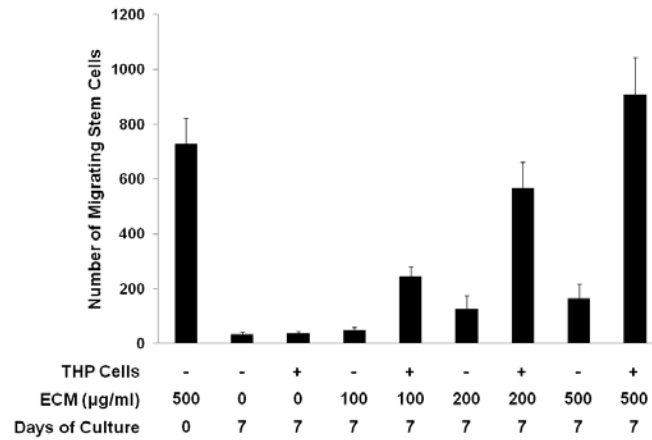
Figure 47. Migration of human perivascular stem cells showed that the perivascular stem cells migrated towards THP-1 cell conditioned medium in a dose dependent fashion. Culturing of the THP-1 cells in the presence of ECM degradation products potentiated the chemotactic potential of the resulting conditioned medium. Error bars represent Mean $\pm$ SEM (n=4).

Further work showed that there was a dose dependent increase in HMGB1 in the conditioned media supplemented with ECM degradation products (Figure 48). Additionally, blockade of the HMGB1 molecule in the conditioned medium (Figure 49) or a potential receptor target of HMGB1 on human perivascular stem cells resulted in a decrease in migration (Figure 50). RT-qPCR showed that ECM degradation products increase HMGB1 expression in THP-1 cells (Figure 50).
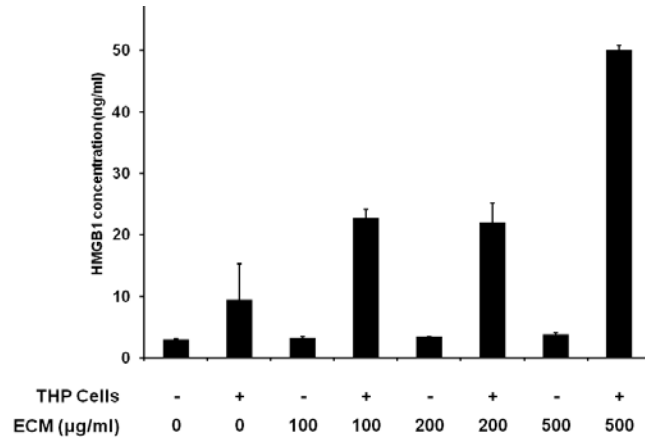
Figure 48. Conditioned medias were assessed for HMGB1 content by ELISA. THP-1 conditioned medium that contained ECM degradation products showed a greater concentration of HMGB1, but ECM degradation products in the absence of THP-1 cells did not have a greater amount of HMGB1. This suggests that the HMGB1 was cell derived.
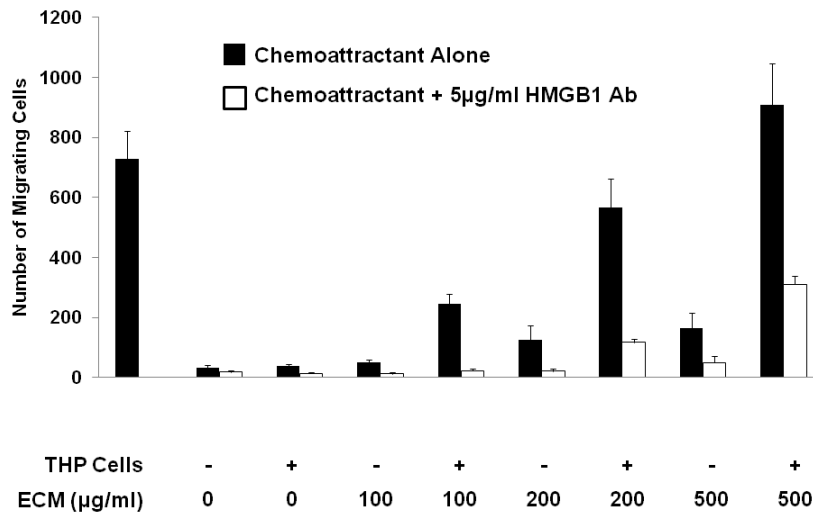
Figure 49. Addition of an HMGB1 antibody to the conditioned medium abrogated the chemotactic potential of the conditioned medium for human perivascular stem cells.
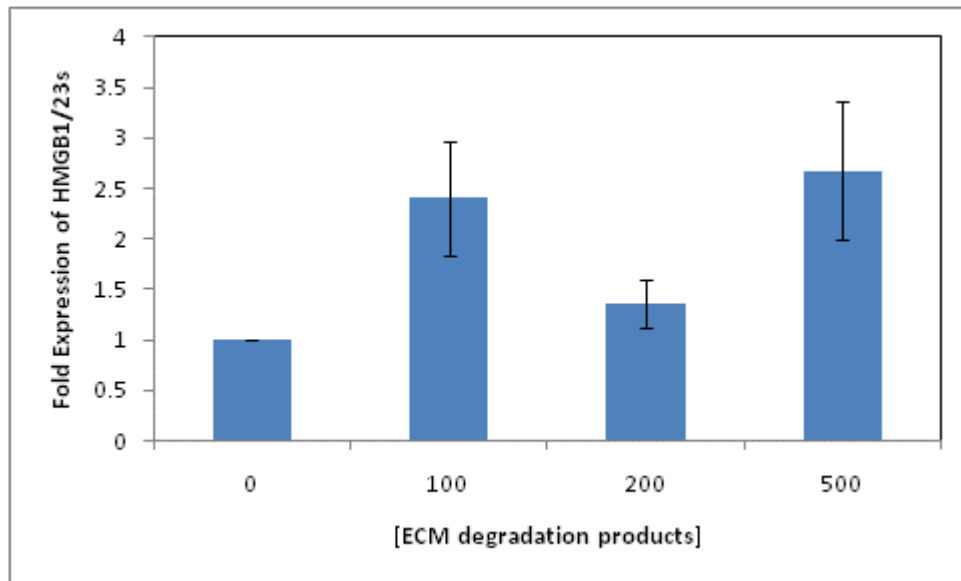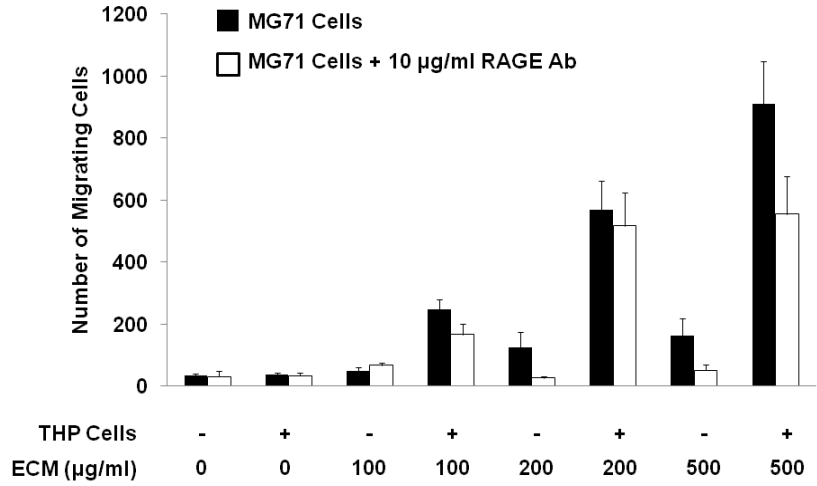
Figure 50. (Above) Blockade of the RAGE receptor on human perivascular stem cells via antibody partially limited the migration of human perivascular stem cells in vitro. (Below) RT-qPCR for HMGB1 expression following THP-1 cell culture showed that ECM degradation products cause an increase in THP-1 cell mRNA expression for HMGB1.

5.6.3 Development of a murine model of volumetric muscle injury

The findings of the present thesis showed that the peptides created from *ex vivo* pepsin mediated degradation of ECM scaffolds results in the site directed accumulation of progenitor cells that not only express markers of mesodermal progenitor cells, but are also capable of neuroectodermal and mesodermal differentiation *in vitro* when isolated. Based on these findings, it was postulated that one mechanism by which ECM scaffolds promote constructive remodeling of soft tissues is via site directed recruitment of progenitor cells to a site of injury by cryptic peptides released following *in vivo* degradation of the implanted ECM scaffold. However, there were notable limitations to the work discussed in the present thesis. The model of digit amputation injury utilized was a non-regnerating model of injury, but treatment with ECM degradation products did not actually result in constructive remodeling of the digit itself. Additionally, in previous preclinical and clinical studies that have observed constructive remodeling at a site of injury have always utilized intact ECM scaffolds as opposed to the degradation products.

To address these limitations, it is important to develop a non-regenerating model of injury in which ECM scaffolds do promote constructive remodeling of the injured tissue. Previous studies have shown in multiple injury models in various organs that replacement of injured muscle of any kind with a degradable ECM scaffold eventually results in constructive remodeling of the injured tissue (Badylak, Lantz et al. 1989; Badylak, Meurling et al. 2000; Badylak, Kokini et al. 2002; Kochupura, Azeloglu et al. 2005; Turner, Yates et al. 2010; Badylak, Hoppo et al. 2011). Thus, a volumetric skeletal muscle injury be an ideal model in which to directly investigate the role of ECM degradation upon subsequent mechanisms thought to contribute to constructive remodeling of the site of injury.

In order to parallel the work completed in the present thesis, adult 6-8 week old C57/BL6 mice were subjected to a 3mm long, full width defect to the fascia lata muscle the left hindleg (Figure 51). Nonresorbable 7-0 Prolene sutures were used to delineate the deep borders of the wound (Figure 52). An ECM sheet was fastened to either side of the fasica lata muscle so as to create a pocket within the site of muscle injury (Figure 53). The defect was filled with a hydrated three dimensional powdered construct composed of ECM, and allowed to remodel for 14 days. At 14 post days post-surgery and ECM implantation, the site of muscle injury still showed evidence of the ECM construct occupying the defect site (Figure 54). Histologic examination of the site of ECM implantation at days 7 and 14 post-surgery showed a dense mononuclear response at the site of ECM implantation (Figure 55, Figure 56).
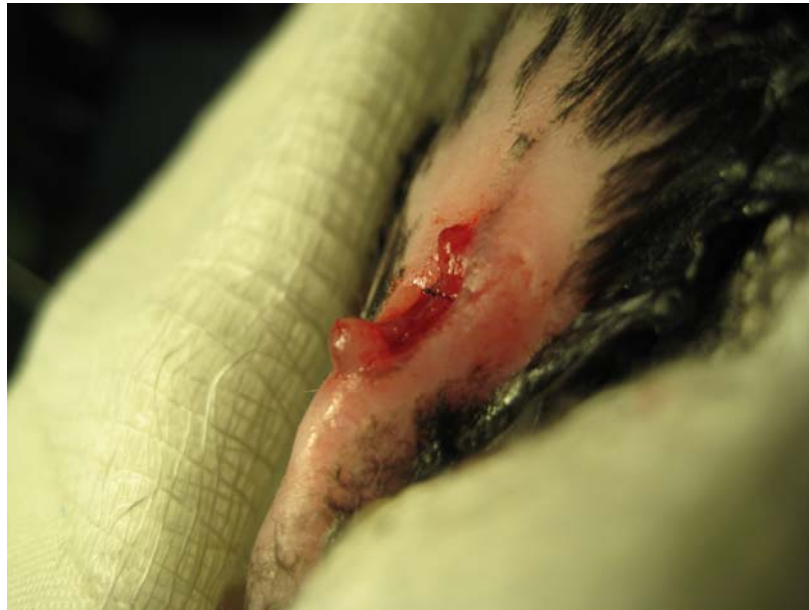
Figure 51. A 3 mm long, full width defect was created in the fascia lata muscle of the left hindleg of adult

C57/BL6 mice.

Figure 52. Non-resorbable 7-0 Prolene sutures were laid at the bottom of the defect to delineate the deep

border of the wound site.
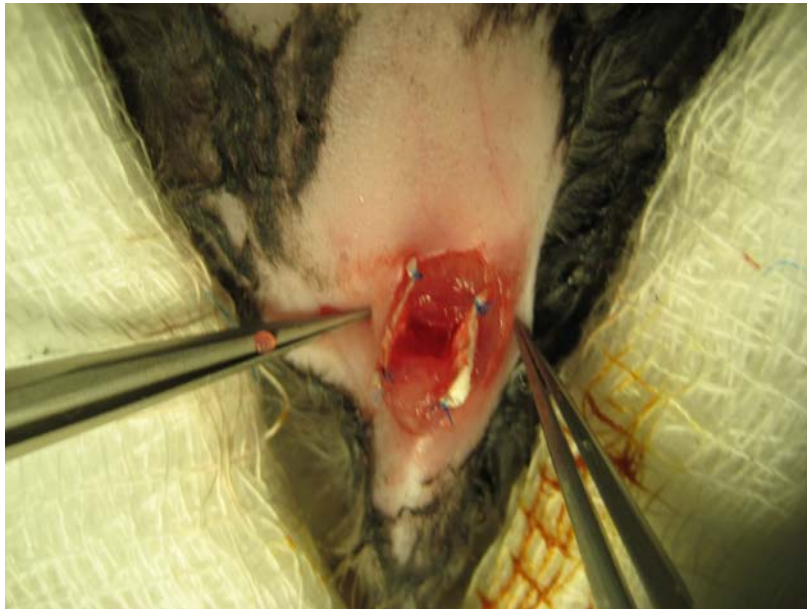
Figure 53. An ECM scaffold composed of porcine urinary bladder was sutured to the lateral edge of the

proximal and distal ends of the injured fascia lata muscle. A pocket was created at the site of injury that can be filled

with any construct of interest.

Figure 54. Following creation of the defect and filling of the defect with a construct composed of powdered porcine urinary bladder extracellular matrix, the site of implantation has begun to remodel at day 14 post-implantation.
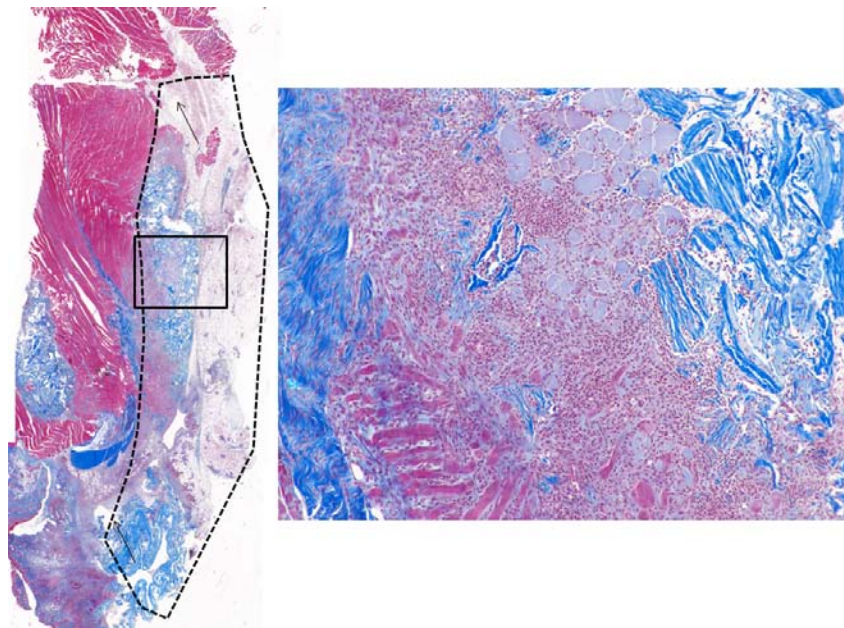
Figure 55. Histologic examination of Trichrome stained sections of muscle injury showed a dense mononuclear infiltrate at the site of ECM implantation at 7 days post-surgery. Dashed lines indicate the site of ECM implantation, and the rectangle indicates the location of the high magnification image.
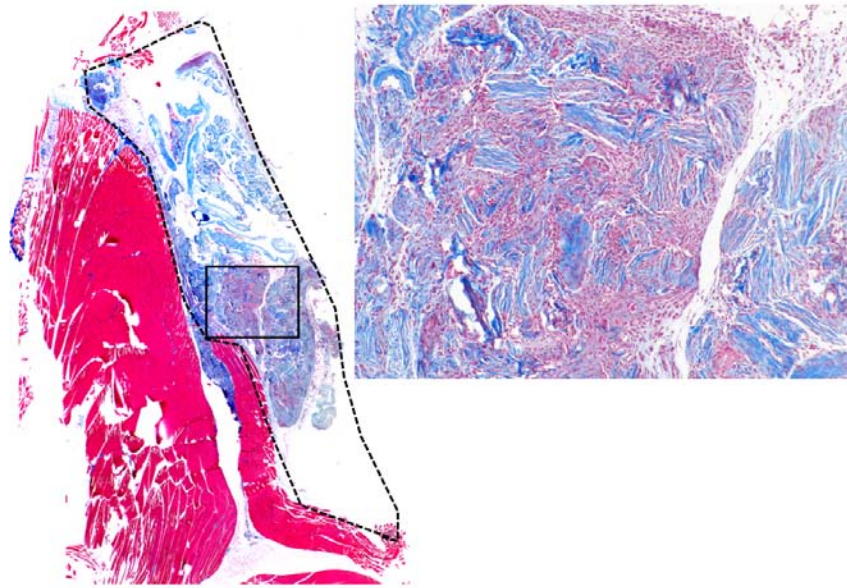
Figure 56. Histologic examination of Trichrome stained sections of muscle injury showed a dense mononuclear infiltrate at the site of ECM implantation at 14 days post-surgery. Dashed lines indicate the site of ECM implantation, and the rectangle indicates the location of the high magnification image.

5.7   OVERALL CONCLUSIONS

Overall, the findings of the present thesis: [1] showed that *ex vivo* generated ECM degradation products were chemotactic for progenitor cells *in vitro* and promoted the site directed recruitment of progenitor cells *in vivo*, [2] identified a single cryptic peptide from the mixture of ECM degradation products with similar *in vitro* and *in vivo* properties for progenitor cells, and [3]   showed that the single cryptic peptide also had the potential to alter progenitor cell differentiation *in vitro* and *in vivo*, specifically along an osteogenic lineage.

The findings of the thesis have laid the foundations for future studies to directly address the interaction between ECM degradation, progenitor cell recruitment, immune cell polarization,

and integrin signaling in mediating site-appropriate and functional tissue deposition at a site of

ECM implantation.

APPENDIX A

PARTIAL LIST OF COMMERCIALLY AVAILABLE ECM SCAFFOLDS

.

Product	Company	Tissue Source	Format	Application
AlloDerm	Lifecell	Human skin	Cross-linked	Soft tissue repair
AlloPatch®	Musculoskeletal Transplant Foundation	Human fascia lata	Cross-linked	Orthpedic applications
Axis™	Mentor	Human dermis	Natural	Pelvic organ prolapsed
CollaMend®	Bard	Porcine dermis	Cross-linked	Soft tissue repair
CuffPatch™	Arthrotek	Porcine small intestinal submucosa (SIS)	Cross-linked	Reinforcement of soft tissues
DurADAPT™	Pegasus Biologicals	Horse pericardium	Cross-linked	Dura repair
Dura-Guard®	Synovis Surgical	Bovine pericardium		Spinal and cranial repair
Durasis®	Cook SIS	Porcine small intestinal submucosa (SIS)	Natural	Repair dura matter
Durepair®	TEI Biosciences	Fetal bovine skin	Natural	Repair of cranial or spinal dura
FasLata®	Bard	Cadaveric fascia lata	Natural	Soft tissue repair
Graft Jacket®	Wright Medical Tech	Human skin	Cross-linked	Foot ulcers

Oasis®	Healthpoint	Porcine small intestinal submucosa (SIS)	Natural	Partial & full thickness wounds; superficial and second degree burns
NeoForm	Mentor Worldwide LLC	Human dermis		Tendon, breast
OrthADAPT™	Pegasus Biologicals	Horse pericardium	Cross-linked	Reinforcement, repair and reconstruction of soft tissue in orthopedics
Pelvicol®	Bard	Porcine dermis	Cross-linked	Soft tissue repair
Peri-Guard®	Synovis Surgical	Bovine pericardium		Pericardial and soft tissue repair
Permacol™	Tissue Science Laboratories	Porcine skin	Cross-linked	Soft connective tissue repair
PriMatrix™	TEI Biosciences	Fetal bovine skin	Natural	Wound management
Restore™	DePuy	Porcine small intestinal submucosa (SIS)	Natural	Reinforcement of soft tissues
Stratasis®	Cook SIS	Porcine small intestinal submucosa (SIS)	Natural	Treatment of urinary incontinence
SurgiMend™	TEI Biosciences	Fetal bovine skin	Natural	Surgical repair of damaged or ruptured soft tissue membranes
Surgisis®	Cook SIS	Porcine small intestinal submucosa (SIS)	Natural	Soft tissue repair and reinforcement
Suspend™	Mentor	Human fascia lata	Natural	Urethral sling
TissueMend®	TEI Biosciences	Fetal bovine skin	Natural	Surgical repair and reinforcement of soft tissue in rotator cuff

Vascu-Guard®	Synovis Surgical	Bovine pericardium		Reconstruction of blood vessels in neck, legs, and arms
Veritas®	Synovis Surgical	Bovine pericardium		Soft tissue repair
Xelma™	Molnlycke	ECM protein, PGA, water		Venous leg ulcers
Xenform™	TEI Biosciences	Fetal bovine skin	Natural	Abdominal and pelvic soft tissue applications
Zimmer®	Tissue Science Laboratories	Procine dermis	Cross-linked	Orthopedic applications

APPENDIX B

MATLAB SCRIPT FOR ISOLATING NUCLEI AND COLLAGEN FROM

TRICHROME IMAGES

```
% [pixels,percentage] = filterImage(filename, showImage, color1, color2)
%
% GAG quantification in an Alcean Blue stained slide. This program
% essentially takes advantage of the fact that GAGs stain light blue in an
% Alcean Blue stain. By converting images from RGB (i.e. TIF format) to an
% HSV (hue/saturation/intensity) image. The hue consists of 256 different
% ranging from 0 to 255, and MATLAB uses a scale of 0 to 1 to distinguish
% between different hues. Because intensities of colors and lighting can
% differ from image to to image (due to variability in slides and
% microscope image capturing conditions, etc etc), the color cutoffs
% (color1 and color 2) should be optimized for each set of images.
%
% This program is only intended for TIF files!
%
% Inputs:      filename = full pathway of the TIF file (EX: 'C:\..\test.tif')
%
%              showImage = boolean character;
%                      1 => shows filtered image containing elastin
%                      0 => does not show any image
%
%              color1/color2 - the range of colors to extract; always 0<x<255
%                      color1 < color2 always; On a scale of 0 to 255, each
%                      hue has a unique number associated with it; For the
%                      Alcean Blue stain looking for GAGs, it seems that 110
%                      to about 170 seems to be a fairly good range for
%                      getting the GAG staining (i.e. color1=110, color2=170)
%
%
% Outputs:     pixels = total number of pixels that are elastin positive
%              percentage = percentage of total image area that is elastin
%                             positive
%
%
% Vineet Agrawal; January 5, 2009
```

```matlab
function [filtImage,pixels,percentage] = filtImage(filename, showImage,
color1, color2)

rgbImage = imread(filename);     % loads TIF file into RGB format
hsvImage = rgb2hsv(rgbImage);      % converts RGB format to an intensity file
gImage = hsvImage(:,:,1);

% Filtered image, starts of all white
fImage = ones(size(gImage))-1;
% Total number of positive pixels
pixels = 0;

% Goes through intensity image and filters away high intensities (whiter)
% and keeps lower intensities (blacker) pixels. The sensitivity of the
% filtration is dependent upon threshold.
%
% color1 = 31, color2 = 51 for yellow
% color1 = 62, color2 = 102 for green
for a = 1:size(gImage,1)
    for b = 1:size(gImage,2)
        if gImage(a,b) >= color1/255 && gImage(a,b) <= color2/255
            if gImage(a,b) >= 31/255 && gImage(a,b) <= 61/255
            fImage(a,b) = 1;
            pixels = pixels+1;
            hsvImage(a,b,3) = 1;
            end
        end
    end
end

%fImage = imfill(gImage,'holes');
fImage2 = bwmorph(fImage,'clean');
fImage2 = bwmorph(fImage2,'fill');
fImage3 = bwmorph(fImage2,'shrink',Inf);
%fImage3 = imoverlay(fImage,fImage2,[0.3 1 0.3]);
figure; imagesc(fImage2); colormap(gray);
figure; imagesc(fImage3); colormap(gray);
length(find(fImage3 == 1))
%fImage2 = bwperim(fImage);
%figure; imagesc(fImage2); colormap(gray);
figure; imagesc(imoverlay(fImage2,fImage3,[1 0 0]));
%figure; imagesc(fImage3);


% if showImage does not equal zero, the filtered image is shown
if showImage
    figure; subplot(2,1,1); imagesc(fImage); colormap(gray);
    subplot(2,1,2); imagesc(hsv2rgb(hsvImage));
end

% Divides by total number of pixels in image to get percentage of area that
% is positive.
percentage = pixels/(size(gImage,1)*size(gImage,2));
```

APPENDIX C

LIST OF CONFERENCE PROCEEDINGS AND MANUSCRIPTS

The following is a list of refereed conference proceeding and manuscripts, either accepted or in preparation, that have materialized during my tenure as a graduate student in the Badylak laboratory.

C.1   LIST OF REFEREED MANUSCRIPTS

Agrawal V, Kelly J, Tottey S, Daly K, Johnson SA, Siu BF, Reing JE, Badylak SF. An Isolated Cryptic Peptide Influences Osteogenesis and Bone Remodeling in an Adult Mammalian Model of Digit Amputation. Tissue Engineering Part A 2011. PMID: 21740273.

Agrawal V, Tottey S, Johnson SA, Freund JM, Siu BF, Badylak SF. Recruitment of progenitor cells by an ECM cryptic peptide in a mouse model of digit amputation. Tissue Engineering Part A 2011. PMID: 21563860.

Agrawal V, Johnson SA, Reing J, Zhang L, Tottey S, Wang G, Hirschi KK, Braunhut S, Gudas LJ, Badylak SF. An epimorphic regeneration approach to tissue replacement in adult mammals. Proceedings of the National Academy of Sciences 2010. 107(8): 3351-5. PMID: 19966310 (Cover Image). PMCID: PMC2840465.

Agrawal V, Brown BN, Beattie AJ, Gilbert TW, Badylak SF. Evidence of Innervation following Extracellular Matrix Scaffold Mediated Remodeling of Muscular Tissues. Journal of Tissue Engineering and Regenerative Medicine 2009. 3(8): 590-600. PMID: 19701935.

Gilbert TW, Agrawal V, Gilbert MR, Povirk KM, Badylak SF, Rosen CA. Liver Derived Extracellular Matrix as a Biologic Scaffold Material for Acute Vocal Fold Repair. Laryngoscope 2009, 119(9): 1856-63. PMID: 19572393.

Agrawal V, Siu BF, Chao H, Hirschi KK, Raborn E, Johnson SA, Tottey S, Hurley KB, Medberry CJ, Badylak SF. Characterization of Sox2+ cell population following digit amputation and treatment with ECM degradation products. In preparation for submission to Cells Tissues Organs. 2011.

C.2   LIST OF REFEREED CONFERENCE PROCEEDINGS

Agrawal V, Tottey S, Johnson SA, Freund JM, Siu B, Badylak SF. Matricryptic Peptides Regulate Progenitor Cell Recruitment and Differentiation In Vivo and In Vitro. AAP/ASCI Joint Meeting 2011, Chicago, IL, April 2011.

Agrawal V, Johnson SA, Tottey S, Hurley KB, Siu B, Reing J, Zhang L, Badylak SF. ECM degradation products recruit progenitor cells to a site of injury: a non-blastemal epimorphic approach to regenerative medicine. Orlando, FL. TERMIS meeting North America Chapter, 2010.

Daly KA, Brown B, Agrawal V, Badylak SF. Damage Associated Molecular Patterns (DAMPs) and Macrophages in the Host Immune and Remodeling Response to Xenogeneic Biologic Scaffolds. Sydney, Australia. TERMIS meeting Asia-Pacific Chapter, 2010.

Agrawal V, Johnson SA, Hurley KB, Reing J, Zhang L, Tottey S, Badylak SF. Matricryptic Peptides Recruit Endogenous Progenitor Cells in vivo in an Adult Mammalian Model of Digit Amputation. Amercian Physicians Scientists Association National Meeting, Chicago, IL, April 2010.

Agrawal V, Johnson SA, Badylak SF. Epimorphic Regeneration: A Truly "Regenerative Medicine" Approach to Tissue and Organ Replacement. Annual Hilton Head Workshop, Hilton Head Island, SC, April 2010.

Agrawal V, Johnson SA, Reing J, Zhang L, Tottey S, Wang G, Hirschi KK, Braunhut S, Gudas LJ, Badylak SF. An epimorphic, non-blastemal approach to limb/digit reconstruction in adult mammals. Armed Forces Institute for Regenerative Medicine Annual Meeting, Tampa, FL, January 2010.

Gilbert TW, Agrawal V, Beattie AJ, Braunhut SJ, Crisan M, Freytes DO, Gudas LJ, Heber-Katz E, Hirschi KK, Huard J, Johnson SA, Peault B, Reing JE, Tottey S, Yoder MC, Zantop T, Zhang L, Badylak SF. ECM Scaffold Degradation Products Recruit Progenitor Cells to the Site of Remodeling. Wound Healing: Science and Industry, St. Thomas, USVI, December 2009.

Agrawal V, Johnson SA, Reing J, Zhang L, Tottey S, Wang G, Hirschi KK, Braunhut S, Gudas LJ, Badylak SF. An Epimorphic Approach to Tissue Regeneration via Recruitment of Endogenous Stem Cells to a Site of Injury in an Adult Mammalian Model of Digit Amputation. World Stem Cell Summit, Baltimore, MD, September 2009.

Gilbert TW, Gilbert M, Povirk KM, Agrawal V, Badylak SF, Rosen CA. Evaluation of Porcine Liver Stroma for Treatment of Vocal Fold Injury. Meeting of the American Laryngological Association, Pheonix, AZ, May 2009.

Agrawal V, Brennan EP, Reing J, Freytes DO, Badylak SF. Intestinal Progenitor Cells Preferentially Migrate and Proliferate in Response to Degradation Products of Small Intestinal Submucosa Extracellular Matrix Bioscaffolds, Regenerate International Conference, Toronto, Canada, June 2007.

149

BIBLIOGRAPHY

Abdallah, B. M., C. H. Jensen, G. Gutierrez, R. G. Leslie, T. G. Jensen and M. Kassem (2004). "Regulation of human skeletal stem cells differentiation by Dlk1/Pref-1." J Bone Miner Res **19**(5): 841-52.

Adair-Kirk, T. L. and R. M. Senior (2008). "Fragments of extracellular matrix as mediators of inflammation." Int J Biochem Cell Biol **40**(6-7): 1101-10.

Agrawal, V., B. N. Brown, A. J. Beattie, T. W. Gilbert and S. F. Badylak (2009). "Evidence of innervation following extracellular matrix scaffold-mediated remodelling of muscular tissues." J Tissue Eng Regen Med **3**(8): 590-600.

Agrawal, V., S. A. Johnson, J. Reing, L. Zhang, S. Tottey, G. Wang, K. K. Hirschi, S. Braunhut, L. J. Gudas and S. F. Badylak (2010). "Epimorphic regeneration approach to tissue replacement in adult mammals." Proc Natl Acad Sci U S A **107**(8): 3351-5.

Agrawal, V., J. Kelly, S. Tottey, K. Daly, S. A. Johnson, B. F. Siu, J. E. Reing and S. F. Badylak (2011). "An Isolated Cryptic Peptide Influences Osteogenesis and Bone Remodeling in an Adult Mammalian Model of Digit Amputation." Tissue Eng Part A.

Agrawal, V., S. Tottey, S. A. Johnson, J. M. Freund, B. F. Siu and S. F. Badylak (2011). "Recruitment of Progenitor Cells by an Extracellular Matrix Cryptic Peptide in a Mouse Model of Digit Amputation." Tissue Eng Part A.

Agrez, M. V., R. C. Bates, A. W. Boyd and G. F. Burns (1991). "Arg-Gly-Asp-containing peptides expose novel collagen receptors on fibroblasts: implications for wound healing." Cell Regul **2**(12): 1035-44.

Ai-Aql, Z. S., A. S. Alagl, D. T. Graves, L. C. Gerstenfeld and T. A. Einhorn (2008). "Molecular mechanisms controlling bone formation during fracture healing and distraction osteogenesis." J Dent Res **87**(2): 107-18.

Aksu, A. E., J. P. Rubin, J. R. Dudas and K. G. Marra (2008). "Role of gender and anatomical region on induction of osteogenic differentiation of human adipose-derived stem cells." Ann Plast Surg **60**(3): 306-22.

Allman, A. J., T. B. McPherson, S. F. Badylak, L. C. Merrill, B. Kallakury, C. Sheehan, R. H. Raeder and D. W. Metzger (2001). "Xenogeneic extracellular matrix grafts elicit a TH2-restricted immune response." Transplantation **71**(11): 1631-40.

Allman, A. J., T. B. McPherson, L. C. Merrill, S. F. Badylak and D. W. Metzger (2002). "The Th2-restricted immune response to xenogeneic small intestinal submucosa does not influence systemic protective immunity to viral and bacterial pathogens." Tissue Eng **8**(1): 53-62.

Androjna, C., R. K. Spragg and K. A. Derwin (2007). "Mechanical conditioning of cell-seeded small intestine submucosa: a potential tissue-engineering strategy for tendon repair." Tissue Eng **13**(2): 233-43.

Anton, E. S., J. A. Kreidberg and P. Rakic (1999). "Distinct functions of alpha3 and alpha(v) integrin receptors in neuronal migration and laminar organization of the cerebral cortex." Neuron **22**(2): 277-89.

Autelitano, D. J., A. Rajic, A. I. Smith, M. C. Berndt, L. L. Ilag and M. Vadas (2006). "The cryptome: a subset of the proteome, comprising cryptic peptides with distinct bioactivities." Drug Discov Today **11**(7-8): 306-14.

Avilion, A. A., S. K. Nicolis, L. H. Pevny, L. Perez, N. Vivian and R. Lovell-Badge (2003). "Multipotent cell lineages in early mouse development depend on S OX2 function." Genes Dev **17**(1): 126-40.

Badylak, S., K. Kokini, B. Tullius, A. Simmons-Byrd and R. Morff (2002). "Morphologic study of small intestinal submucosa as a body wall repair device." J Surg Res **103**(2): 190-202.

Badylak, S., K. Kokini, B. Tullius and B. Whitson (2001). "Strength over time of a resorbable bioscaffold for body wall repair in a dog model." J Surg Res **99**(2): 282-7.

Badylak, S., S. Meurling, M. Chen, A. Spievack and A. Simmons-Byrd (2000). "Resorbable bioscaffold for esophageal repair in a dog model." J Pediatr Surg **35**(7): 1097-103.

Badylak, S. F. (2002). "The extracellular matrix as a scaffold for tissue reconstruction." Semin Cell Dev Biol **13**(5): 377-83.

Badylak, S. F. (2007). "The extracellular matrix as a biologic scaffold material." Biomaterials **28**(25): 3587-93.

Badylak, S. F., T. Hoppo, A. Nieponice, T. W. Gilbert, J. M. Davison and B. A. Jobe "Esophageal preservation in five male patients after endoscopic inner-layer circumferential resection in the setting of superficial cancer: a regenerative medicine approach with a biologic scaffold." Tissue Eng Part A **17**(11-12): 1643-50.

Badylak, S. F., T. Hoppo, A. Nieponice, T. W. Gilbert, J. M. Davison and B. A. Jobe (2011). "Esophageal preservation in five male patients after endoscopic inner-layer circumferential resection in the setting of superficial cancer: a regenerative medicine approach with a biologic scaffold." Tissue Eng Part A **17**(11-12): 1643-50.

Badylak, S. F., P. V. Kochupura, I. S. Cohen, S. V. Doronin, A. E. Saltman, T. W. Gilbert, D. J. Kelly, R. A. Ignotz and G. R. Gaudette (2006). "The use of extracellular matrix as an inductive scaffold for the partial replacement of functional myocardium." Cell Transplant **15 Suppl 1**: S29-40.

Badylak, S. F., G. C. Lantz, A. Coffey and L. A. Geddes (1989). "Small intestinal submucosa as a large diameter vascular graft in the dog." J Surg Res **47**(1): 74-80.

Badylak, S. F., K. Park, N. Peppas, G. McCabe and M. Yoder (2001). "Marrow-derived cells populate scaffolds composed of xenogeneic extracellular matrix." Exp Hematol **29**(11): 1310-8.

Badylak, S. F., J. E. Valentin, A. K. Ravindra, G. P. McCabe and A. M. Stewart-Akers (2008). "Macrophage phenotype as a determinant of biologic scaffold remodeling." Tissue Eng Part A **14**(11): 1835-42.

Badylak, S. F., D. A. Vorp, A. R. Spievack, A. Simmons-Byrd, J. Hanke, D. O. Freytes, A. Thapa, T. W. Gilbert and A. Nieponice (2005). "Esophageal reconstruction with ECM and muscle tissue in a dog model." J Surg Res **128**(1): 87-97.

Baer, D. G., M. A. Dubick, J. C. Wenke, K. V. Brown, L. L. McGhee, V. A. Convertino, L. C. Cancio, S. E. Wolf and L. H. Blackbourne (2009). "Combat casualty care research at the U.S. Army Institute of Surgical Research." J R Army Med Corps **155**(4): 327-32.

Baltus, G. A., M. P. Kowalski, H. Zhai, A. V. Tutter, D. Quinn, D. Wall and S. Kadam (2009). "Acetylation of sox2 induces its nuclear export in embryonic stem cells." Stem Cells **27**(9): 2175-84.

Banfi, G., G. Lombardi, A. Colombini and G. Lippi (2010). "Bone metabolism markers in sports medicine." Sports Med **40**(8): 697-714.

Bang, O. Y., J. S. Lee, P. H. Lee and G. Lee (2005). "Autologous mesenchymal stem cell transplantation in stroke patients." Ann Neurol **57**(6): 874-82.

Barker, N., J. H. van Es, J. Kuipers, P. Kujala, M. van den Born, M. Cozijnsen, A. Haegebarth, J. Korving, H. Begthel, P. J. Peters and H. Clevers (2007). "Identification of stem cells in small intestine and colon by marker gene Lgr5." Nature **449**(7165): 1003-7.

Barmparas, G., K. Inaba, P. G. Teixeira, J. J. Dubose, M. Criscuoli, P. Talving, D. Plurad, D. Green and D. Demetriades (2010). "Epidemiology of post-traumatic limb amputation: a National Trauma Databank analysis." Am Surg **76**(11): 1214-22.

Barnes, C. A., J. Brison, R. Michel, B. N. Brown, D. G. Castner, S. F. Badylak and B. D. Ratner (2011). "The surface molecular functionality of decellularized extracellular matrices." Biomaterials **32**(1): 137-43.

Barth, D., O. Kyrieleis, S. Frank, C. Renner and L. Moroder (2003). "The role of cystine knots in collagen folding and stability, part II. Conformational properties of (Pro-Hyp-Gly)n model trimers with N- and C-terminal collagen type III cystine knots." Chemistry **9**(15): 3703-14.

Basu-Roy, U., D. Ambrosetti, R. Favaro, S. K. Nicolis, A. Mansukhani and C. Basilico "The transcription factor Sox2 is required for osteoblast self-renewal." Cell Death Differ **17**(8): 1345-53.

Beattie, A. J., T. W. Gilbert, J. P. Guyot, A. J. Yates and S. F. Badylak (2008). "Chemoattraction of Progenitor Cells by Remodeling Extracellular Matrix Scaffolds." Tissue Eng Part A.

Beattie, A. J., T. W. Gilbert, J. P. Guyot, A. J. Yates and S. F. Badylak (2009). "Chemoattraction of progenitor cells by remodeling extracellular matrix scaffolds." Tissue Eng Part A **15**(5): 1119-25.

Berkowitz, B. A., C. L. Bevins and M. A. Zasloff (1990). "Magainins: a new family of membrane-active host defense peptides." Biochem Pharmacol **39**(4): 625-9.

Bianchi, M. E. (2007). "DAMPs, PAMPs and alarmins: all we need to know about danger." J Leukoc Biol **81**(1): 1-5.

Biernaskie, J., M. Paris, O. Morozova, B. M. Fagan, M. Marra, L. Pevny and F. D. Miller (2009). "SKPs derive from hair follicle precursors and exhibit properties of adult dermal stem cells." Cell Stem Cell **5**(6): 610-23.

Bongso, A., C. Y. Fong and K. Gauthaman (2008). "Taking stem cells to the clinic: Major challenges." J Cell Biochem **105**(6): 1352-60.

Borgens, R. B. (1982). "Mice regrow the tips of their foretoes." Science **217**(4561): 747-50.

Boruch, A. V., A. Nieponice, I. R. Qureshi, T. W. Gilbert and S. F. Badylak (2010). "Constructive remodeling of biologic scaffolds is dependent on early exposure to physiologic bladder filling in a canine partial cystectomy model." J Surg Res **161**(2): 217-25.

Brennan, E. P., J. Reing, D. Chew, J. M. Myers-Irvin, E. J. Young and S. F. Badylak (2006). "Antibacterial activity within degradation products of biological scaffolds composed of extracellular matrix." Tissue Eng **12**(10): 2949-55.

Brennan, E. P., X. H. Tang, A. M. Stewart-Akers, L. J. Gudas and S. F. Badylak (2008). "Chemoattractant activity of degradation products of fetal and adult skin extracellular matrix for keratinocyte progenitor cells." J Tissue Eng Regen Med **2**(8): 491-8.

Brockes, J. P. and A. Kumar (2005). "Appendage regeneration in adult vertebrates and implications for regenerative medicine." Science **310**(5756): 1919-23.

Brown, B., K. Lindberg, J. Reing, D. B. Stolz and S. F. Badylak (2006). "The basement membrane component of biologic scaffolds derived from extracellular matrix." Tissue Eng **12**(3): 519-26.

Brown, B. N., C. A. Barnes, R. T. Kasick, R. Michel, T. W. Gilbert, D. Beer-Stolz, D. G. Castner, B. D. Ratner and S. F. Badylak (2010). "Surface characterization of extracellular matrix scaffolds." Biomaterials **31**(3): 428-37.

Brown, B. N., J. E. Valentin, A. M. Stewart-Akers, G. P. McCabe and S. F. Badylak (2009). "Macrophage phenotype and remodeling outcomes in response to biologic scaffolds with and without a cellular component." Biomaterials **30**(8): 1482-91.

Brown, D. M., S. P. Hong, C. L. Farrell, G. F. Pierce and R. K. Khouri (1995). "Platelet-derived growth factor BB induces functional vascular anastomoses in vivo." Proc Natl Acad Sci U S A **92**(13): 5920-4.

Caione, P., N. Capozza, D. Zavaglia, G. Palombaro and R. Boldrini (2006). "In vivo bladder regeneration using small intestinal submucosa: experimental study." Pediatr Surg Int **22**(7): 593-9.

Camargo, F. D., R. Green, Y. Capetanaki, K. A. Jackson and M. A. Goodell (2003). "Single hematopoietic stem cells generate skeletal muscle through myeloid intermediates." Nat Med **9**(12): 1520-7.

Campana, L., L. Bosurgi and P. Rovere-Querini (2008). "HMGB1: a two-headed signal regulating tumor progression and immunity." Curr Opin Immunol **20**(5): 518-23.

Ceder, J. A., L. Jansson, L. Helczynski and P. A. Abrahamsson (2008). "Delta-like 1 (Dlk-1), a novel marker of prostate basal and candidate epithelial stem cells, is downregulated by notch signalling in intermediate/transit amplifying cells of the human prostate." Eur Urol **54**(6): 1344-53.

Chan, R. J. and M. C. Yoder (2004). "The multiple facets of hematopoietic stem cells." Curr Neurovasc Res **1**(3): 197-206.

Chavakis, E., A. Aicher, C. Heeschen, K. Sasaki, R. Kaiser, N. El Makhfi, C. Urbich, T. Peters, K. Scharffetter-Kochanek, A. M. Zeiher, T. Chavakis and S. Dimmeler (2005). "Role of beta2-integrins for homing and neovascularization capacity of endothelial progenitor cells." J Exp Med **201**(1): 63-72.

Chen, S. L., W. W. Fang, F. Ye, Y. H. Liu, J. Qian, S. J. Shan, J. J. Zhang, R. Z. Chunhua, L. M. Liao, S. Lin and J. P. Sun (2004). "Effect on left ventricular function of intracoronary transplantation of autologous bone marrow mesenchymal stem cell in patients with acute myocardial infarction." Am J Cardiol **94**(1): 92-5.

Chow, A., D. Lucas, A. Hidalgo, S. Mendez-Ferrer, D. Hashimoto, C. Scheiermann, M. Battista, M. Leboeuf, C. Prophete, N. van Rooijen, M. Tanaka, M. Merad and P. S. Frenette (2011). "Bone marrow CD169+ macrophages promote the retention of hematopoietic stem and progenitor cells in the mesenchymal stem cell niche." J Exp Med **208**(2): 261-71.

Chun, S. Y., G. J. Lim, T. G. Kwon, E. K. Kwak, B. W. Kim, A. Atala and J. J. Yoo (2007). "Identification and characterization of bioactive factors in bladder submucosa matrix." Biomaterials **28**(29): 4251-6.

Clark, L. D., R. K. Clark and E. Heber-Katz (1998). "A new murine model for mammalian wound repair and regeneration." Clin Immunol Immunopathol **88**(1): 35-45.

Clarke, K. M., G. C. Lantz, S. K. Salisbury, S. F. Badylak, M. C. Hiles and S. L. Voytik (1996). "Intestine submucosa and polypropylene mesh for abdominal wall repair in dogs." J Surg Res **60**(1): 107-14.

Cobb, M. A., S. F. Badylak, W. Janas and F. A. Boop (1996). "Histology after dural grafting with small intestinal submucosa." Surg Neurol **46**(4): 389-93; discussion 393-4.

Crapo, P. M., T. W. Gilbert and S. F. Badylak (2011). "An overview of tissue and whole organ decellularization processes." Biomaterials **32**(12): 3233-43.

Crisan, M., S. Yap, L. Casteilla, C. W. Chen, M. Corselli, T. S. Park, G. Andriolo, B. Sun, B. Zheng, L. Zhang, C. Norotte, P. N. Teng, J. Traas, R. Schugar, B. M. Deasy, S. Badylak, H. J. Buhring, J. P. Giacobino, L. Lazzari, J. Huard and B. Peault (2008). "A perivascular origin for mesenchymal stem cells in multiple human organs." Cell Stem Cell **3**(3): 301-13.

Davis, G. E. (2010). "Matricryptic sites control tissue injury responses in the cardiovascular system: relationships to pattern recognition receptor regulated events." J Mol Cell Cardiol **48**(3): 454-60.

Davis, G. E., K. J. Bayless, M. J. Davis and G. A. Meininger (2000). "Regulation of tissue injury responses by the exposure of matricryptic sites within extracellular matrix molecules." Am J Pathol **156**(5): 1489-98.

Davis, N. F., A. Callanan, B. B. McGuire, R. Mooney, H. D. Flood and T. M. McGloughlin (2011). "Porcine extracellular matrix scaffolds in reconstructive urology: An ex vivo comparative study of their biomechanical properties." J Mech Behav Biomed Mater **4**(3): 375-82.

De Bari, C., F. Dell'Accio, J. Vanlauwe, J. Eyckmans, I. M. Khan, C. W. Archer, E. A. Jones, D. McGonagle, T. A. Mitsiadis, C. Pitzalis and F. P. Luyten (2006). "Mesenchymal multipotency of adult human periosteal cells demonstrated by single-cell lineage analysis." Arthritis Rheum **54**(4): 1209-21.

De Mori, R., S. Straino, A. Di Carlo, A. Mangoni, G. Pompilio, R. Palumbo, M. E. Bianchi, M. C. Capogrossi and A. Germani (2007). "Multiple effects of high mobility group box protein 1 in skeletal muscle regeneration." Arterioscler Thromb Vasc Biol **27**(11): 2377-83.

Dec, W. (2006). "A meta-analysis of success rates for digit replantation." Tech Hand Up Extrem Surg **10**(3): 124-9.

Derwin, K. A., S. F. Badylak, S. P. Steinmann and J. P. Iannotti (2010). "Extracellular matrix scaffold devices for rotator cuff repair." J Shoulder Elbow Surg **19**(3): 467-76.

Dickinson, B. P., R. K. Ashley, K. L. Wasson, C. O'Hara, J. Gabbay, J. B. Heller and J. P. Bradley (2008). "Reduced morbidity and improved healing with bone morphogenic protein-2 in older patients with alveolar cleft defects." Plast Reconstr Surg **121**(1): 209-17.

Discher, D. E., D. J. Mooney and P. W. Zandstra (2009). "Growth factors, matrices, and forces combine and control stem cells." Science **324**(5935): 1673-7.

Ellis, S. J. and G. Tanentzapf "Integrin-mediated adhesion and stem-cell-niche interactions." Cell Tissue Res **339**(1): 121-30.

Eng, L. F., R. S. Ghirnikar and Y. L. Lee (2000). "Glial fibrillary acidic protein: GFAP-thirty-one years (1969-2000)." Neurochem Res **25**(9-10): 1439-51.

Epstein, W. L. and H. I. Maibach (1965). "Cell renewal in human epidermis." Arch Dermatol **92**(4): 462-8.

Falanga, V. (2005). "Wound healing and its impairment in the diabetic foot." Lancet **366**(9498): 1736-43.

Fauquier, T., K. Rizzoti, M. Dattani, R. Lovell-Badge and I. C. Robinson (2008). "SOX2-expressing progenitor cells generate all of the major cell types in the adult mouse pituitary gland." Proc Natl Acad Sci U S A **105**(8): 2907-12.

Fernando, W. A., E. Leininger, J. Simkin, N. Li, C. A. Malcom, S. Sathyamoorthi, M. Han and K. Muneoka "Wound healing and blastema formation in regenerating digit tips of adult mice." Dev Biol **350**(2): 301-10.

Flaim, C. J., S. Chien and S. N. Bhatia (2005). "An extracellular matrix microarray for probing cellular differentiation." Nat Methods **2**(2): 119-25.

Freytes, D. O., S. F. Badylak, T. J. Webster, L. A. Geddes and A. E. Rundell (2004). "Biaxial strength of multilaminated extracellular matrix scaffolds." Biomaterials **25**(12): 2353-61.

Freytes, D. O., J. Martin, S. S. Velankar, A. S. Lee and S. F. Badylak (2008). "Preparation and rheological characterization of a gel form of the porcine urinary bladder matrix." Biomaterials **29**(11): 1630-7.

Frid, M. G., V. A. Kale and K. R. Stenmark (2002). "Mature vascular endothelium can give rise to smooth muscle cells via endothelial-mesenchymal transdifferentiation: in vitro analysis." Circ Res **90**(11): 1189-96.

Friedenstein, A. J., K. V. Petrakova, A. I. Kurolesova and G. P. Frolova (1968). "Heterotopic of bone marrow. Analysis of precursor cells for osteogenic and hematopoietic tissues." Transplantation **6**(2): 230-47.

Friedenstein, A. J., S. Piatetzky, II and K. V. Petrakova (1966). "Osteogenesis in transplants of bone marrow cells." J Embryol Exp Morphol **16**(3): 381-90.

Ganz, T. (2003). "Defensins: antimicrobial peptides of innate immunity." Nat Rev Immunol **3**(9): 710-20.

Gatenby, P. A., R. E. Callard and A. Basten (1984). "T cells, T cell subsets and immunoregulation." Aust N Z J Med **14**(1): 89-96.

Gilbert, T. W., J. M. Freund and S. F. Badylak (2009). "Quantification of DNA in biologic scaffold materials." J Surg Res **152**(1): 135-9.

Gilbert, T. W., S. Gilbert, M. Madden, S. D. Reynolds and S. F. Badylak (2008). "Morphologic assessment of extracellular matrix scaffolds for patch tracheoplasty in a canine model." Ann Thorac Surg **86**(3): 967-74; discussion 967-74.

Gilbert, T. W., M. S. Sacks, J. S. Grashow, S. L. Woo, S. F. Badylak and M. B. Chancellor (2006). "Fiber kinematics of small intestinal submucosa under biaxial and uniaxial stretch." J Biomech Eng **128**(6): 890-8.

Gilbert, T. W., A. M. Stewart-Akers and S. F. Badylak (2007). "A quantitative method for evaluating the degradation of biologic scaffold materials." Biomaterials **28**(2): 147-50.

Gilbert, T. W., A. M. Stewart-Akers, A. Simmons-Byrd and S. F. Badylak (2007). "Degradation and remodeling of small intestinal submucosa in canine Achilles tendon repair." J Bone Joint Surg Am **89**(3): 621-30.

Gilbert, T. W., A. M. Stewart-Akers, J. Sydeski, T. D. Nguyen, S. F. Badylak and S. L. Woo (2007). "Gene expression by fibroblasts seeded on s mall intestinal submucosa and subjected to cyclic stretching." Tissue Eng **13**(6): 1313-23.

Gregory, C. A., W. G. Gunn, A. Peister and D. J. Prockop (2004). "An Alizarin red-based assay of mineralization by adherent cells in culture: comparison with cetylpyridinium chloride extraction." Anal Biochem **329**(1): 77-84.

Han, M., X. Yang, J. E. Farrington and K. Muneoka (2003). "Digit regeneration is regulated by Msx1 and BMP4 in fetal mice." Development **130**(21): 5123-32.

Han, M., X. Yang, J. Lee, C. H. Allan and K. Muneoka (2008). "Development and regeneration of the neonatal digit tip in mice." Dev Biol **315**(1): 125-35.

Hans, F. and S. Dimitrov (2001). "Histone H3 phosphorylation and cell division." Oncogene **20**(24): 3021-7.

Harada, K., M. Friedman, J. J. Lopez, S. Y. Wang, J. Li, P. V. Prasad, J. D. Pearlman, E. R. Edelman, F. W. Sellke and M. Simons (1996). "Vascular endothelial growth factor administration in chronic myocardial ischemia." Am J Physiol **270**(5 Pt 2): H1791-802.

Hechavarria, D., A. Dewilde, S. Braunhut, M. Levin and D. L. Kaplan "BioDome regenerative sleeve for biochemical and biophysical stimulation of tissue regeneration." Med Eng Phys **32**(9): 1065-73.

Hocking, D. C. and K. Kowalski (2002). "A cryptic fragment from fibronectin's III1 module localizes to lipid rafts and stimulates cell growth and contractility." J Cell Biol **158**(1): 175-84.

Hodde, J. P., S. F. Badylak and K. D. Shelbourne (1997). "The Effect of Range of Motion on Remodeling of Small Intestinal Submucosa (SIS) When Used as an Achilles Tendon Repair Material in the Rabbit." Tissue Engineering **3**(1): 27-37.

Horton, M. A., J. H. Spragg, S. C. Bodary and M. H. Helfrich (1994). "Recognition of cryptic sites in human and mouse laminins by rat osteoclasts is mediated by beta 3 and beta 1 integrins." Bone **15**(6): 639-46.

Horwitz, E. M., P. L. Gordon, W. K. Koo, J. C. Marx, M. D. Neel, R. Y. McNall, L. Muul and T. Hofmann (2002). "Isolated allogeneic bone marrow-derived mesenchymal cells engraft and stimulate growth in children with osteogenesis imperfecta: Implications for cell therapy of bone." Proc Natl Acad Sci U S A **99**(13): 8932-7.

Humphries, J. D., A. Byron and M. J. Humphries (2006). "Integrin ligands at a glance." J Cell Sci **119**(Pt 19): 3901-3.

Humphries, M. J. (2009). "Cell adhesion assays." Methods Mol Biol **522**: 203-10.

Hutton, S. R. and L. H. Pevny (2011). "SOX2 expression levels distinguish between neural progenitor populations of the developing dorsal telencephalon." Dev Biol **352**(1): 40-7.

Ito, Y., H. Hayashi, M. Taira, M. Tatibana, Y. Tabata and K. Isono (1991). "Depression of liver-specific gene expression in regenerating rat liver: a putative cause for liver dysfunction after hepatectomy." J Surg Res **51**(2): 143-7.

Jackson, K. A., S. M. Majka, H. Wang, J. Pocius, C. J. Hartley, M. W. Majesky, M. L. Entman, L. H. Michael, K. K. Hirschi and M. A. Goodell (2001). "Regeneration of ischemic cardiac muscle and vascular endothelium by adult stem cells." J Clin Invest **107**(11): 1395-402.

Janssens, S., C. Dubois, J. Bogaert, K. Theunissen, C. Deroose, W. Desmet, M. Kalantzi, L. Herbots, P. Sinnaeve, J. Dens, J. Maertens, F. Rademakers, S. Dymarkowski, O. Gheysens, J. Van Cleemput, G. Bormans, J. Nuyts, A. Belmans, L. Mortelmans, M.

Boogaerts and F. Van de Werf (2006). "Autologous bone marrow-derived stem-cell transfer in patients with ST-segment elevation myocardial infarction: double-blind, randomised controlled trial." <u>Lancet</u> **367**(9505): 113-21.

Janssens, S., K. Theunissen, M. Boogaerts and F. Van de Werf (2006). "Bone marrow cell transfer in acute myocardial infarction." <u>Nat Clin Pract Cardiovasc Med</u> **3 Suppl 1**: S69-72.

Jeong, G. K., H. S. Sandhu and J. Farmer (2005). "Bone morphogenic proteins: applications in spinal surgery." <u>HSS J</u> **1**(1): 110-7.

Kamiya, A., S. Kakinuma, Y. Yamazaki and H. Nakauchi (2009). "Enrichment and clonal culture of progenitor cells during mouse postnatal liver development in mice." <u>Gastroenterology</u> **137**(3): 1114-26, 1126 e1-14.

Kanatsu-Shinohara, M., M. Takehashi, S. Takashima, J. Lee, H. Morimoto, S. Chuma, A. Raducanu, N. Nakatsuji, R. Fassler and T. Shinohara (2008). "Homing of mouse spermatogonial stem cells to germline niche depends on beta1-integrin." <u>Cell Stem Cell</u> **3**(5): 533-42.

Kanoupakis, E. M., E. G. Manios, E. M. Kallergis, H. E. Mavrakis, C. A. Goudis, I. G. Saloustros, M. E. Milathianaki, G. I. Chlouverakis and P. E. Vardas (2010). "Serum markers of collagen turnover predict future shocks in implantable cardioverter-defibrillator recipients with dilated cardiomyopathy on optimal treatment." <u>J Am Coll Cardiol</u> **55**(24): 2753-9.

Kelly, D. J., A. B. Rosen, A. J. Schuldt, P. V. Kochupura, S. V. Doronin, I. A. Potapova, E. U. Azeloglu, S. F. Badylak, P. R. Brink, I. S. Cohen and G. R. Gaudette (2009). "Increased myocyte content and mechanical function within a tissue-engineered myocardial patch following implantation." <u>Tissue Eng Part A</u> **15**(8): 2189-201.

Keung, A. J., S. Kumar and D. V. Schaffer (2010). "Presentation counts: microenvironmental regulation of stem cells by biophysical and material cues." <u>Annu Rev Cell Dev Biol</u> **26**: 533-56.

Kienstra, K. A., K. A. Jackson and K. K. Hirschi (2008). "Injury mechanism dictates contribution of bone marrow-derived cells to murine hepatic vascular regeneration." <u>Pediatr Res</u> **63**(2): 131-6.

Kim, J. Y., X. Xin, E. K. Moioli, J. Chung, C. H. Lee, M. Chen, S. Y. Fu, P. D. Koch and J. J. Mao (2010). "Regeneration of Dental-Pulp-like Tissue by Chemotaxis-Induced Cell Homing." <u>Tissue Eng Part A</u>.

Kim, J. Y., X. Xin, E. K. Moioli, J. Chung, C. H. Lee, M. Chen, S. Y. Fu, P. D. Koch and J. J. Mao (2010). "Regeneration of Dental-Pulp-like Tissue by Chemotaxis-Induced Cell Homing." <u>Tissue Eng Part A</u> **16**(10): 3023-3031.

Kitahara, T., Y. Takeishi, T. Arimoto, T. Niizeki, Y. Koyama, T. Sasaki, S. Suzuki, N. Nozaki, O. Hirono, J. Nitobe, T. Watanabe and I. Kubota (2007). "Serum carboxy-terminal telopeptide of type I collagen (ICTP) predicts cardiac events in chronic heart failure patients with preserved left ventricular systolic function." <u>Circ J</u> **71**(6): 929-35.

Kochupura, P. V., E. U. Azeloglu, D. J. Kelly, S. V. Doronin, S. F. Badylak, I. B. Krukenkamp, I. S. Cohen and G. R. Gaudette (2005). "Tissue-engineered myocardial patch derived from extracellular matrix provides regional mechanical function." <u>Circulation</u> **112**(9 Suppl): I144-9.

Kragl, M., D. Knapp, E. Nacu, S. Khattak, M. Maden, H. H. Epperlein and E. M. Tanaka (2009). "Cells keep a memory of their tissue origin during axolotl limb regeneration." Nature **460**(7251): 60-5.

Kropp, B. P., B. L. Eppley, C. D. Prevel, M. K. Rippy, R. C. Harruff, S. F. Badylak, M. C. Adams, R. C. Rink and M. A. Keating (1995). "Experimental assessment of small intestinal submucosa as a bladder wall substitute." Urology **46**(3): 396-400.

Kropp, B. P., M. K. Rippy, S. F. Badylak, M. C. Adams, M. A. Keating, R. C. Rink and K. B. Thor (1996). "Regenerative urinary bladder augmentation using small intestinal submucosa: urodynamic and histopathologic assessment in long-term canine bladder augmentations." J Urol **155**(6): 2098-104.

Kumar, A., J. W. Godwin, P. B. Gates, A. A. Garza-Garcia and J. P. Brockes (2007). "Molecular basis for the nerve dependence of limb regeneration in an adult vertebrate." Science **318**(5851): 772-7.

Lackie, J. M., P. C. Wilkinson and Society for Experimental Biology (Great Britain) (1981). Biology of the chemotactic response. Cambridge ; New York, Cambridge University Press.

Lagasse, E., H. Connors, M. Al-Dhalimy, M. Reitsma, M. Dohse, L. Osborne, X. Wang, M. Finegold, I. L. Weissman and M. Grompe (2000). "Purified hematopoietic stem cells can differentiate into hepatocytes in vivo." Nat Med **6**(11): 1229-34.

Langer, R. and J. P. Vacanti (1993). "Tissue engineering." Science **260**(5110): 920-6.

Lantz, G. C., S. F. Badylak, A. C. Coffey, L. A. Geddes and W. E. Blevins (1990). "Small intestinal submucosa as a small-diameter arterial graft in the dog." J Invest Surg **3**(3): 217-27.

Lantz, G. C., S. F. Badylak, A. C. Coffey, L. A. Geddes and G. E. Sandusky (1992). "Small intestinal submucosa as a superior vena cava graft in the dog." J Surg Res **53**(2): 175-81.

Lee, C. H., J. L. Cook, A. Mendelson, E. K. Moioli, H. Yao and J. J. Mao "Regeneration of the articular surface of the rabbit synovial joint by cell homing: a proof of concept study." Lancet **376**(9739): 440-8.

Lee, C. H., J. L. Cook, A. Mendelson, E. K. Moioli, H. Yao and J. J. Mao (2010). "Regeneration of the articular surface of the rabbit synovial joint by cell homing: a proof of concept study." Lancet **376**(9739): 440-8.

Lee, L. P., P. Y. Lau and C. W. Chan (1995). "A simple and efficient treatment for fingertip injuries." J Hand Surg [Br] **20**(1): 63-71.

Lee, S. T., J. I. Yun, Y. S. Jo, M. Mochizuki, A. J. van der Vlies, S. Kontos, J. E. Ihm, J. M. Lim and J. A. Hubbell (2011). "Engineering integrin signaling for promoting embryonic stem cell self-renewal in a precisely defined niche." Biomaterials **31**(6): 1219-26.

Leone, D. P., J. B. Relvas, L. S. Campos, S. Hemmi, C. Brakebusch, R. Fassler, C. Ffrench-Constant and U. Suter (2005). "Regulation of neural progenitor proliferation and survival by beta1 integrins." J Cell Sci **118**(Pt 12): 2589-99.

Lewis, J. P. and F. E. Trobaugh, Jr. (1964). "Haematopoietic Stem Cells." Nature **204**: 589-90.

Li, C., F. Yang and A. Sheppard (2009). "Adult Stem Cells and Mammalian Epimorphic Regeneration-Insights from Studying Annual Renewal of Deer Antlers." Curr Stem Cell Res Ther.

Li, F., W. Li, S. Johnson, D. Ingram, M. Yoder and S. Badylak (2004). "Low-molecular-weight peptides derived from extracellular matrix as chemoattractants for primary endothelial cells." Endothelium **11**(3-4): 199-206.

Li, J., G. Pan, K. Cui, Y. Liu, S. Xu and D. Pei (2007). "A dominant-negative form of mouse SOX2 induces trophectoderm differentiation and progressive polyploidy in mouse embryonic stem cells." J Biol Chem **282**(27): 19481-92.

Locatelli, F., S. Corti, C. Donadoni, M. Guglieri, F. Capra, S. Strazzer, S. Salani, R. Del Bo, F. Fortunato, A. Bordoni and G. P. Comi (2003). "Neuronal differentiation of murine bone marrow Thy-1- and Sca-1-positive cells." J Hematother Stem Cell Res **12**(6): 727-34.

Lolmede, K., L. Campana, M. Vezzoli, L. Bosurgi, R. Tonlorenzi, E. Clementi, M. E. Bianchi, G. Cossu, A. A. Manfredi, S. Brunelli and P. Rovere-Querini (2009). "Inflammatory and alternatively activated human macrophages attract vessel-associated stem cells, relying on separate HMGB1- and MMP-9-dependent pathways." J Leukoc Biol **85**(5): 779-87.

Lopes, M. F., A. Cabrita, J. Ilharco, P. Pessa, J. Paiva-Carvalho, A. Pires and J. Patricio (2006). "Esophageal replacement in rat using porcine intestinal submucosa as a patch or a tube-shaped graft." Dis Esophagus **19**(4): 254-9.

Lutton, C. and B. Goss (2008). "Caring about microenvironments." Nat Biotechnol **26**(6): 613-4.

Majka, S. M., K. A. Jackson, K. A. Kienstra, M. W. Majesky, M. A. Goodell and K. K. Hirschi (2003). "Distinct progenitor populations in skeletal muscle are bone marrow derived and exhibit different cell fates during vascular regeneration." J Clin Invest **111**(1): 71-9.

Mannion, R. J., A. M. Nowitzke and M. J. Wood (2010). "Promoting fusion in minimally invasive lumbar interbody stabilization with low-dose bone morphogenic protein-2-but what is the cost?" Spine J.

Mansukhani, A., D. Ambrosetti, G. Holmes, L. Cornivelli and C. Basilico (2005). "Sox2 induction by FGF and FGFR2 activating mutations inhibits Wnt signaling and osteoblast differentiation." J Cell Biol **168**(7): 1065-76.

Mantovani, A., A. Sica, S. Sozzani, P. Allavena, A. Vecchi and M. Locati (2004). "The chemokine system in diverse forms of macrophage activation and polarization." Trends Immunol **25**(12): 677-86.

Marra, K. G., A. J. Defail, J. A. Clavijo-Alvarez, S. F. Badylak, A. Taieb, B. Schipper, J. Bennett and J. P. Rubin (2008). "FGF-2 enhances vascularization for adipose tissue engineering." Plast Reconstr Surg **121**(4): 1153-64.

Mase, V. J., Jr., J. R. Hsu, S. E. Wolf, J. C. Wenke, D. G. Baer, J. Owens, S. F. Badylak and T. J. Walters "Clinical application of an acellular biologic scaffold for surgical repair of a large, traumatic quadriceps femoris muscle defect." Orthopedics **33**(7): 511.

Mase, V. J., Jr., J. R. Hsu, S. E. Wolf, J. C. Wenke, D. G. Baer, J. Owens, S. F. Badylak and T. J. Walters (2010). "Clinical application of an acellular biologic scaffold for surgical repair of a large, traumatic quadriceps femoris muscle defect." Orthopedics **33**(7): 511.

McKinney-Freeman, S. L., K. A. Jackson, F. D. Camargo, G. Ferrari, F. Mavilio and M. A. Goodell (2002). "Muscle-derived hematopoietic stem cells are hematopoietic in origin." Proc Natl Acad Sci U S A **99**(3): 1341-6.

Medberry, C. J., S. Tottey, H. Jiang, S. A. Johnson and S. F. Badylak (2010). "Resistance to Infection of Five Different Materials in a Rat Body Wall Model." J Surg Res **Epub Sep 17**.

Medberry, C. J., S. Tottey, H. Jiang, S. A. Johnson and S. F. Badylak (2010). "Resistance to Infection of Five Different Materials in a Rat Body Wall Model." J Surg Res.

Melman, L., E. D. Jenkins, N. A. Hamilton, L. C. Bender, M. D. Brodt, C. R. Deeken, S. C. Greco, M. M. Frisella and B. D. Matthews (2011). "Early biocompatibility of crosslinked

and non-crosslinked biologic meshes in a porcine model of ventral hernia repair." <u>Hernia</u> **15**(2): 157-64.

Metcalf, M. H., F. H. Savoie and B. Kellum (2002). "Surgical technique for xenograft (SIS) augmentation of rotator-cuff repairs." <u>Oper Tech Orthop</u> **12**: 204-8.

Metcalfe, A. D. and M. W. Ferguson (2005). "Harnessing wound healing and regeneration for tissue engineering." <u>Biochem Soc Trans</u> **33**(Pt 2): 413-7.

Michalopoulos, G. K. (2007). "Liver regeneration." <u>J Cell Physiol</u> **213**(2): 286-300.

Mohammad, K. S. and D. A. Neufeld (2000). "Denervation retards but does not prevent toetip regeneration." <u>Wound Repair Regen</u> **8**(4): 277-81.

Moist, L. M., N. Muirhead, L. D. Wazny, K. L. Gallo, A. P. Heidenheim and A. A. House (2006). "Erythropoietin dose requirements when converting from subcutaneous to intravenous administration among patients on hemodialysis." <u>Ann Pharmacother</u> **40**(2): 198-203.

Monaghan, J. R., L. G. Epp, S. Putta, R. B. Page, J. A. Walker, C. K. Beachy, W. Zhu, G. M. Pao, I. M. Verma, T. Hunter, S. V. Bryant, D. M. Gardiner, T. T. Harkins and S. R. Voss (2009). "Microarray and cDNA sequence analysis of transcription during nerve-dependent limb regeneration." <u>BMC Biol</u> **7**: 1.

Mongan, N. P., K. M. Martin and L. J. Gudas (2006). "The putative human stem cell marker, Rex-1 (Zfp42): structural classification and expression in normal human epithelial and carcinoma cell cultures." <u>Mol Carcinog</u> **45**(12): 887-900.

Moore, A. J., W. D. Beazley, M. C. Bibby and D. A. Devine (1996). "Antimicrobial activity of cecropins." <u>J Antimicrob Chemother</u> **37**(6): 1077-89.

Moore, A. J., D. A. Devine and M. C. Bibby (1994). "Preliminary experimental anticancer activity of cecropins." <u>Pept Res</u> **7**(5): 265-9.

Morgan, T. H. (1901). <u>Regeneration</u>. New York,

London,, The Macmillan Company;

Macmillan & Co., ltd.

Mukai, H., Y. Hokari, T. Seki, T. Takao, M. Kubota, Y. Matsuo, H. Tsukagoshi, M. Kato, H. Kimura, Y. Shimonishi, Y. Kiso, Y. Nishi, K. Wakamatsu and E. Munekata (2008). "Discovery of mitocryptide-1, a neutrophil-activating cryptide from healthy porcine heart." <u>J Biol Chem</u> **283**(45): 30596-605.

Mukai, H., T. Seki, H. Nakano, Y. Hokari, T. Takao, M. Kawanami, H. Tsukagoshi, H. Kimura, Y. Kiso, Y. Shimonishi, Y. Nishi and E. Munekata (2009). "Mitocryptide-2: purification, identification, and characterization of a novel cryptide that activates neutrophils." <u>J Immunol</u> **182**(8): 5072-80.

Nakamoto, T., K. H. Kain and M. H. Ginsberg (2004). "Neurobiology: New connections between integrins and axon guidance." <u>Curr Biol</u> **14**(3): R121-3.

Nelson, C. M. and M. J. Bissell (2006). "Of extracellular matrix, scaffolds, and signaling: tissue architecture regulates development, homeostasis, and cancer." <u>Annu Rev Cell Dev Biol</u> **22**: 287-309.

Neufeld, D. A. and K. S. Mohammad (2000). "Fluorescent bone viewed through toenails of living animals: a method to observe bone regrowth." <u>Biotech Histochem</u> **75**(6): 259-63.

Neufeld, D. A. and W. Zhao (1993). "Phalangeal regrowth in rodents: postamputational bone regrowth depends upon the level of amputation." <u>Prog Clin Biol Res</u> **383A**: 243-52.

Neufeld, D. A. and W. Zhao (1995). "Bone regrowth after digit tip amputation in mice is equivalent in adults and neonates." <u>Wound Repair Regen</u> **3**(4): 461-6.

Ng, J. H. and L. L. Ilag (2006). "Cryptic protein fragments as an emerging source of peptide drugs." IDrugs **9**(5): 343-6.

Nichol, J. W. and A. Khademhosseini (2009). "Modular Tissue Engineering: Engineering Biological Tissues from the Bottom Up." Soft Matter **5**(7): 1312-1319.

Nieponice, A., T. W. Gilbert and S. F. Badylak (2006). "Reinforcement of esophageal anastomoses with an extracellular matrix scaffold in a canine model." Ann Thorac Surg **82**(6): 2050-8.

Nieponice, A., K. McGrath, I. Qureshi, E. J. Beckman, J. D. Luketich, T. W. Gilbert and S. F. Badylak (2009). "An extracellular matrix scaffold for esophageal stricture prevention after circumferential EMR." Gastrointest Endosc **69**(2): 289-96.

Oates, P. S. and A. R. West (2006). "Heme in intestinal epithelial cell turnover, differentiation, detoxification, inflammation, carcinogenesis, absorption and motility." World J Gastroenterol **12**(27): 4281-95.

Okamoto, R., T. Yajima, M. Yamazaki, T. Kanai, M. Mukai, S. Okamoto, Y. Ikeda, T. Hibi, J. Inazawa and M. Watanabe (2002). "Damaged epithelia regenerated by bone marrow-derived cells in the human gastrointestinal tract." Nat Med **8**(9): 1011-7.

Ota, T., T. W. Gilbert, S. F. Badylak, D. Schwartzman and M. A. Zenati (2007). "Electromechanical characterization of a t issue-engineered myocardial patch derived from extracellular matrix." J Thorac Cardiovasc Surg **133**(4): 979-85.

Ott, H. C., B. Clippinger, C. Conrad, C. Schuetz, I. Pomerantseva, L. Ikonomou, D. Kotton and J. P. Vacanti (2010). "Regeneration and orthotopic transplantation of a bioartificial lung." Nat Med **16**(8): 927-33.

Ott, H. C., T. S. Matthiesen, S. K. Goh, L. D. Black, S. M. Kren, T. I. Netoff and D. A. Taylor (2008). "Perfusion-decellularized matrix: using nature's platform to engineer a bioartificial heart." Nat Med **14**(2): 213-21.

Owen, M. (1988). "Marrow stromal stem cells." J Cell Sci Suppl **10**: 63-76.

Parekh, A., B. Mantle, J. Banks, J. D. Swarts, S. F. Badylak, J. E. Dohar and P. A. Hebda (2009). "Repair of the tympanic membrane with urinary bladder matrix." Laryngoscope **119**(6): 1206-13.

Petersen, T. H., E. A. Calle, M. B. Colehour and L. E. Niklason "Matrix Composition and Mechanics of Decellularized Lung Scaffolds." Cells Tissues Organs.

Petersen, T. H., E. A. Calle, L. Zhao, E. J. Lee, L. Gui, M. B. Raredon, K. Gavrilov, T. Yi, Z. W. Zhuang, C. Breuer, E. Herzog and L. E. Niklason "Tissue-engineered lungs for in vivo implantation." Science **329**(5991): 538-41.

Pimenta, D. C. and I. Lebrun (2007). "Cryptides: buried secrets in proteins." Peptides **28**(12): 2403-10.

Pope, J. C. t., M. M. Davis, E. R. Smith, Jr., M. J. Walsh, P. K. Ellison, R. C. Rink and B. P. Kropp (1997). "The ontogeny of canine small intestinal submucosa regenerated bladder." J Urol **158**(3 Pt 2): 1105-10.

Porto, A., R. Palumbo, M. Pieroni, G. Aprigliano, R. Chiesa, F. Sanvito, A. Maseri and M. E. Bianchi (2006). "Smooth muscle cells in human atherosclerotic plaques secrete and proliferate in response to high mobility group box 1 protein." FASEB J **20**(14): 2565-6.

Prevel, C. D., B. L. Eppley, D. J. Summerlin, J. R. Jackson, M. McCarty and S. F. Badylak (1995). "Small intestinal submucosa: utilization for repair of rodent abdominal wall defects." Ann Plast Surg **35**(4): 374-80.

Ranzato, E., M. Patrone, M. Pedrazzi and B. Burlando (2009). "HMGb1 promotes scratch wound closure of HaCaT keratinocytes via ERK1/2 activation." Mol Cell Biochem **332**(1-2): 199-205.

Raymond, K., M. A. Deugnier, M. M. Faraldo and M. A. Glukhova (2009). "Adhesion within the stem cell niches." Curr Opin Cell Biol **21**(5): 623-9.

Record, R. D., D. Hillegonds, C. Simmons, R. Tullius, F. A. Rickey, D. Elmore and S. F. Badylak (2001). "In vivo degradation of 14C-labeled small intestinal submucosa (SIS) when used for urinary bladder repair." Biomaterials **22**(19): 2653-9.

Reginelli, A. D., Y. Q. Wang, D. Sassoon and K. Muneoka (1995). "Digit tip regeneration correlates with regions of Msx1 (Hox 7) expression in fetal and newborn mice." Development **121**(4): 1065-76.

Reing, J. E., L. Zhang, J. Myers-Irvin, K. E. Cordero, D. O. Freytes, E. Heber-Katz, K. Bedelbaeva, D. McIntosh, A. Dewilde, S. J. Braunhut and S. F. Badylak (2009). "Degradation products of extracellular matrix affect cell migration and proliferation." Tissue Eng Part A **15**(3): 605-14.

Ritenour, A. E., L. H. Blackbourne, J. F. Kelly, D. F. McLaughlin, L. A. Pearse, J. B. Holcomb and C. E. Wade (2010). "Incidence of primary blast injury in US military overseas contingency operations: a retrospective study." Ann Surg **251**(6): 1140-4.

Robinson, K. A., J. Li, M. Mathison, A. Redkar, J. Cui, N. A. Chronos, R. G. Matheny and S. F. Badylak (2005). "Extracellular matrix scaffold for cardiac repair." Circulation **112**(9 Suppl): I135-43.

Rogozinski, A., C. Rogozinski and G. Cloud (2009). "Accelerating autograft maturation in instrumented posterolateral lumbar spinal fusions without donor site morbidity." Orthopedics **32**(11): 809.

Sanchez Alvarado, A. (2000). "Regeneration in the metazoans: why does it happen?" Bioessays **22**(6): 578-90.

Sarikaya, A., R. Record, C. C. Wu, B. Tullius, S. Badylak and M. Ladisch (2002). "Antimicrobial activity associated with extracellular matrices." Tissue Eng **8**(1): 63-71.

Schieber, M. H., C. E. Lang, K. T. Reilly, P. McNulty and A. Sirigu (2009). "Selective activation of human finger muscles after stroke or amputation." Adv Exp Med Biol **629**: 559-75.

Schotte, O. E. and C. B. Smith (1959). "Wound Healing Processes in Amputated Mouse Digits." Biological Bulletin **117**(3): 546-561.

Schotte, O. E. and C. B. Smith (1961). "Effects of ACTH and of cortisone upon amputational wound healing processes in mice digits." J Exp Zool **146**: 209-29.

Sellaro, T. L., A. K. Ravindra, D. B. Stolz and S. F. Badylak (2007). "Maintenance of hepatic sinusoidal endothelial cell phenotype in vitro using organ-specific extracellular matrix scaffolds." Tissue Eng **13**(9): 2301-10.

Shen, C. N., J. M. Slack and D. Tosh (2000). "Molecular basis of transdifferentiation of pancreas to liver." Nat Cell Biol **2**(12): 879-87.

Shih, Y. R., K. F. Tseng, H. Y. Lai, C. H. Lin and O. K. Lee (2011). "Matrix stiffness regulation of integrin-mediated mechanotransduction during osteogenic differentiation of human mesenchymal stem cells." J Bone Miner Res **26**(4): 730-8.

Spangrude, G. J., S. Heimfeld and I. L. Weissman (1988). "Purification and characterization of mouse hematopoietic stem cells." Science **241**(4861): 58-62.

Spangrude, G. J. and R. Scollay (1990). "A simplified method for enrichment of mouse hematopoietic stem cells." Exp Hematol **18**(8): 920-6.

Steinau, H. U., A. Daigeler, S. Langer, L. Steinstrasser, J. Hauser, O. Goertz and M. Lehnhardt (2010). "Limb salvage in malignant tumors." <u>Semin Plast Surg</u> **24**(1): 18-33.

Stinner, D. J., T. C. Burns, K. L. Kirk, C. R. Scoville, J. R. Ficke and J. R. Hsu (2010). "Prevalence of late amputations during the current conflicts in Afghanistan and Iraq." <u>Mil Med</u> **175**(12): 1027-9.

Suzuki, A., A. Iwama, H. Miyashita, H. Nakauchi and H. Taniguchi (2003). "Role for growth factors and extracellular matrix in controlling differentiation of prospectively isolated hepatic stem cells." <u>Development</u> **130**(11): 2513-24.

Tottey, S., M. Corselli, E. M. Jeffries, R. Londono, B. Peault and S. F. Badylak "Extracellular matrix degradation products and low-oxygen conditions enhance the regenerative potential of perivascular stem cells." <u>Tissue Eng Part A</u> **17**(1-2): 37-44.

Tottey, S., M. Corselli, E. M. Jeffries, R. Londono, B. Peault and S. F. Badylak (2011). "Extracellular matrix degradation products and low-oxygen conditions enhance the regenerative potential of perivascular stem cells." <u>Tissue Eng Part A</u> **17**(1-2): 37-44.

Tottey, S., S. A. Johnson, P. M. Crapo, J. E. Reing, L. Zhang, H. Jiang, C. J. Medberry, B. Reines and S. F. Badylak (2010). "The effect of source animal age upon extracellular matrix scaffold properties." <u>Biomaterials</u> **32**(1): 128-36.

Trouba, K. J., E. M. Wauson and R. L. Vorce (2000). "Sodium arsenite inhibits terminal differentiation of murine C3H 10T1/2 preadipocytes." <u>Toxicol Appl Pharmacol</u> **168**(1): 25-35.

Tsuchiya, A., T. Heike, S. Baba, H. Fujino, K. Umeda, Y. Matsuda, M. Nomoto, T. Ichida, Y. Aoyagi and T. Nakahata (2007). "Long-term culture of postnatal mouse hepatic stem/progenitor cells and their relative developmental hierarchy." <u>Stem Cells</u> **25**(4): 895-902.

Turner, N. J. and S. F. Badylak "Regeneration of skeletal muscle." <u>Cell Tissue Res</u>.

Turner, N. J., A. J. Yates, Jr., D. J. Weber, I. R. Qureshi, D. B. Stolz, T. W. Gilbert and S. F. Badylak (2010). "Xenogeneic extracellular matrix as an inductive scaffold for regeneration of a functioning musculotendinous junction." <u>Tissue Eng Part A</u> **16**(11): 3309-17.

Tyndall, A. and D. E. Furst (2007). "Adult stem cell treatment of scleroderma." <u>Curr Opin Rheumatol</u> **19**(6): 604-10.

Uygun, B. E., A. Soto-Gutierrez, H. Yagi, M. L. Izamis, M. A. Guzzardi, C. Shulman, J. Milwid, N. Kobayashi, A. Tilles, F. Berthiaume, M. Hertl, Y. Nahmias, M. L. Yarmush and K. Uygun (2010). "Organ reengineering through development of a transplantable recellularized liver graft using decellularized liver matrix." <u>Nat Med</u> **16**(7): 814-20.

Valentin, J. E., J. S. Badylak, G. P. McCabe and S. F. Badylak (2006). "Extracellular matrix bioscaffolds for orthopaedic applications. A comparative histologic study." <u>J Bone Joint Surg Am</u> **88**(12): 2673-86.

Valentin, J. E., A. M. Stewart-Akers, T. W. Gilbert and S. F. Badylak (2009). "Macrophage Participation in the Degradation and Remodeling of ECM Scaffolds." <u>Tissue Eng Part A</u>.

Valentin, J. E., A. M. Stewart-Akers, T. W. Gilbert and S. F. Badylak (2009). "Macrophage participation in the degradation and remodeling of extracellular matrix scaffolds." <u>Tissue Eng Part A</u> **15**(7): 1687-94.

Valentin, J. E., N. J. Turner, T. W. Gilbert and S. F. Badylak "Functional skeletal muscle formation with a biologic scaffold." <u>Biomaterials</u> **31**(29): 7475-84.

van de Rijn, M., S. Heimfeld, G. J. Spangrude and I. L. Weissman (1989). "Mouse hematopoietic stem-cell antigen Sca-1 is a member of the Ly-6 antigen family." <u>Proc Natl Acad Sci U S A</u> **86**(12): 4634-8.

Vogelezang, M. G., Z. Liu, J. B. Relvas, G. Raivich, S. S. Scherer and C. ffrench-Constant (2001). "Alpha4 integrin is expressed during peripheral nerve regeneration and enhances neurite outgrowth." <u>J Neurosci</u> **21**(17): 6732-44.

Watt, F. M. and B. L. Hogan (2000). "Out of Eden: stem cells and their niches." <u>Science</u> **287**(5457): 1427-30.

Weaver, C. D., C. K. Yoshida, I. de Curtis and L. F. Reichardt (1995). "Expression and in vitro function of beta 1-integrin laminin receptors in the developing avian ciliary ganglion." <u>J Neurosci</u> **15**(7 Pt 2): 5275-85.

Witteman, B. P., T. J. Foxwell, S. Monsheimer, A. Gelrud, G. M. Eid, A. Nieponice, R. W. O'Rourke, T. Hoppo, N. D. Bouvy, S. F. Badylak and B. A. Jobe (2009). "Transoral endoscopic inner layer esophagectomy: management of high-grade dysplasia and superficial cancer with organ preservation." <u>J Gastrointest Surg</u> **13**(12): 2104-12.

Wokalek, H. and H. Ruh (1991). "Time course of wound healing." <u>J Biomater Appl</u> **5**(4): 337-62.

Xia, M. and Y. Zhu (2010). "Fibronectin fragment activation of ERK increasing integrin alpha(5) and beta(1) subunit expression to degenerate nucleus pulposus cells." <u>J Orthop Res</u>.

Yu, L., M. Han, M. Yan, E. C. Lee, J. Lee and K. Muneoka "BMP signaling induces digit regeneration in neonatal mice." <u>Development</u> **137**(4): 551-9.

Zadrazil, J., P. Horak, J. Zahalkova, P. Strebl, V. Horcicka, K. Krejci, P. Bachleda, J. Dedochova and I. Valkovsky (2009). "Improvement of cardiovascular risk factors and cosmetic side effects in kidney transplant recipients after conversion to tacrolimus." <u>Biomed Pap Med Fac Univ Palacky Olomouc Czech Repub</u> **153**(1): 67-73.

Zalavras, C. G., R. Gardocki, E. Huang, M. Stevanovic, T. Hedman and J. Tibone (2006). "Reconstruction of large rotator cuff tendon defects with porcine small intestinal submucosa in an animal model." <u>J Shoulder Elbow Surg</u> **15**(2): 224-31.

Zantop, T., T. W. Gilbert, M. C. Yoder and S. F. Badylak (2006). "Extracellular matrix scaffolds are repopulated by bone marrow-derived cells in a mouse model of achilles tendon reconstruction." <u>J Orthop Res</u> **24**(6): 1299-309.

Zhang, X., C. Xie, A. S. Lin, H. Ito, H. Awad, J. R. Lieberman, P. T. Rubery, E. M. Schwarz, R. J. O'Keefe and R. E. Guldberg (2005). "Periosteal progenitor cell fate in segmental cortical bone graft transplantations: implications for functional tissue engineering." <u>J Bone Miner Res</u> **20**(12): 2124-37.

Zhao, W. and D. A. Neufeld (1995). "Bone regrowth in young mice stimulated by nail organ." <u>J Exp Zool</u> **271**(2): 155-9.

Zheng, Y. W. and H. Taniguchi (2003). "Diversity of hepatic stem cells in the fetal and adult liver." <u>Semin Liver Dis</u> **23**(4): 337-48.

Zhou, Q. and D. A. Melton (2008). "Extreme makeover: converting one cell into another." <u>Cell Stem Cell</u> **3**(4): 382-8.

Zhu, H. and A. Dahlstrom (2007). "Glial fibrillary acidic protein-expressing cells in the neurogenic regions in normal and injured adult brains." <u>J Neurosci Res</u> **85**(12): 2783-92.